# *Materials Science View of Grinding and Polishing of Laser Glass Optics*

## OSA Optical Materials Studies Webinar

**December 2, 2016**

**Tayyab Suratwala** suratwala1@llnl.gov
***Optics & Materials Science & Technology***
***Lawrence Livermore National Laboratory***

Lawrence Livermore National Laboratory

LLNL-PRES-712377
This work was performed under the auspices of the U.S. Department of Energy by Lawrence Livermore National Laboratory under Contract DE-AC52-07NA27344. Lawrence Livermore National Security, LLC

# Useful Reading Material

H. Karow, “Fabrication Methods of Precision Optics” John Wiley & Sons (1993)

N. Brown, “Optical Fabrication” LLNL Report MISC4476 (August 1989)

L. Cook, “Chemical Processes in Glass Polishing” Journal of Non-Crystalline Solids 120 (1990) 152-171

T. Izumatani, “Optical Glass” (Kyoritsu Shuppan Company, Tokyo 1984; Lawrence Livermore National Laboratory (USA); American Institute of Physics (New York 1986)

D. Anderson, J. Burge, “The Handbook of Optical Engineering: Chapter 28: Optical Fabrication”

D. Malacara, “Optical Shot Testing” Wiley-Interscience (2007)

Other references quoted through the presentation

# What is optical fabrication?

**The objective of optical fabrication is to manufacture an optical element (e.g., lense, flat, mirror, active optic) which is often made of glass**

**Key Requirements**

1) **Surface Figure (affects wavefront)**

2) **Surface Quality (affects scatter and laser damage resistance)**
   a) **Roughness**
   b) **Sub-surface damage (scratch/dig)**

# NIF concentrates all 192 laser beam energy in a football stadium-sized facility into a $mm^3$

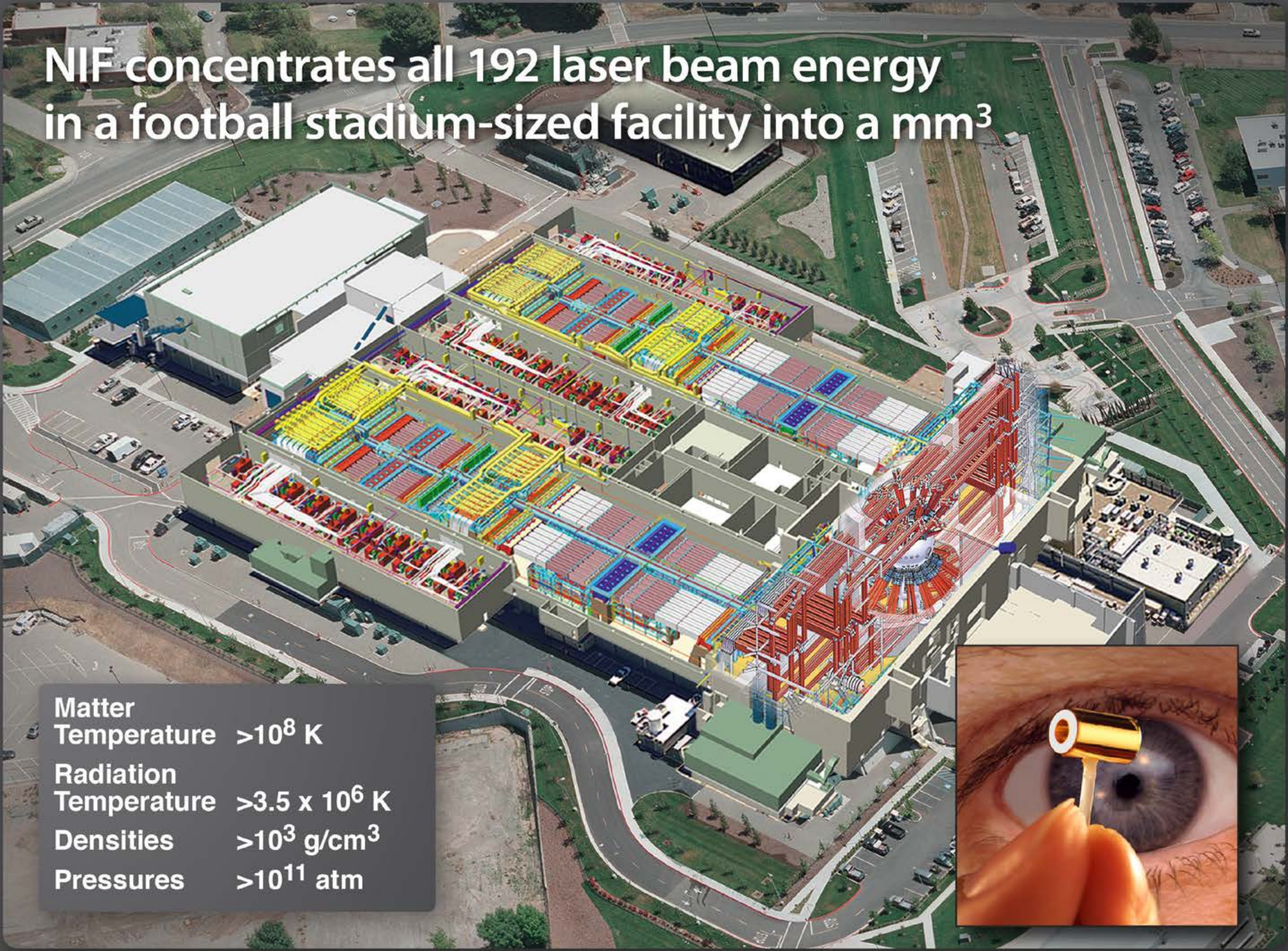

| | |
|---|---|
| **Matter Temperature** | **$>10^8$ K** |
| **Radiation Temperature** | **$>3.5 \times 10^6$ K** |
| **Densities** | **$>10^3$ g/cm$^3$** |
| **Pressures** | **$>10^{11}$ atm** |

# NIF contains >7000 large (0.5 m scale), high precision optics

**KDP**

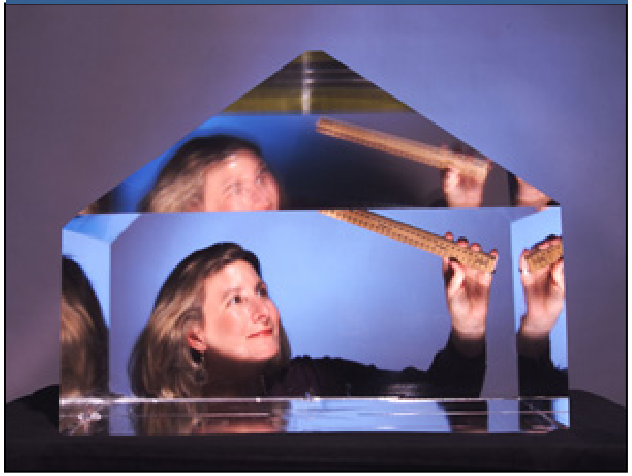

**Laser Phosphate Glass**

**Fused Silica**

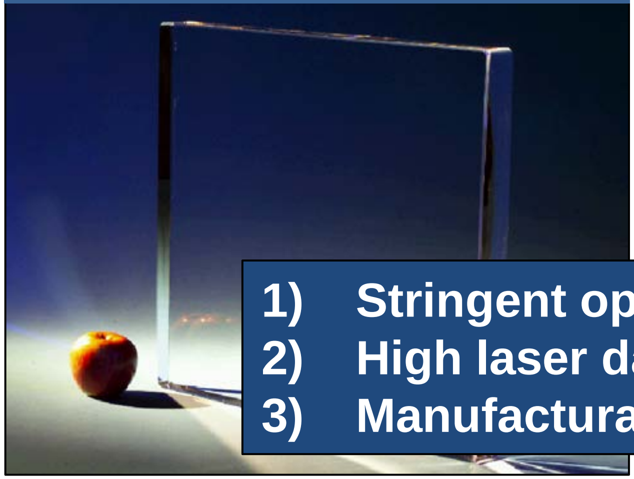

**Borosilicate Glass**

1) Stringent optical requirements
2) High laser damage resistance
3) Manufacturability to 0.5 m size scale

# An example of specifying the requirements of an optic

**Power Spectral Density for Optic Surface**

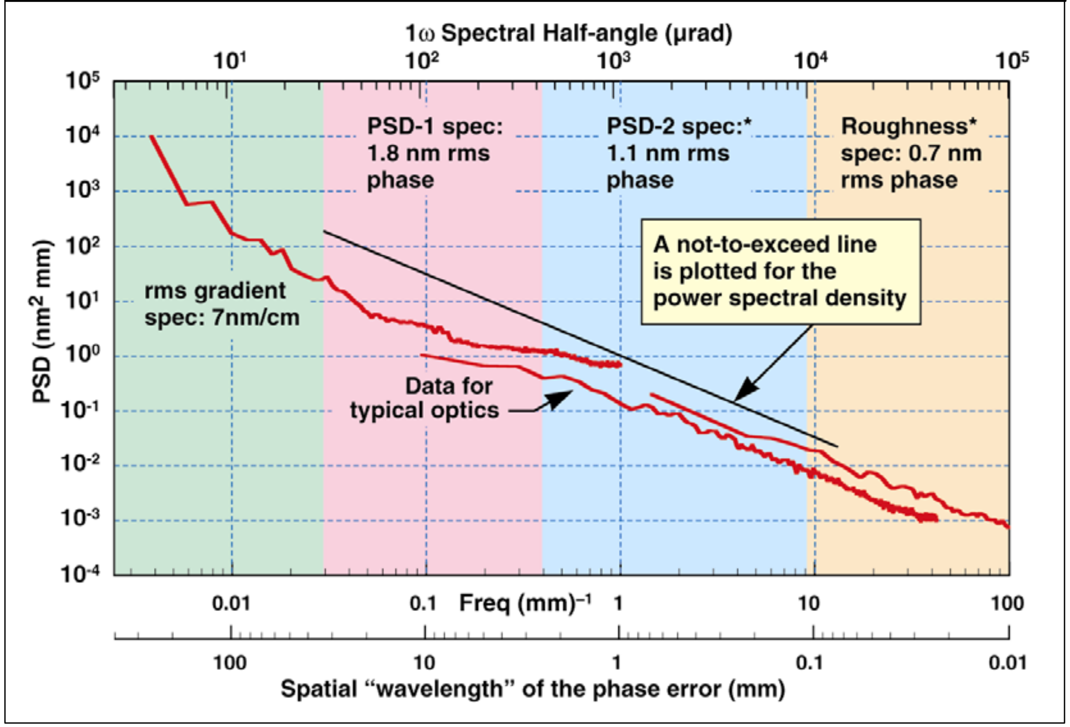

## High Level Requirements[1]

### *Surface*

| | |
|---|---|
| **Peak-to-Valley** | **211 nm (λ/3)** |
| **Gradient** | **<7 nm/cm** |
| **PSD1** | **1.8 nm** |
| **PSD2** | **1.1 nm** |
| **Roughness** | **4-10 Ang** |
| **Scratch/Dig[2]** | **20/10** |

### *Bulk*

| | |
|---|---|
| **Homogeniety** | **<5 ppm** |
| **Inclusions(>5um)** | **0** |
| **Lenslets** | **0** |

**[1] For typical $3\omega$ NIF optics; [2] Post-etch with number of scratches (width>8μm) <12-50**

# Typical steps of an optical fabrication process

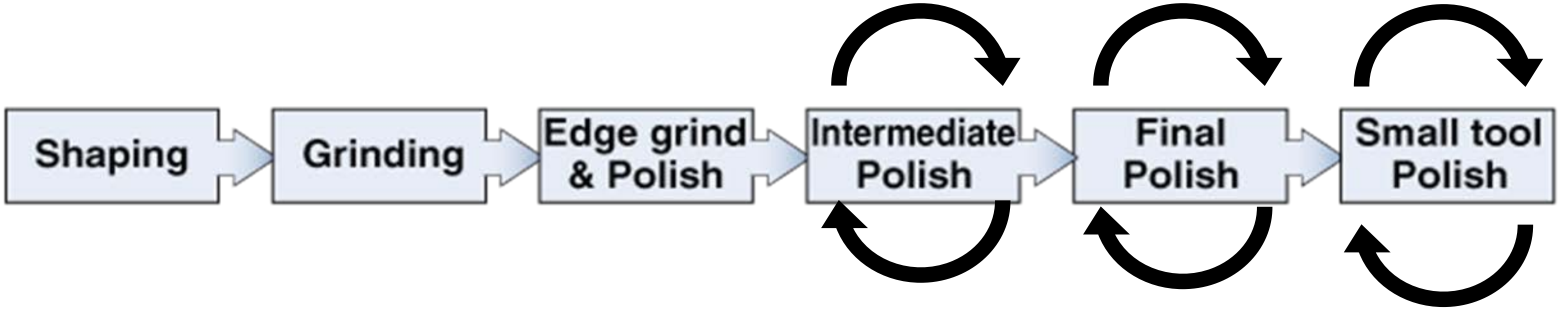

# Examples of grinding techniques

# Examples of polishing techniques

# The complexities of polishing has made is difficult to scientifically design, optimize a process for a given material

## Phenomena affecting Surface Quality

## Phenomena affecting Surface Figure

## Phenomena affecting Roughness

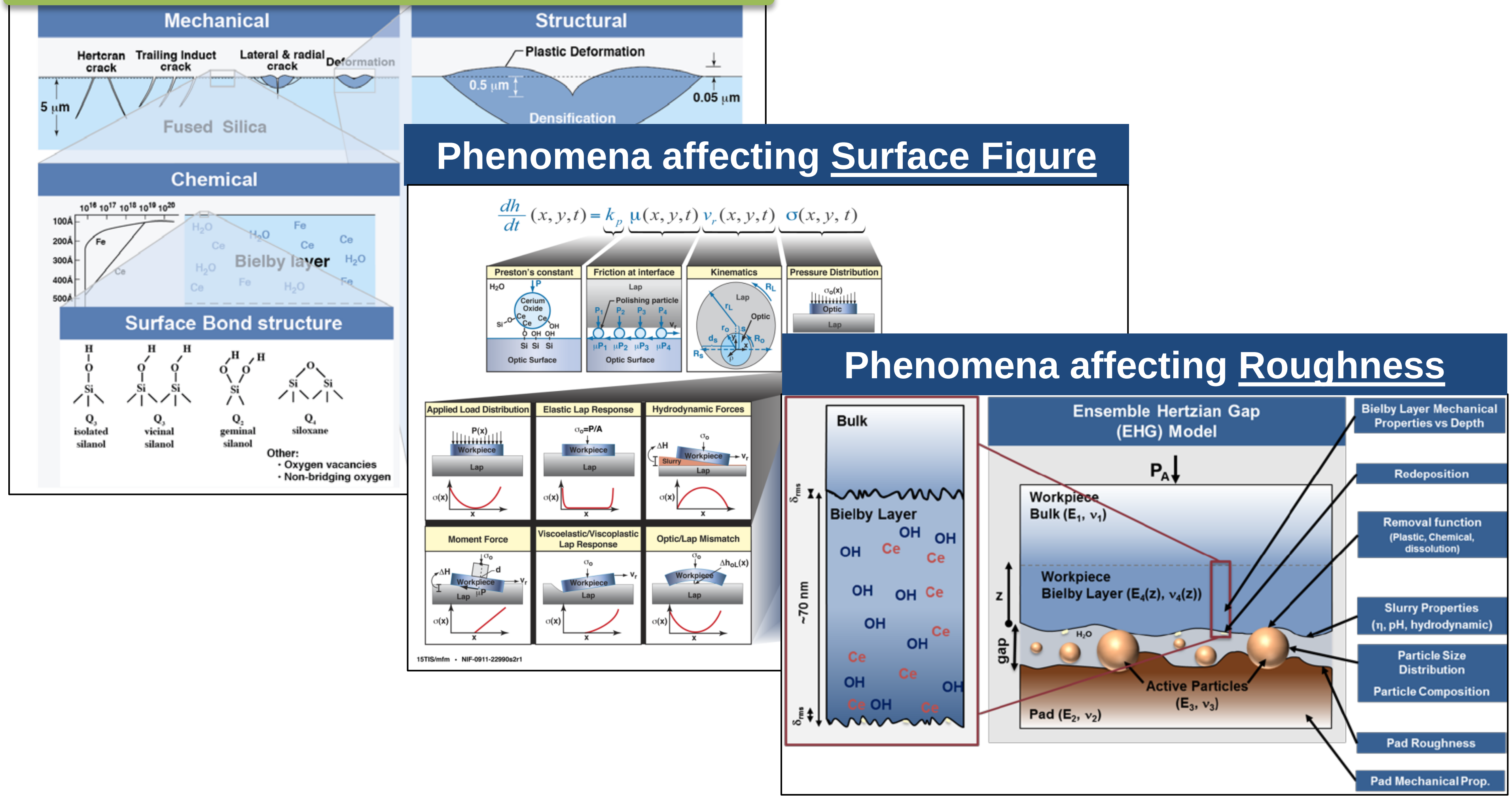

$$\frac{dh}{dt}(x,y,t) = \underbrace{k_p} \; \underbrace{\mu(x,y,t)} \; \underbrace{v_r(x,y,t)} \; \underbrace{\sigma(x,y,t)}$$

# There are numerous mechanical, structural and chemical effects on the glass surface during grinding and polishing

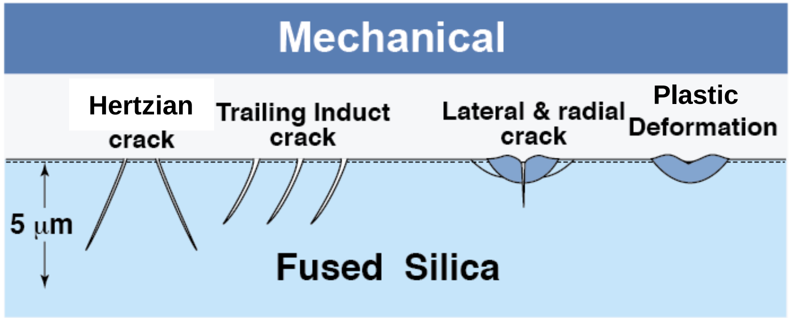

# There are numerous mechanical, structural and chemical effects on the glass surface during grinding and polishing

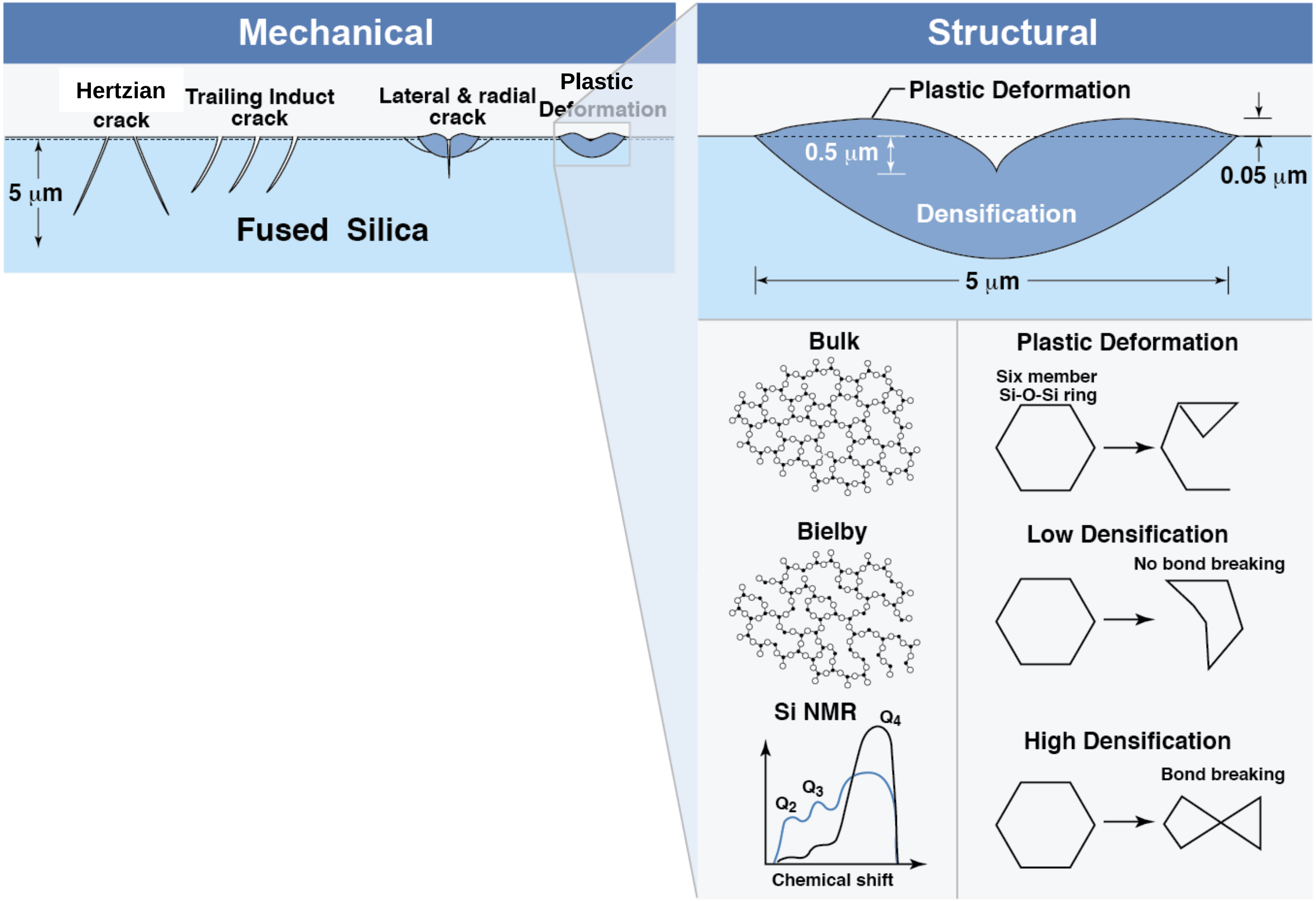

# There are numerous mechanical, structural and chemical effects on the glass surface during grinding and polishing

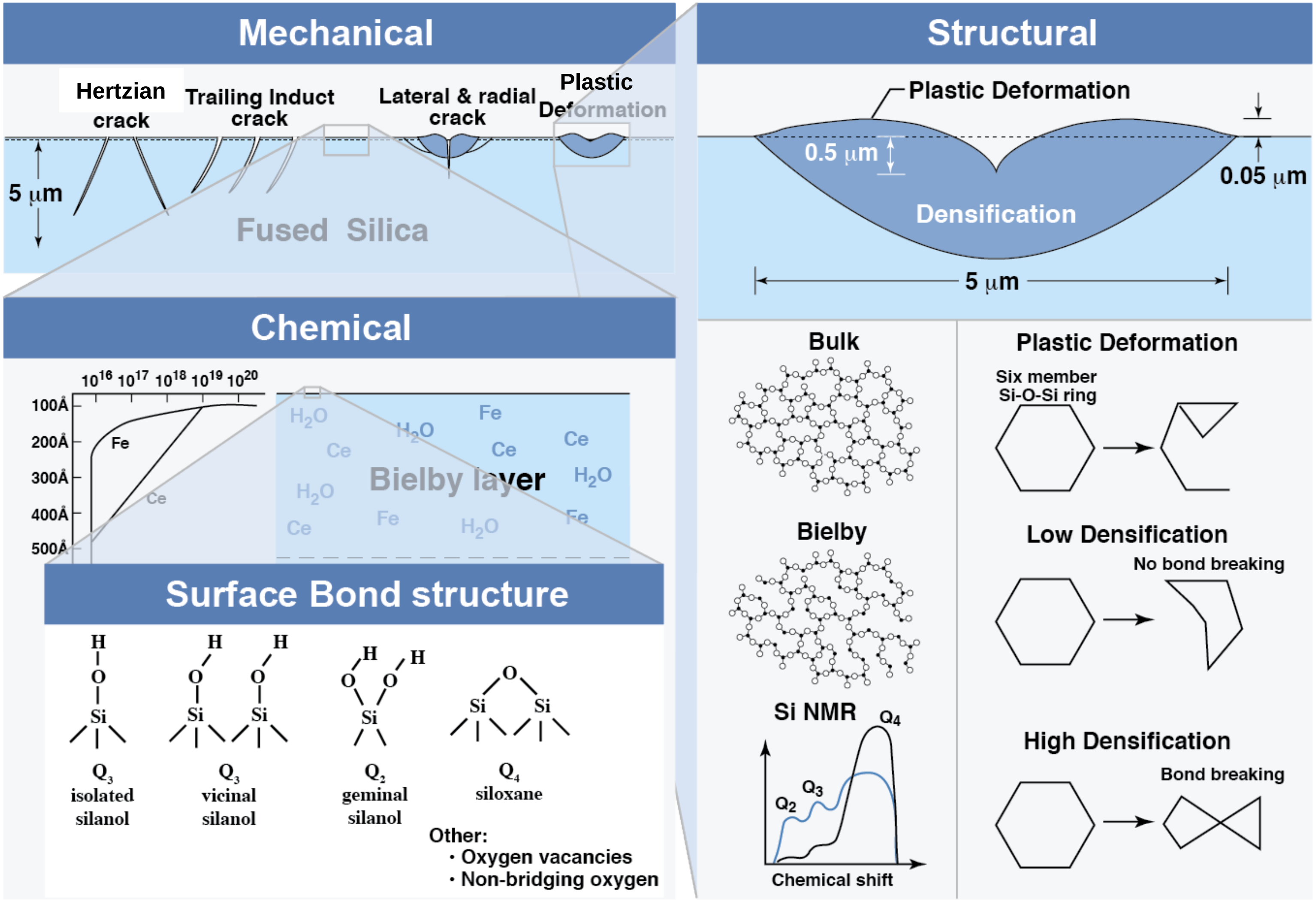

Other:
- Oxygen vacancies
- Non-bridging oxygen

# The load/particle determines the removal mechanism

### Brittle Removal
### Grinding or scratching

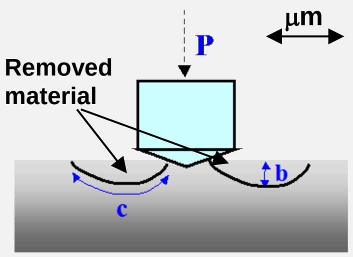

$P_{crit}$>0.1 N

- Material within lateral cracks are removed (grinding process)
- Leads to scratches

### Plastic Removal
### Ductile Polishing

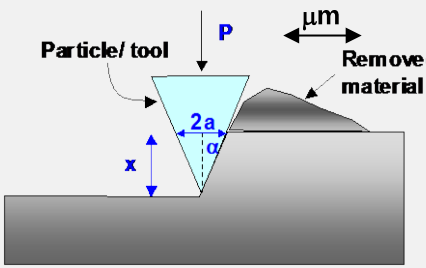

$P_{crit}$> 5x$10^{-5}$ N

- Portion of deformed material removed
- Leads to plastic scratches or sleeks
- Determined removal amount ~1 nm

### Chemical removal
### Chemical Polishing

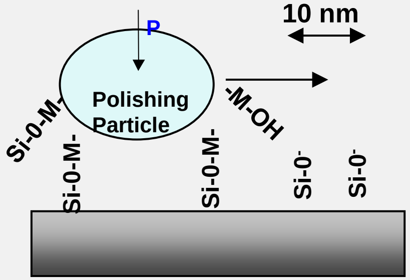

$P_{crit}$< 5x$10^{-5}$ N

- Removal at the molecular level ($Si(OH)_4$) by condensation & hydrolysis
- Creates smooth surface
- Determined removal amount ~0.04 nm

# Approach for the management of sub-surface fractures (i.e. scratches/digs)

**Schematic of material removal during various steps of the grinding/polishing process illustrating surface fracture removal**

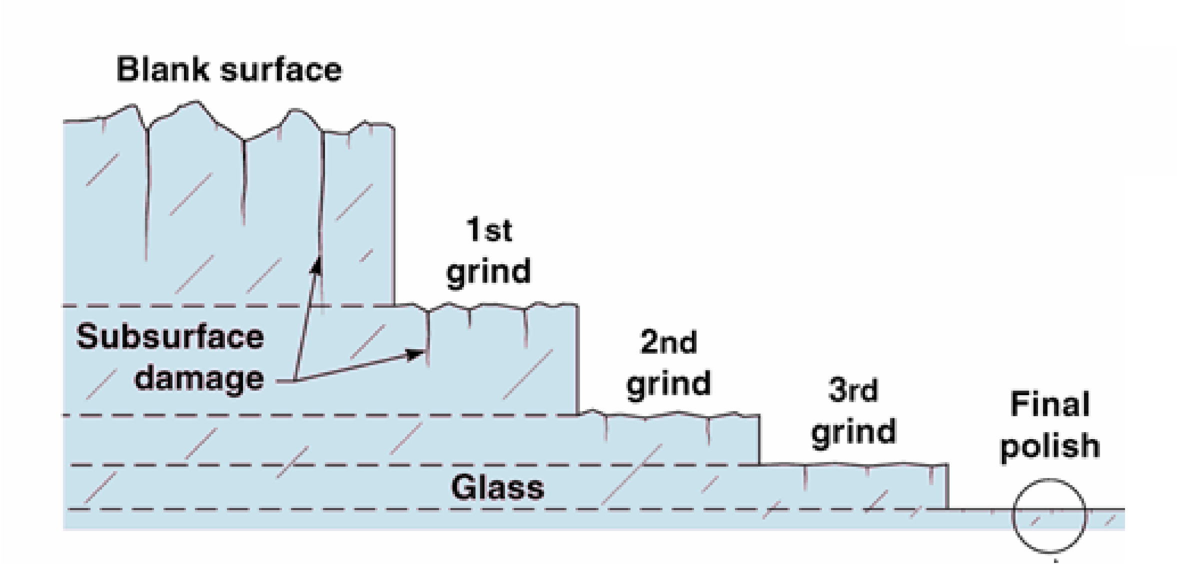

- Removal at each step is aimed at removal of deepest damage decreasing it to the level of deepest damage expected at current step (most economical design)
- Note each subsequent step has much lower removal rate
- This approach has been generally followed for hundreds of years

***Preston (1921), Aleinikov (1957), Edwards & Hed (1987), Brown (1980), Lambropoulos (1996)**

# There are five major areas of effort that have aided in managing sub-surface fractures

## GRINDING

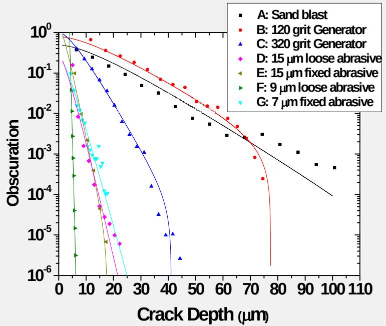

**1. Developed fracture mechanics understanding of sub-surface fracture distributions**

## POLISHING

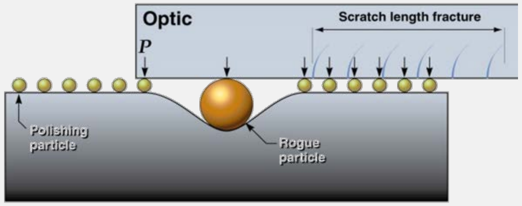

**2. Identified/characterized behavior of rogue particles causing sub-surface fractures**

## CHEMICAL ETCHING

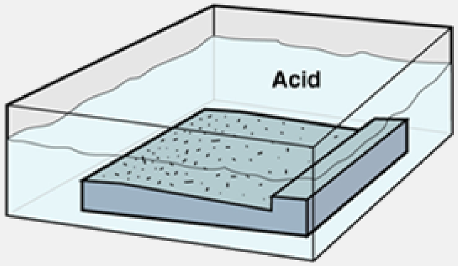

**3. Established techniques using etching to reveal and remove subsurface fractures**

## SCRATCH FORENSICS

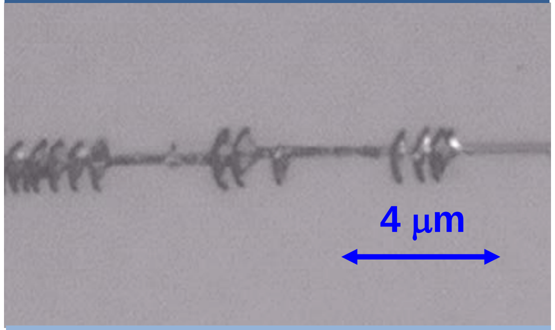

**4. Developed quantitative rules for post-diagnosis of cause of surface fractures**

## LASER DAMAGE

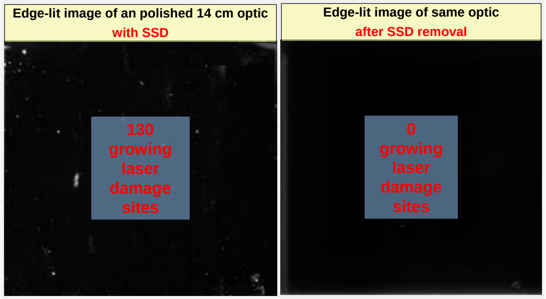
Edge-lit image of an polished 14 cm optic with SSD

Edge-lit image of same optic after SSD removal

**5. Showed link between sub-surface fracture removal & improved laser resistance**

# There are five major areas of effort that have aided in managing sub-surface fractures

## GRINDING

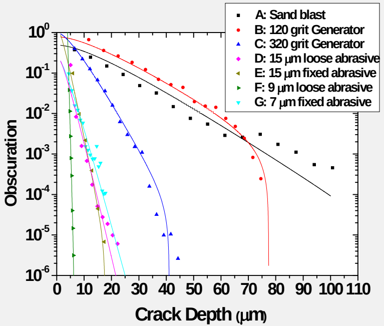

**1. Developed fracture mechanics understanding of sub-surface fracture distributions**

## POLISHING

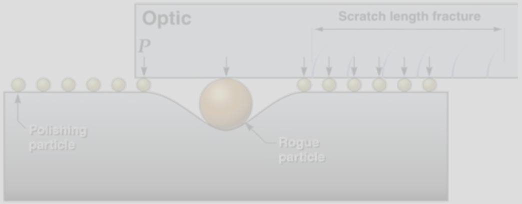

**2. Identified/characterized behavior of rogue particles causing sub-surface fractures**

## CHEMICAL ETCHING

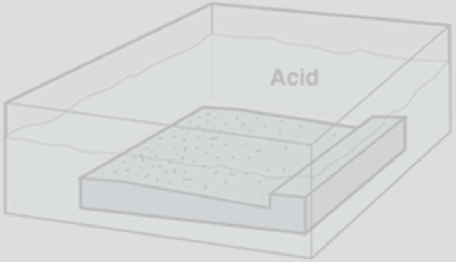

**3. Established techniques using etching to reveal and remove subsurface fractures**

## SCRATCH FORENSICS

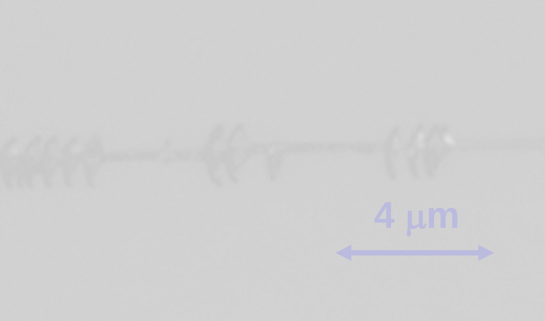

**4. Developed quantitative rules for post-diagnosis of cause of surface fractures**

## LASER DAMAGE


Edge-lit image of an polished 14 cm optic with SSD

Edge-lit image of same optic after SSD removal

**5. Showed link between sub-surface fracture removal & improved laser resistance**

# There are three basic types of cracks created by static brittle indentation

## Hertzian Cracks[1] (blunt)

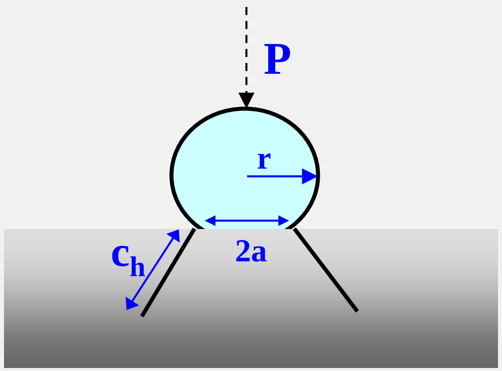

**Initiation**

$$P_c = A\,r$$

**Growth**

$$c_h = \left(\frac{\chi_h P}{K_{Ic}}\right)^{2/3}$$

**Leads to subsurface damage**

## Radial Cracks[1] (sharp)

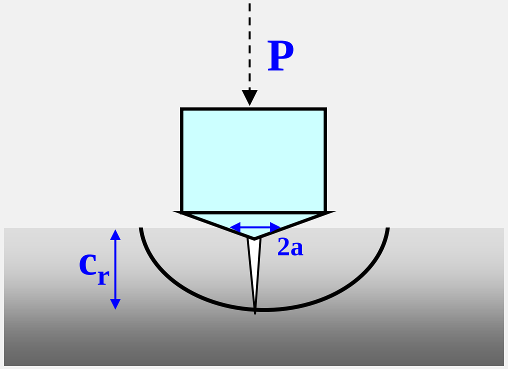

$$P_c = \alpha_r \frac{K_{Ic}^{\,4}}{H^3}$$

$$c_r = \left(\frac{\chi_r P}{K_{Ic}}\right)^{2/3}$$

**Leads to subsurface damage**

## Lateral Cracks[2] (sharp)

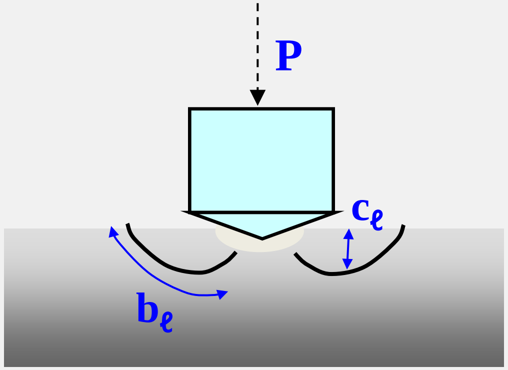

$$P_c = P_{c\ell}$$

$$b_\ell = \frac{\chi_\ell \left(\frac{E}{H}\right)^{3/5} P^{5/8}}{K_{Ic}^{\,1/2} H^{1/8}}$$

$$c_\ell = \frac{\chi_{\ell 2} \left(\frac{E}{H}\right)^{2/5} P^{1/2}}{H^{1/2}}$$

**Leads to material removal**

---

[1] B. Lawn, “Fracture of Brittle Materials” (1993)

[2] I. Hutchings “Tribology:Friction and Wear of Engineering Materials” (1992)

# The fracture initiation and growth constants need to be known to quantitatively use these relationships

| | Hertzian Cracks[1] (blunt) | Radial Cracks[1] (sharp) | Lateral Cracks[2] (sharp) |
|---|---|---|---|
| | 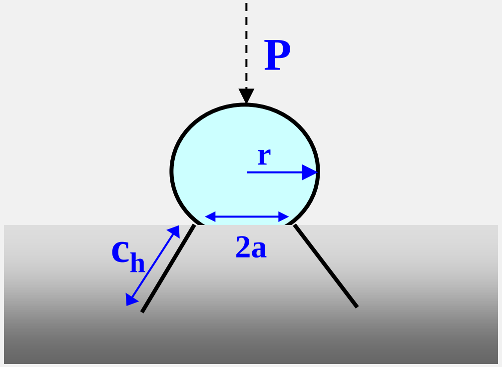 | 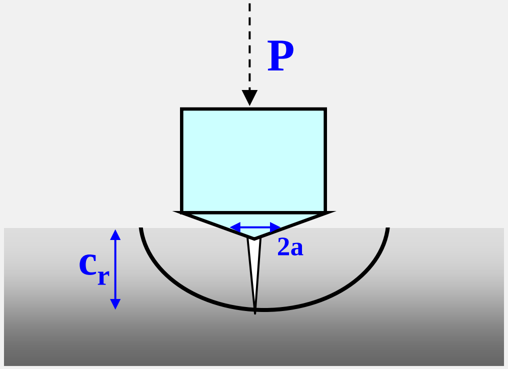 | 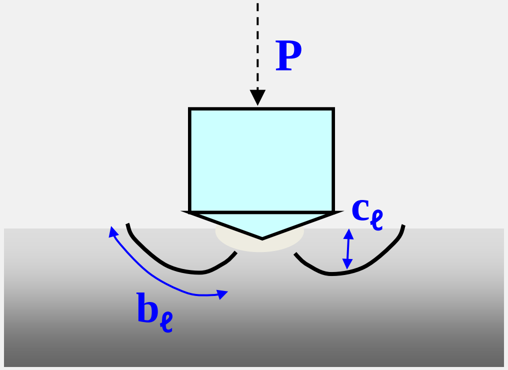 |
| **Initiation** | $P_c = A r$ | $P_c = \alpha_r \dfrac{K_{Ic}^{\,4}}{H^3}$ | $P_c = P_{c\ell}$ |
| **Growth** | $c_h = \left(\dfrac{\chi_h P}{K_{Ic}}\right)^{2/3}$ | $c_r = \left(\dfrac{\chi_r P}{K_{Ic}}\right)^{2/3}$ | $b_\ell = \dfrac{\chi_\ell \left(\dfrac{E}{H}\right)^{3/5} P^{5/8}}{K_{Ic}^{\,1/2} H^{1/8}}$ <br> $c_\ell = \dfrac{\chi_{\ell 2} \left(\dfrac{E}{H}\right)^{2/5} P^{1/2}}{H^{1/2}}$ |
| | **Leads to subsurface damage** | **Leads to subsurface damage** | **Leads to material removal** |

[1] B. Lawn, "Fracture of Brittle Materials" (1993)

[2] I. Hutchings "Tribology:Friction and Wear of Engineering Materials" (1992)

# Friction strongly influences fracture initiation for a sliding particle indentation (i.e. scratching)

## Static Sphere[1]

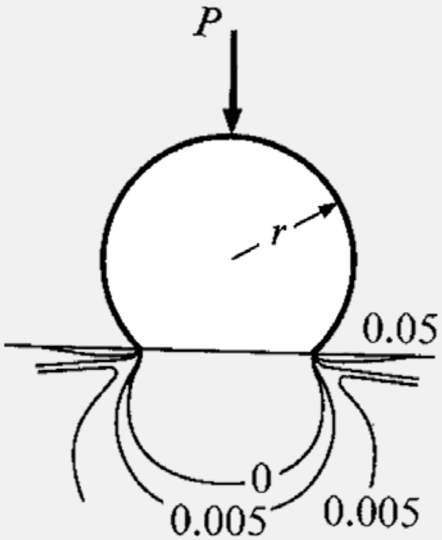

**Initiation**

$$P_c = A\,r$$

**Growth**

$$P = \frac{K_{Ic}}{\chi_h} c^{3/2}$$

## Sliding Sphere[1,2]

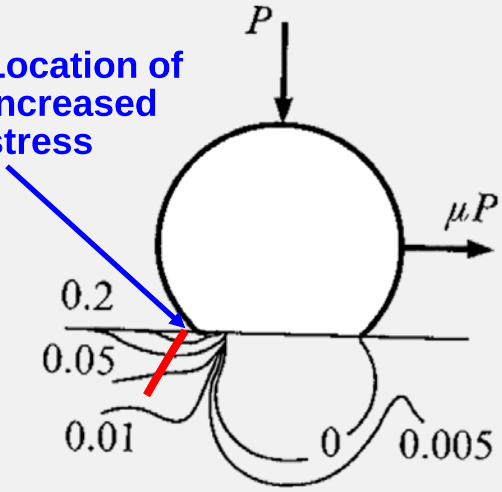

Location of increased stress

$$P_c = \frac{C\,r^2}{(1+B\mu)^3}$$

$$P = \frac{K_{Ic}}{\chi_h (1+\mu^2)^2} c^{3/2}$$

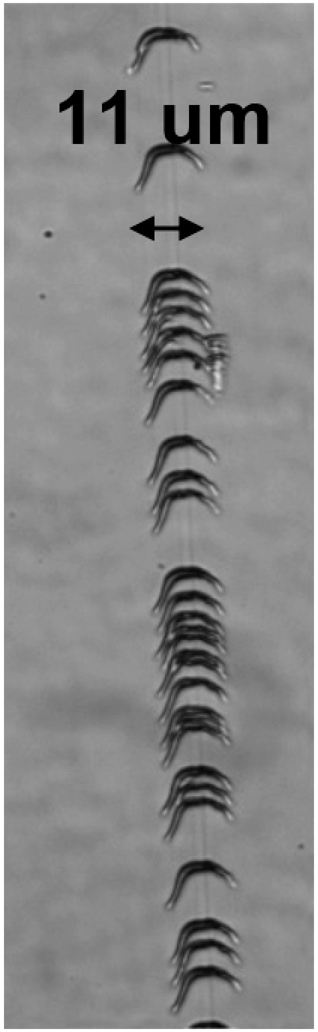

[1] Lawn, Fracture of Brittle Solids (1993)
[2] Lawn, Indentation Fracture: Principles and Applications (1975)

# The effect of load on the fracture behavior of scratches has been measured

**Schematic description of fractures associated with a scratch**

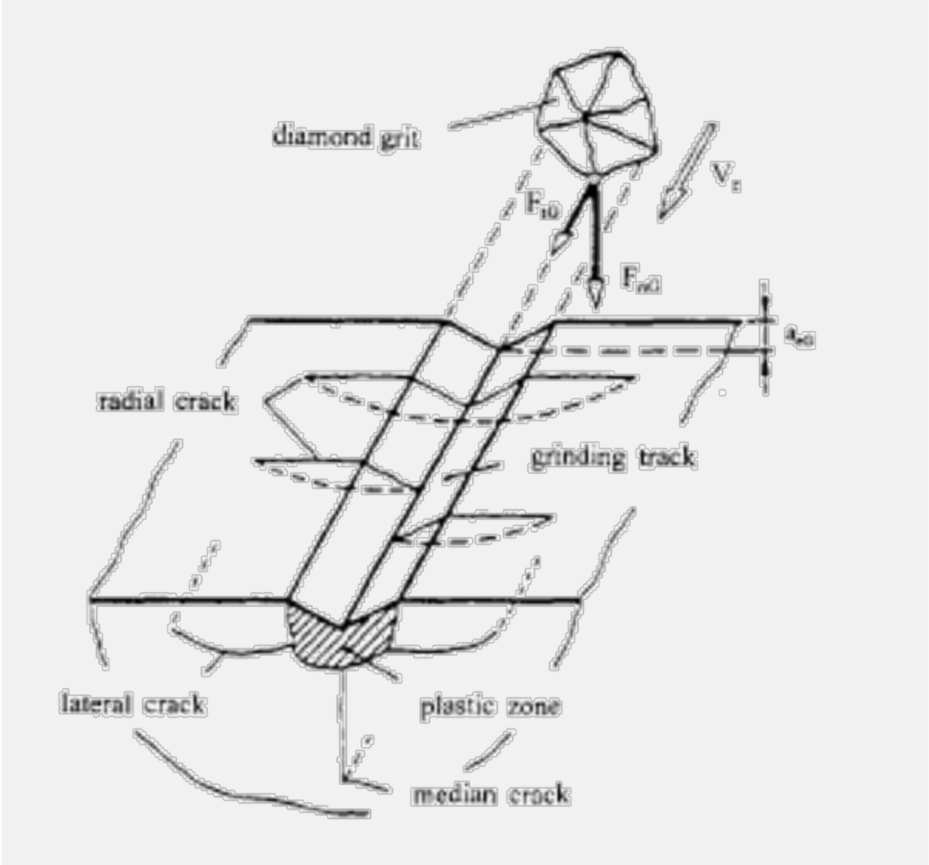

- **At low loads (P<0.1 N),** no cracking is observed just a ductile track
- **At intermediate loads (0.1 N< P < 5 N),** well defined median and lateral cracks form
- **At high loads (P> 5N),** the plastically observed track appears to shatter and the median and lateral crack are not as extending as in the higher end of the intermediate loads

**Refs:** Review: K. Li, Journal of Materials Processing Technology 57 (1996) 206
Review:M. Swain, Proc. R. Soc. London A, 366 (1979) 575

# A wedge or taper polishing* technique was developed to directly measure the SSD distribution

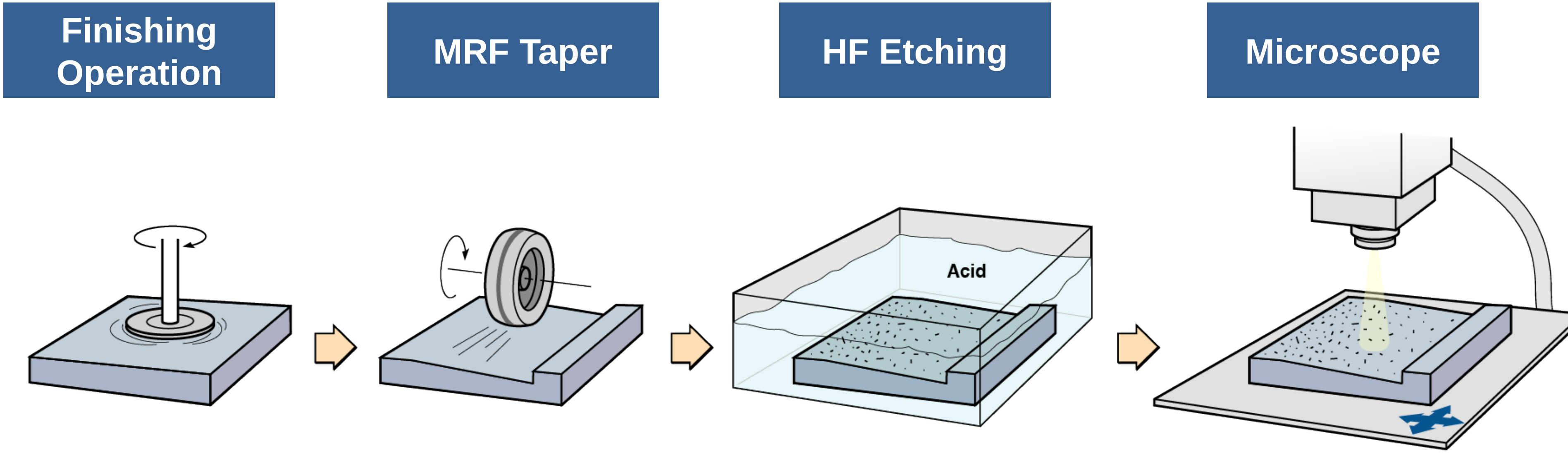

***J. Menapace, SPIE 2005, Boulder Damage Symposium; Based on tapering technique used by Hed & Edwards (1987)**

# GRINDING

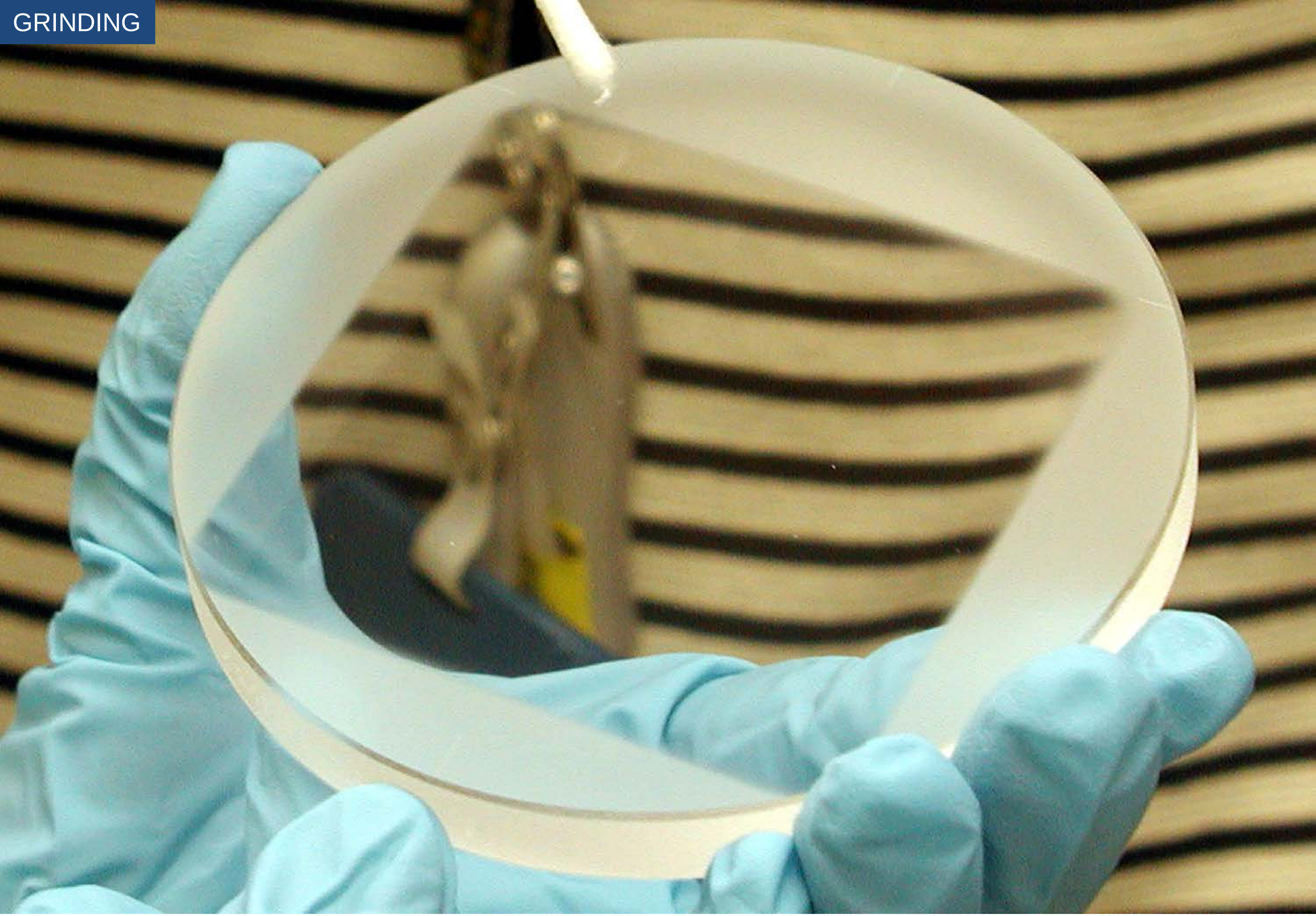

# The SSD depth distribution has been measured for a series of standard grinding processes

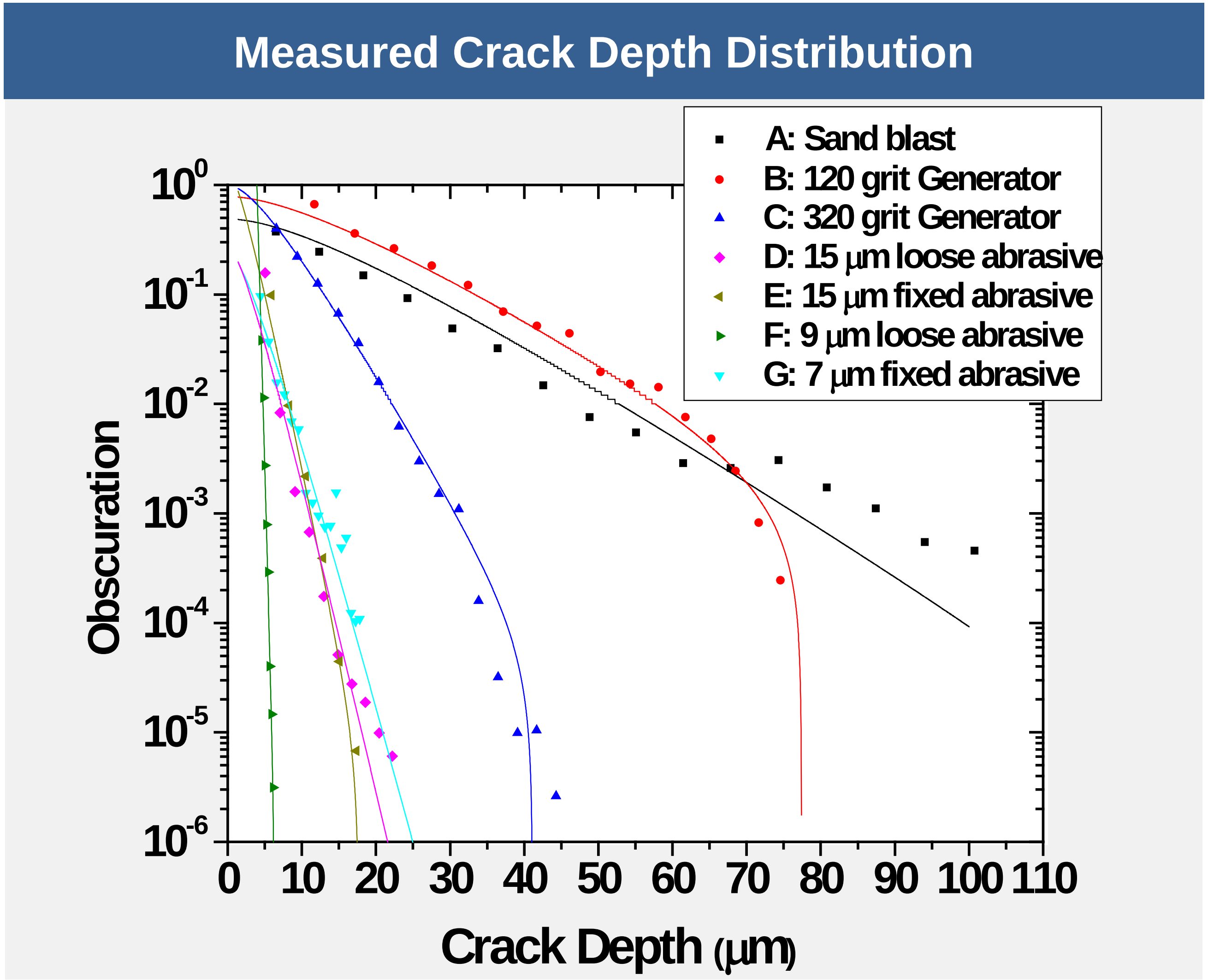

T. Suratwala, JNCS 352 (2006) 5601

# Coarse Generator Grind (120 grit) (Sample B)

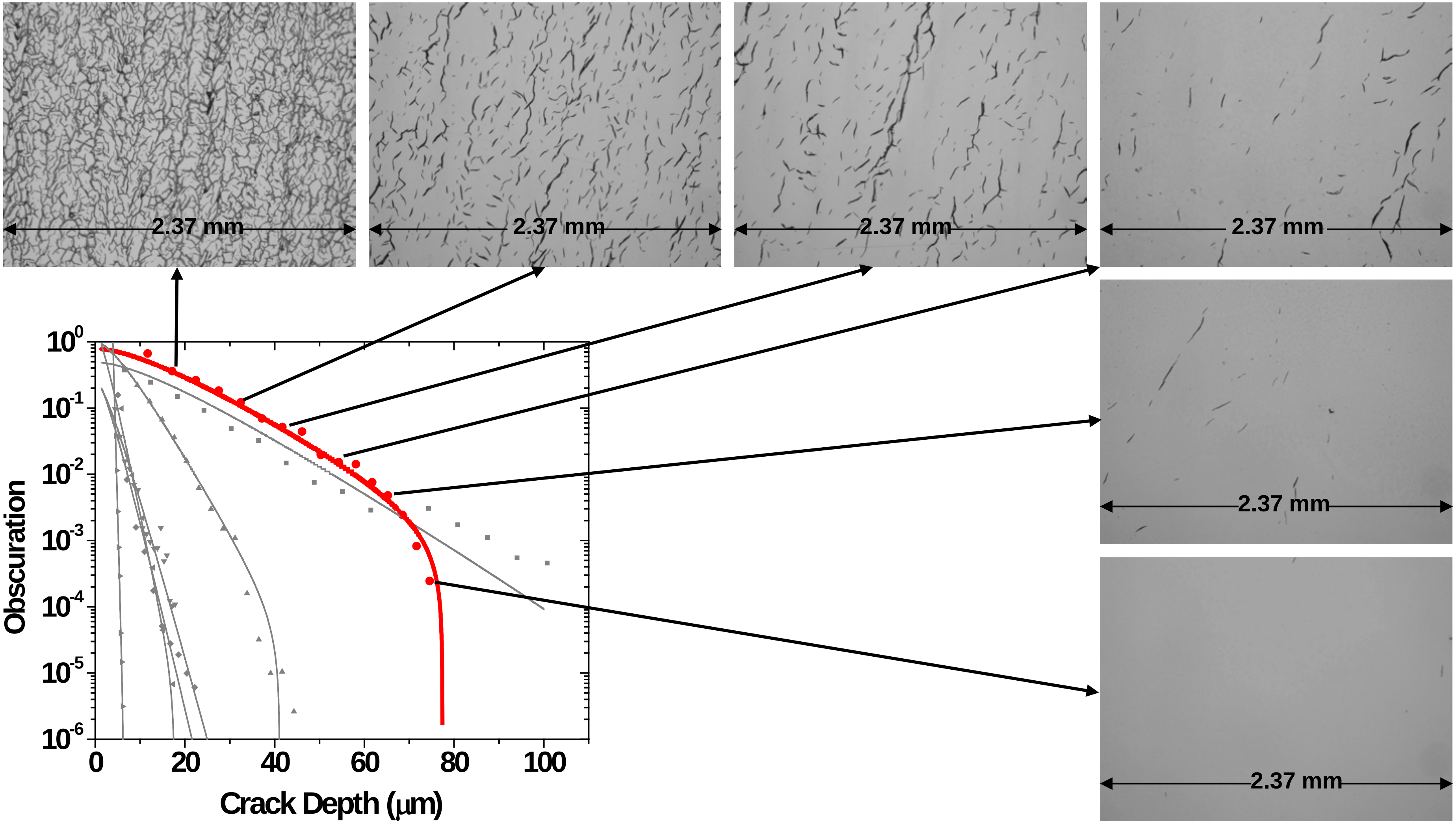

T. Suratwala, JNCS 352 (2006) 5601

# Microscope images of the fractures show a unique size character for each grinding step

**Sand blasted**

**120 Grit (125 μm)**

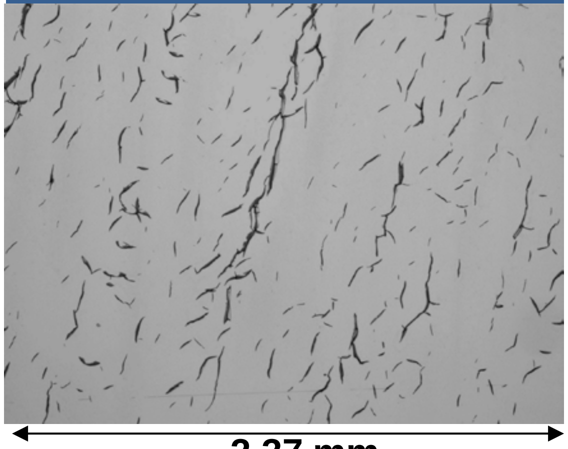

**150 Grit (100 μm)**

**15 μm loose abrasive**

**15 μm fixed abrasive**

**9 μm loose abrasive**

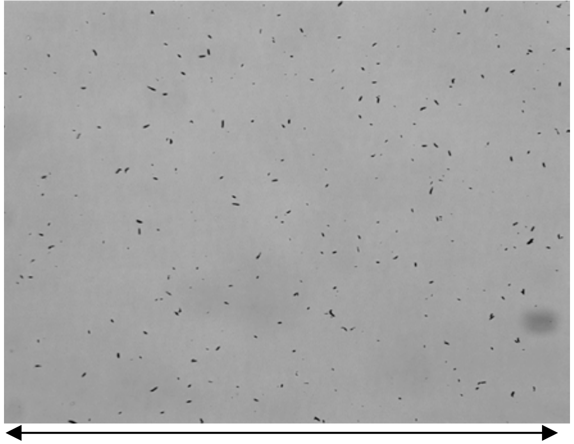

T. Suratwala, JNCS 352 (2006) 5601

# Microscope images of the fractures show a unique size character for each grinding step

**Sand blasted**

**120 Grit (125 μm)**

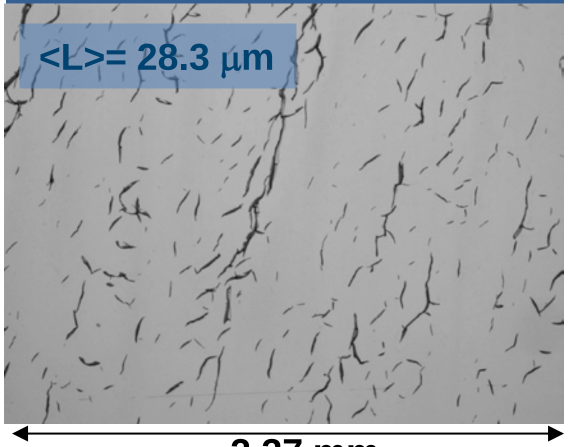

**150 Grit (100 μm)**

**15 μm loose abrasive**

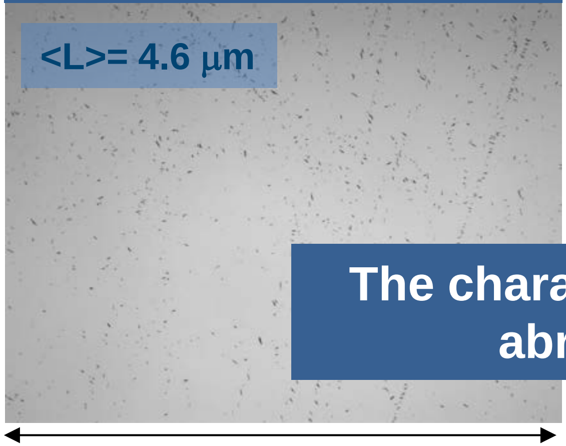

**15 μm fixed abrasive**

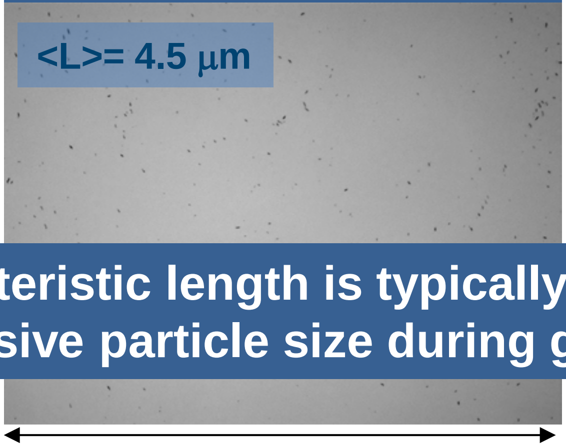

**9 μm loose abrasive**

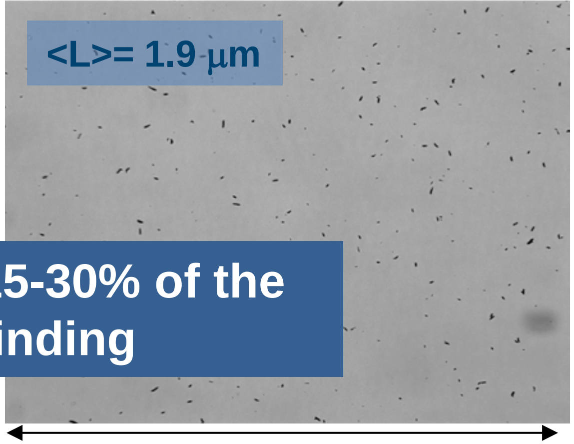

**The characteristic length is typically 15-30% of the abrasive particle size during grinding**

T. Suratwala, JNCS 352 (2006) 5601

# A brittle fracture model has been successfully used to explain the observed distribution of crack depth and lengths

## Schematic of Model*

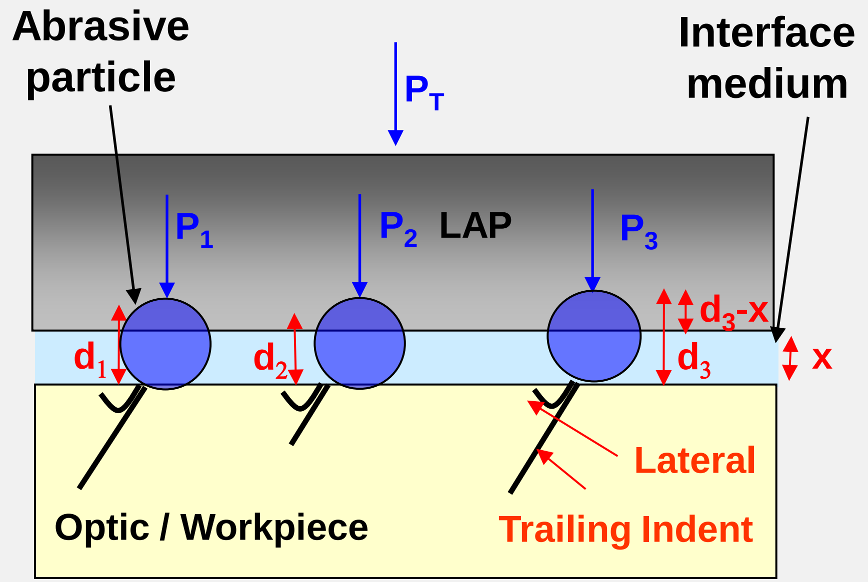

$$P_T = \Sigma P_i \qquad P_i \propto (d_i\text{-}x) \propto d_i$$

**Key assumption:** The load on particle is proportional to its vertical dimension

*T. Suratwala, JNCS 352 (2006) 5601.
*P. Miller, SPIE 5991 (2006).

# We recommend using the '90' rule for material removal ($c_{90}$=0.9<L>) for isolated SSD observed on polished parts

## Measured mean crack length vs SSD depth

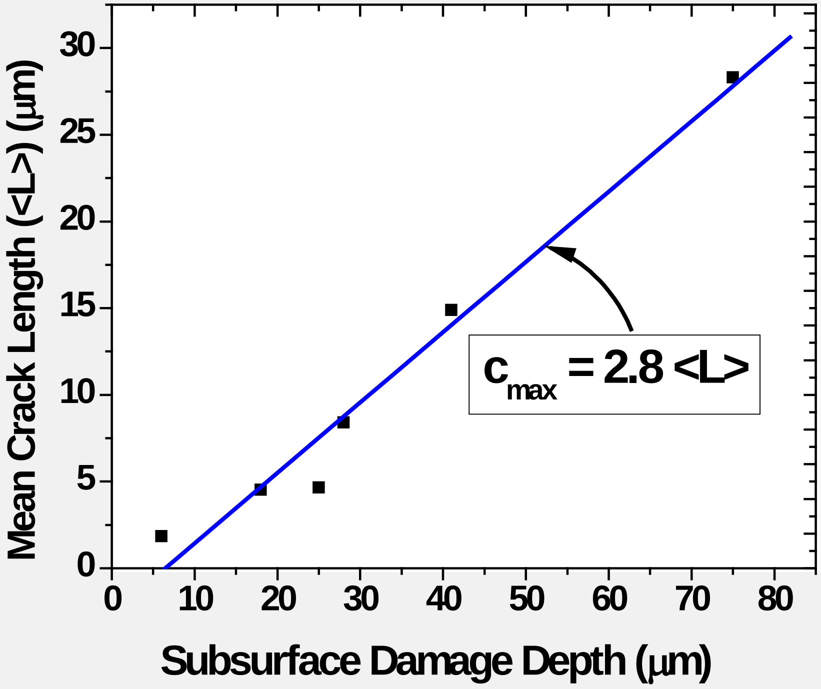

$$c_{\max} = 2.8 < L >$$

## Probability of finding a crack of depth c for a given crack length

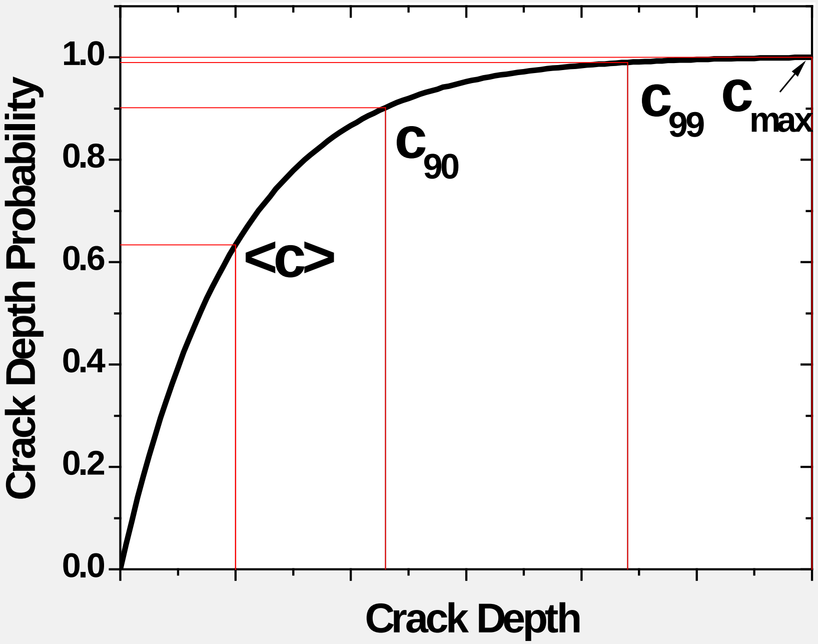

$$c_{90} = 0.9 < L >$$

T. Suratwala, JNCS 352 (2006) 5601

# The addition of a small amount of 15 μm particles in a 9 μm slurry results in a significant increase in SSD

## Particle size distributions of the alumina particles used

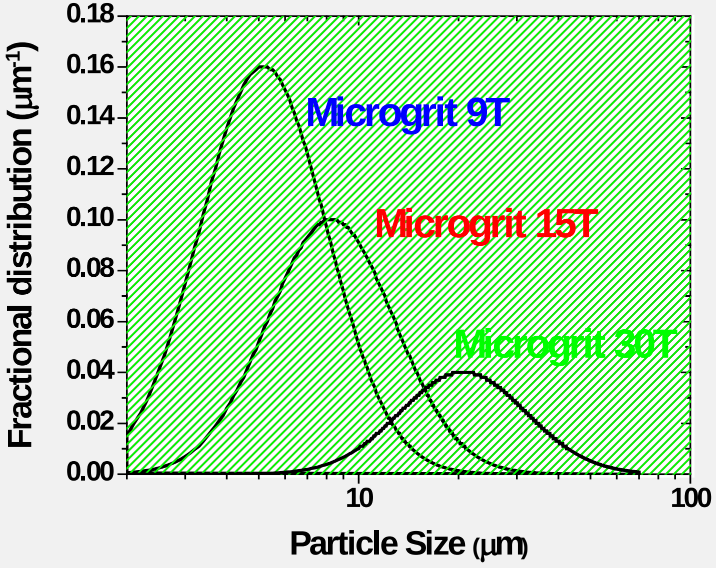

## Crack depth distributions: Loose abrasive grinding with addition of rogue particles

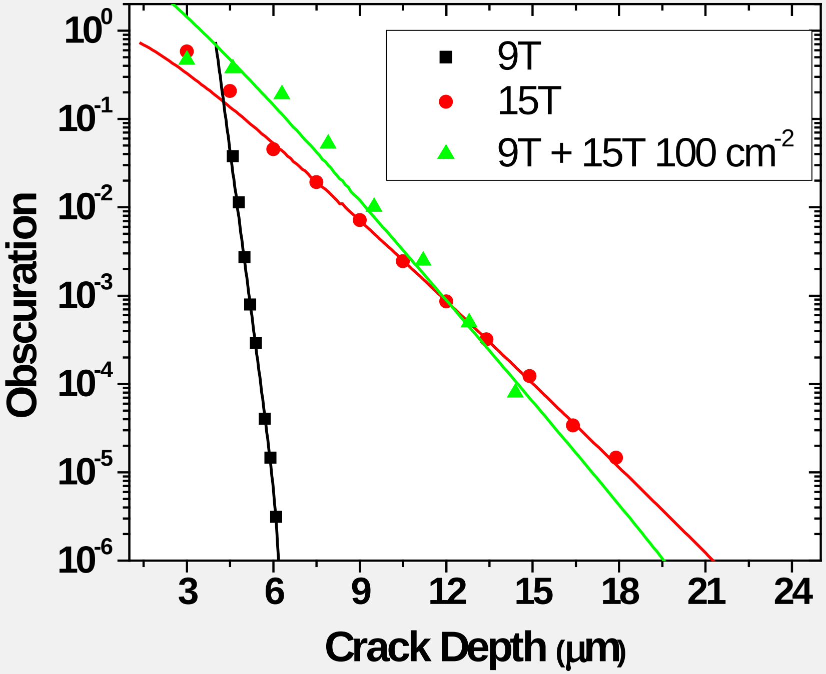

T. Suratwala, JNCS 354 (2006) 2023

# The loaded particles are the largest particles in the abrasive particle distribution

**Abrasive size distribution for 9 µm loose abrasive**

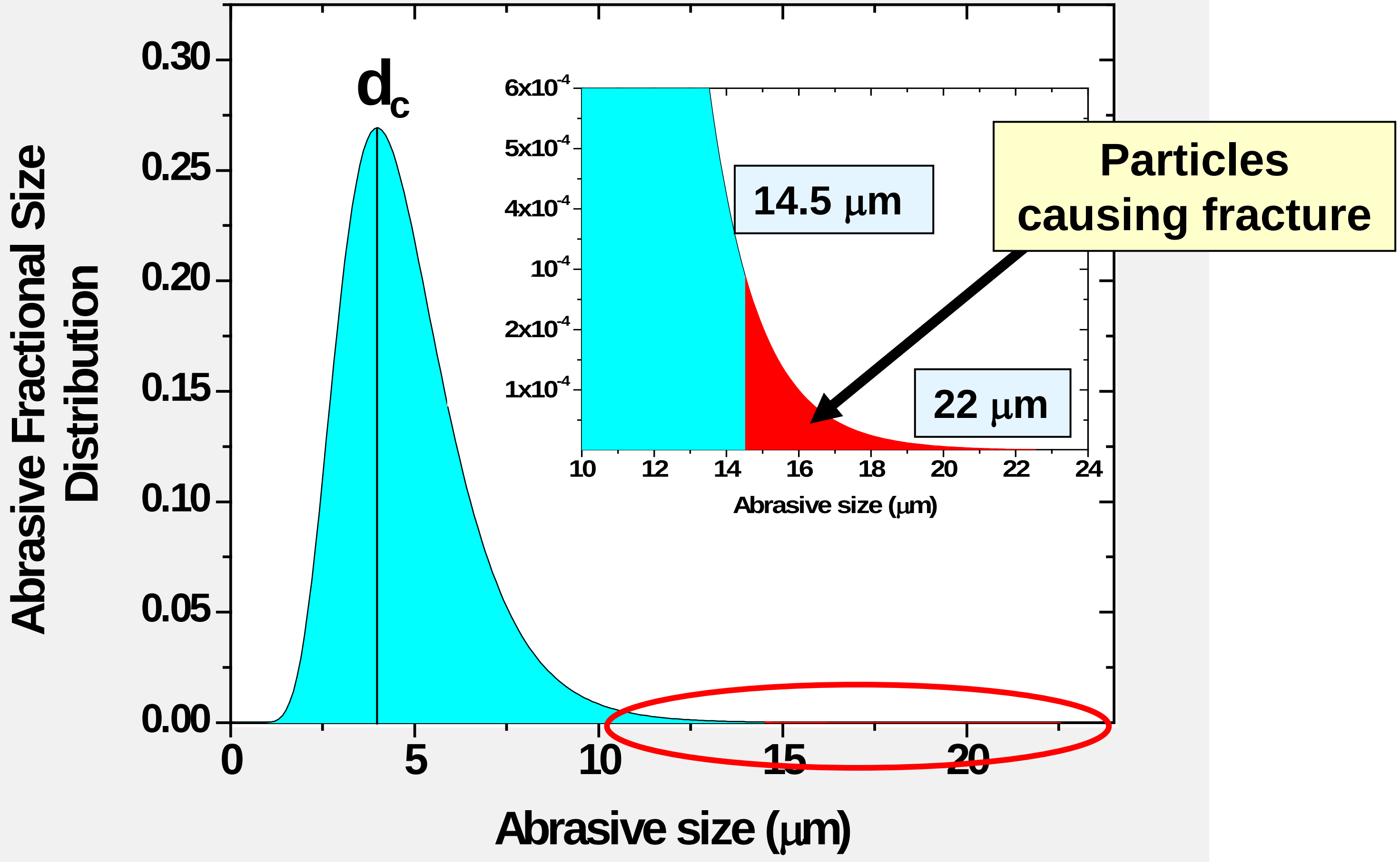

**Particles causing fracture**

T. Suratwala, JNCS 354 (2006) 2023

# There are five major areas of effort that have aided in managing sub-surface fractures

## GRINDING

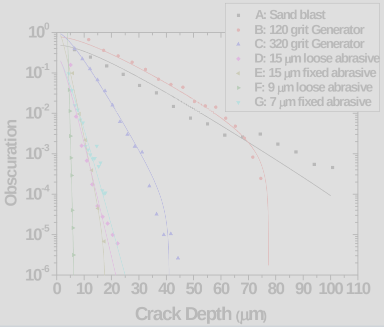

1. Developed fracture mechanics understanding of sub-surface fracture distributions

## POLISHING

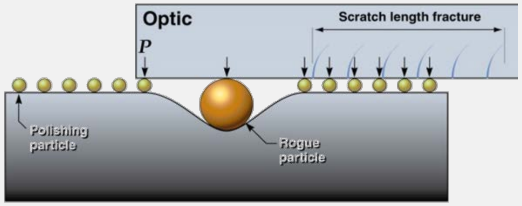

**2. Identified/characterized behavior of rogue particles causing sub-surface fractures**

## CHEMICAL ETCHING

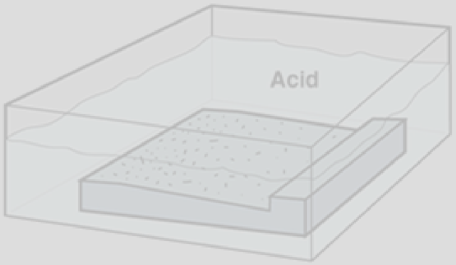

3. Established techniques using etching to reveal and remove subsurface fractures

## SCRATCH FORENSICS

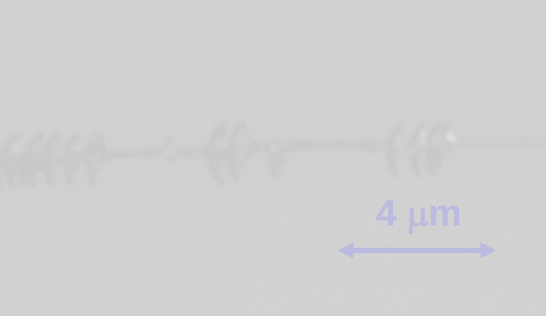

4. Developed quantitative rules for post-diagnosis of cause of surface fractures

## LASER DAMAGE

5. Showed link between sub-surface fracture removal & improved laser resistance

# Rogue particles of diamond were added to a ceria slurry during polishing at various sizes & concentrations

**Particle size distributions of ceria and rogue diamonds**

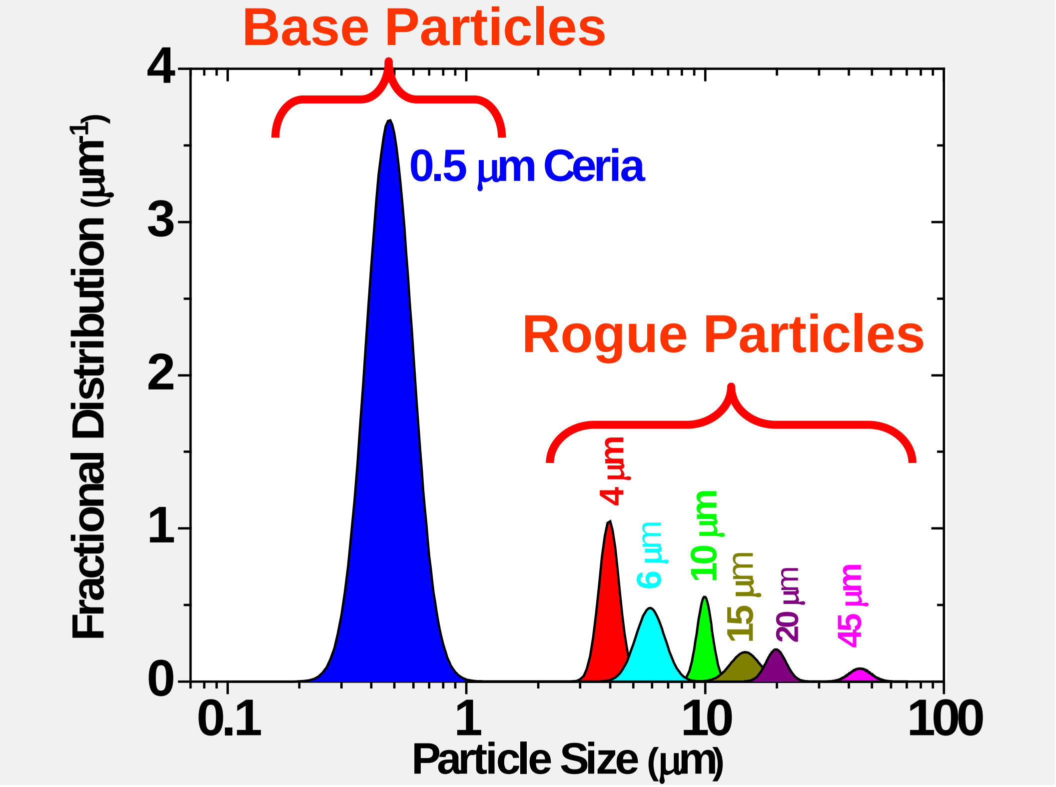

T. Suratwala, JNCS 354 (2006) 2023

# Rogue particles can cause multiple types of scratches

## Plastic
## Abrasive Wear

**Sleek**

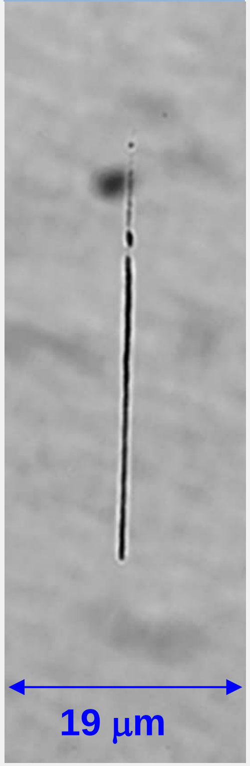

## Mixed
## Brittle fracture / Plastic Abrasive Wear

**Sleek + lateral fracture**

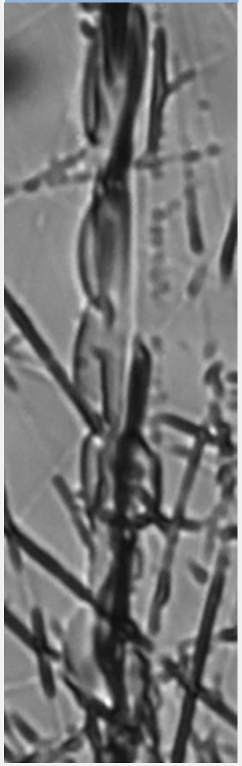

**Sleek + trailing indent fracture**

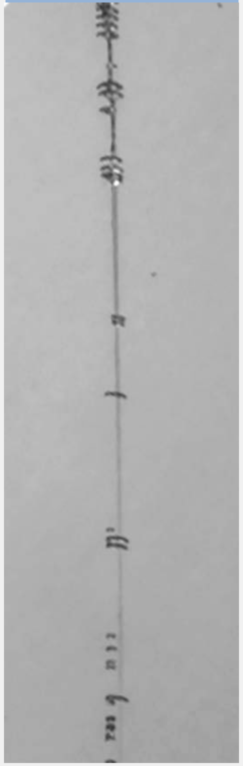

**Sleek + trailing indent + lateral fracture**

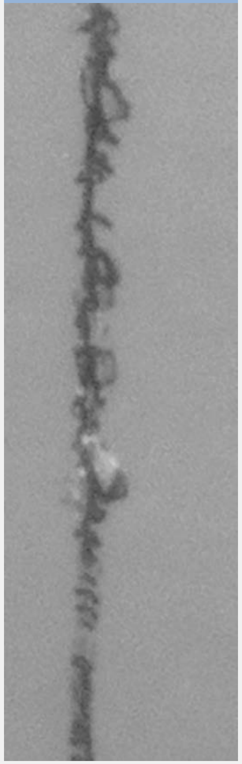

## Brittle
## Fracture

**Trailing indent fracture**

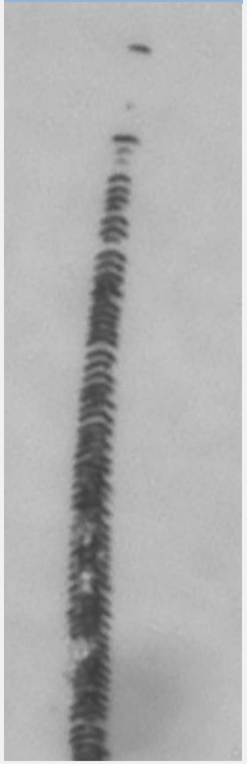

**Trailing indent + lateral fracture**

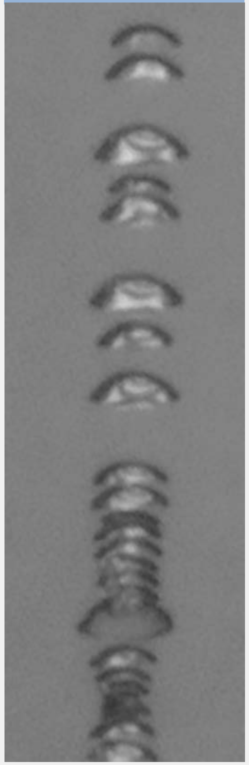

# The scratch length increases with rogue particle size

## Cumulative scratch length distribution

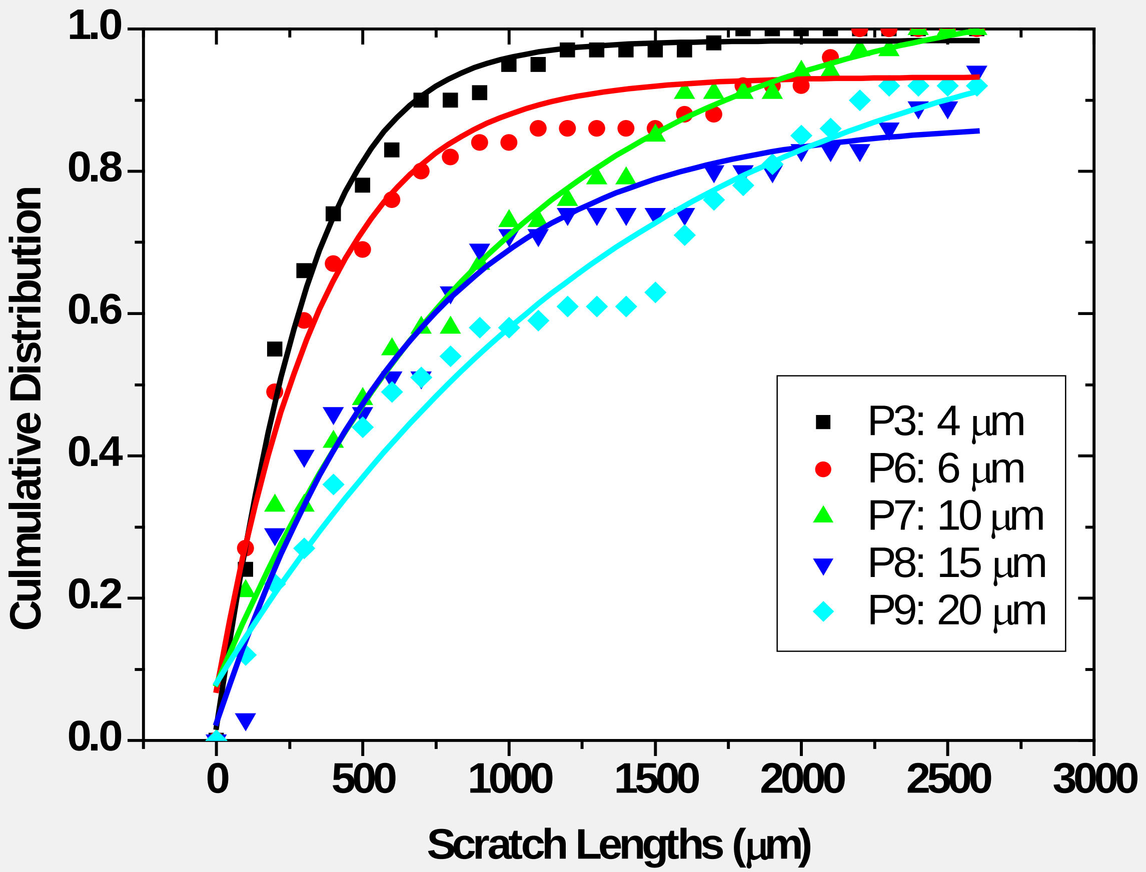

T. Suratwala, JNCS 354 (2006) 2023

# The observed scratch lengths can be explained by the viscoelastic penetration of a rogue particle

$$L_{scratch} = 8.9\,\frac{\nu_{ave}\,\eta\, R^2}{P}$$

$t = t_0$

$P_1$ = *Load on rogue particle*

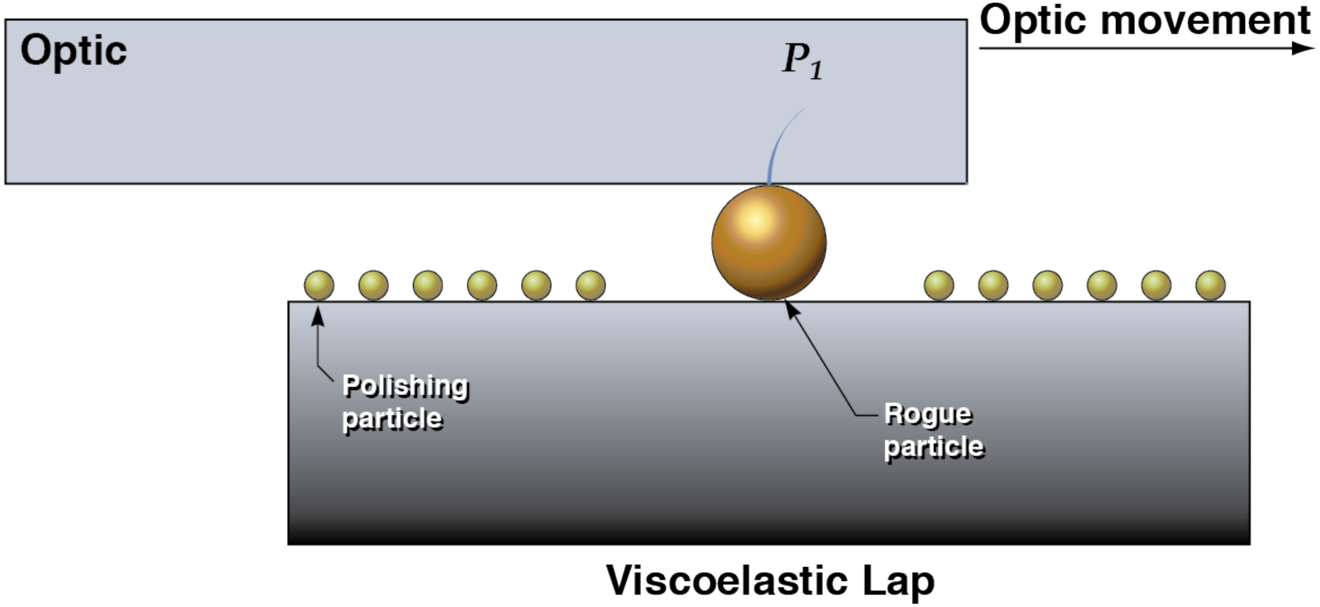

**This behavior has been modeled using hard sphere penetration into a linear viscoelastic lap at large penetration**

T. Suratwala, JNCS 354 (2006) 2023

# The observed scratch lengths can be explained by the viscoelastic penetration of a rogue particle

$$L_{scratch} = 8.9\,\frac{\nu_{ave}\,\eta\,R^2}{P}$$

$t = t_1$

$P_1 = Load\ on\ rogue\ particle$

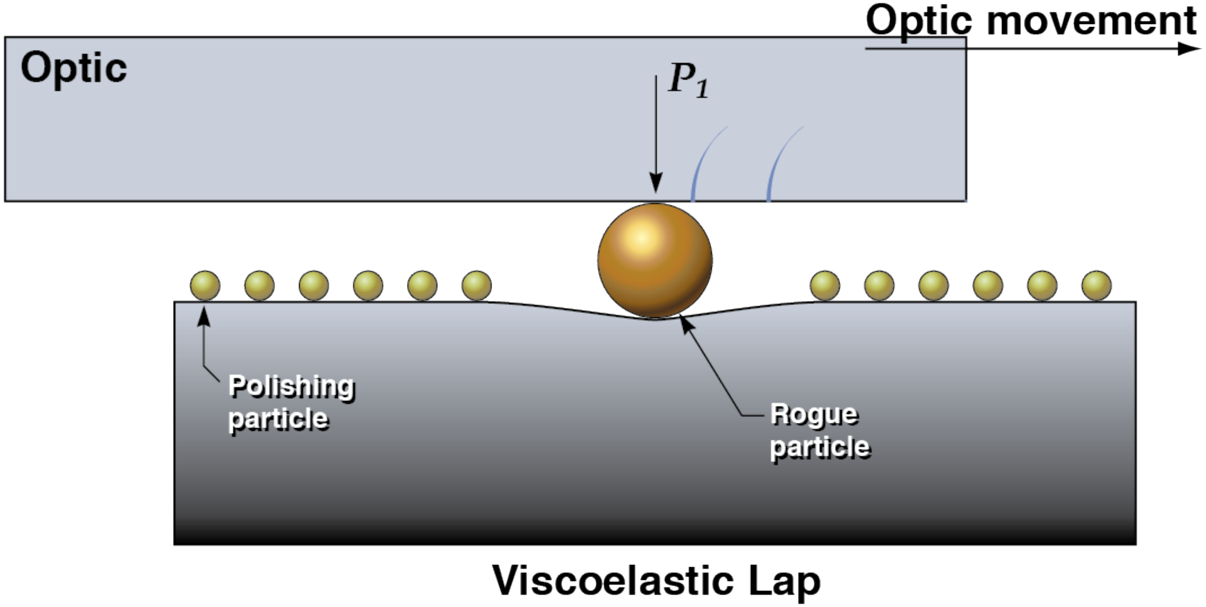

**This behavior has been modeled using hard sphere penetration into a linear viscoelastic lap at large penetration**

T. Suratwala, JNCS 354 (2006) 2023

# The observed scratch lengths can be explained by the viscoelastic penetration of a rogue particle

$$L_{scratch} = 8.9\,\frac{\nu_{ave}\,\eta\, R^2}{P}$$

$t = t_2$

$P_1 = Load\ on\ rogue\ particle$

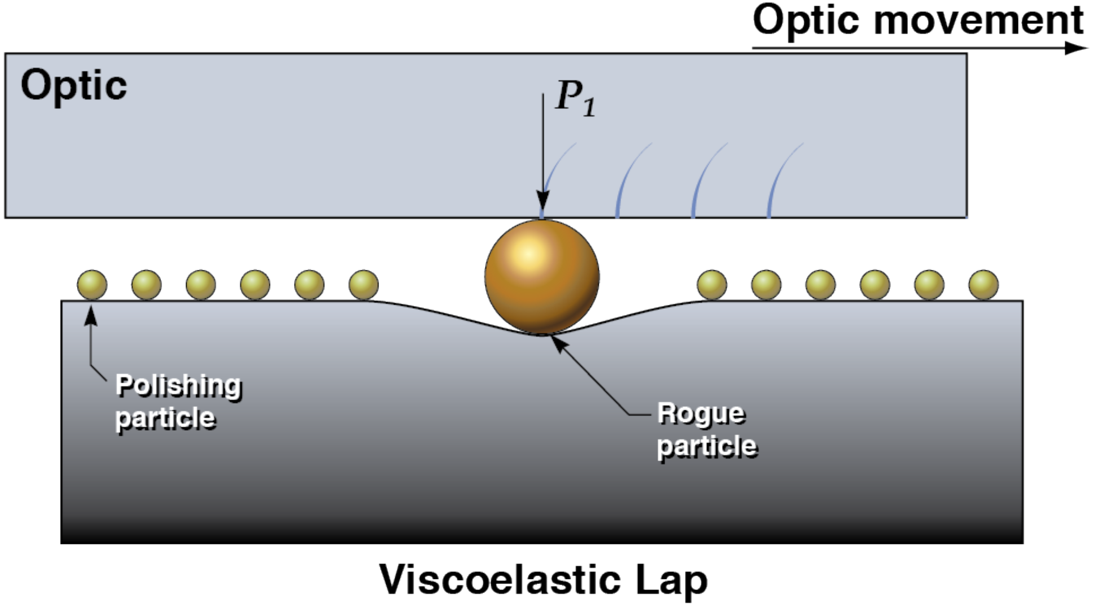

**This behavior has been modeled using hard sphere penetration into a linear viscoelastic lap at large penetration**

T. Suratwala, JNCS 354 (2006) 2023

# The observed scratch lengths can be explained by the viscoelastic penetration of a rogue particle

$$L_{scratch} = 8.9 \frac{\nu_{ave} \eta R^2}{P}$$

$t = t_3$

$P_1 = Load\ on\ rogue\ particle$

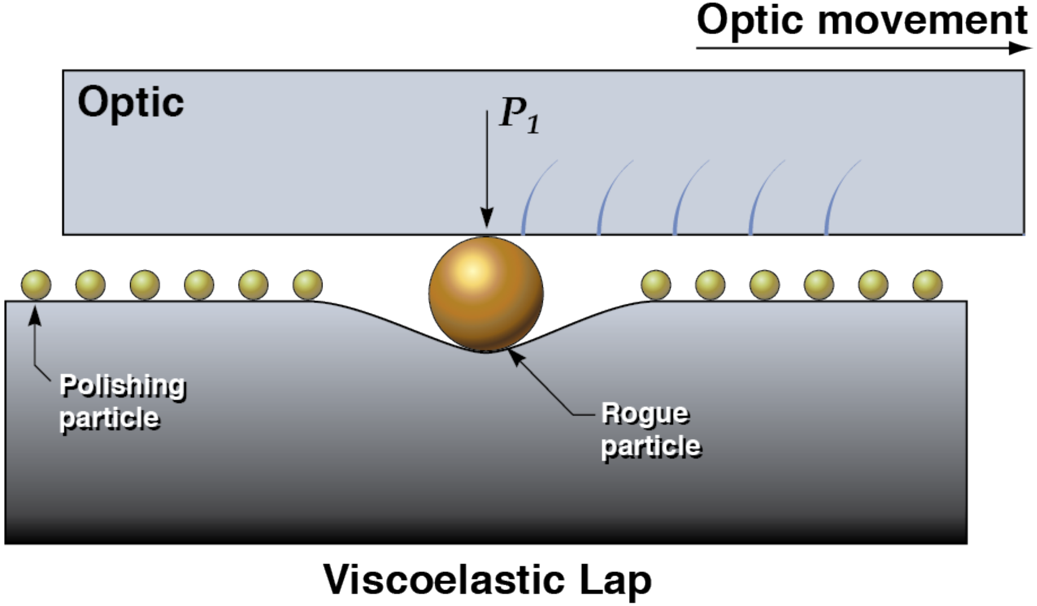

**This behavior has been modeled using hard sphere penetration into a linear viscoelastic lap at large penetration**

T. Suratwala, JNCS 354 (2006) 2023

# The observed scratch lengths can be explained by the viscoelastic penetration of a rogue particle

$$L_{scratch} = 8.9\frac{v_{ave}\eta R^2}{P}$$

$t = t_4$

$P_1 = Load\ on\ rogue\ particle$

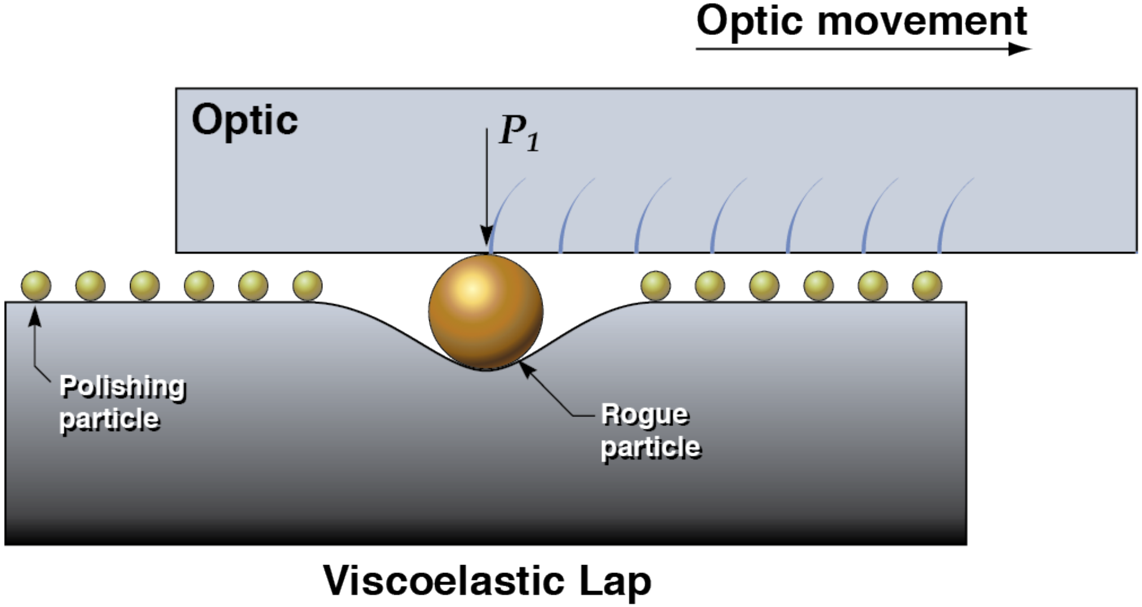

**This behavior has been modeled using hard sphere penetration into a linear viscoelastic lap at large penetration**

T. Suratwala, JNCS 354 (2006) 2023

# The observed scratch lengths can be explained by the viscoelastic penetration of a rogue particle

$$L_{scratch} = 8.9\,\frac{\nu_{ave}\,\eta\,R^2}{P}$$

$t = t_5$
$P = Load\ on\ all\ particles$

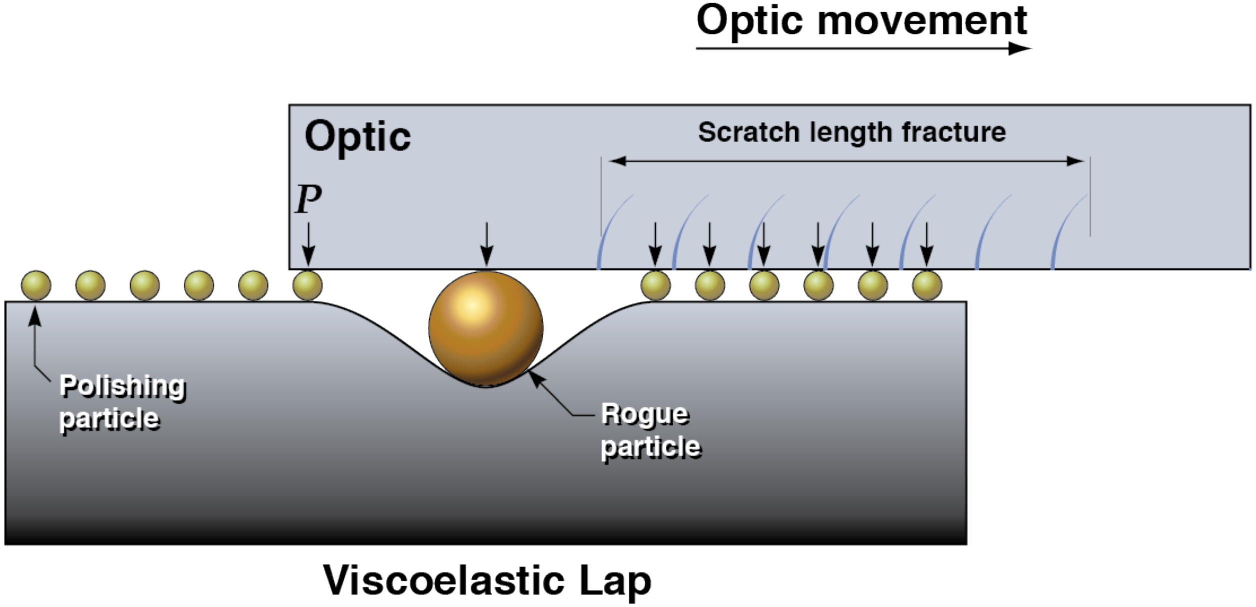

**This behavior has been modeled using hard sphere penetration into a linear viscoelastic lap at large penetration**

T. Suratwala, JNCS 354 (2006) 2023

# The scratch length correlates with viscoelastic model wrt rogue particle size, pressure, lap viscosity, and lap temperature

## Scratch length as a fn of various process parameters

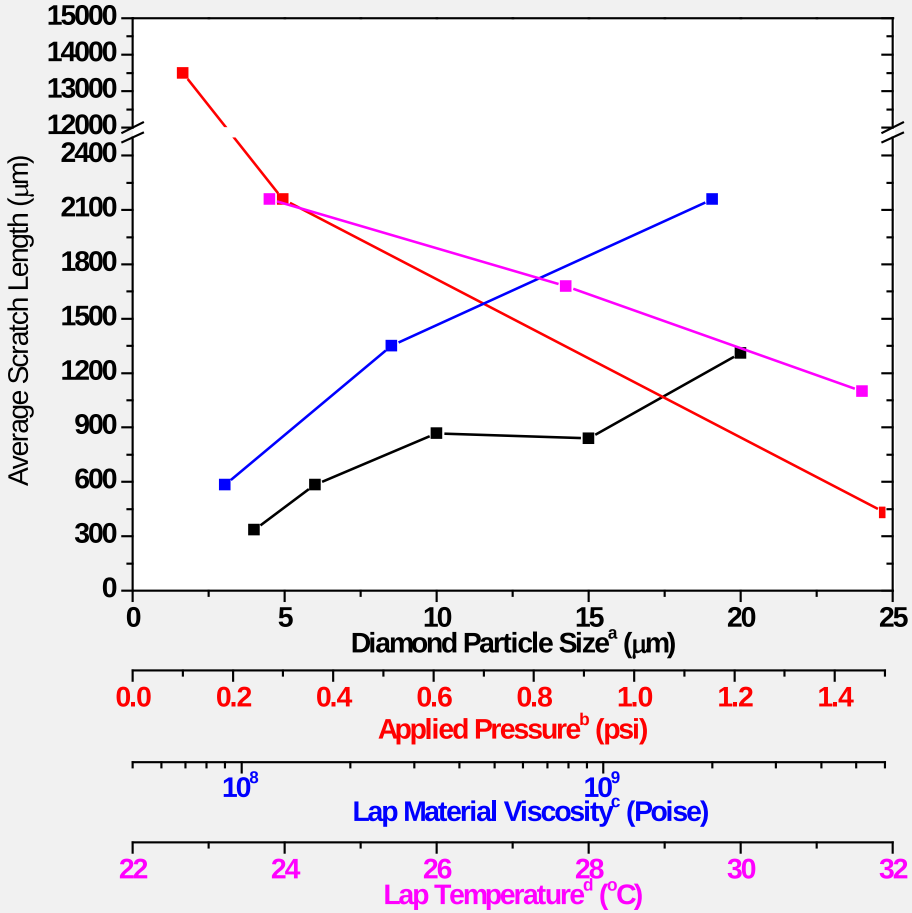

T. Suratwala, JNCS 354 (2006) 2023; T. Suratwala OPN (Sep 2008) 12

# There are five major areas of effort that have aided in managing sub-surface fractures

## GRINDING

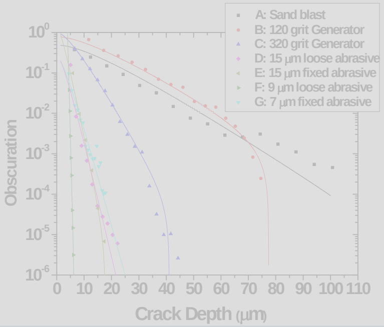

1. Developed fracture mechanics understanding of sub-surface fracture distributions

## POLISHING

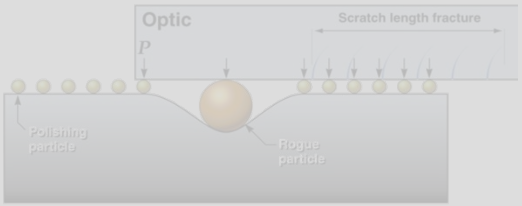

2. Identified/characterized behavior of rogue particles causing sub-surface fractures

## CHEMICAL ETCHING

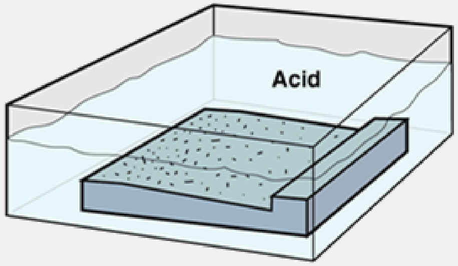

**3. Established techniques using etching to reveal and remove subsurface fractures**

## SCRATCH FORENSICS

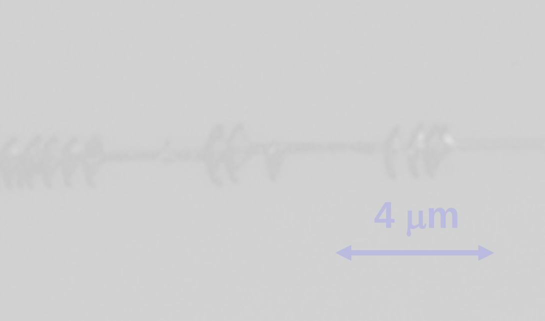

4. Developed quantitative rules for post-diagnosis of cause of surface fractures

## LASER DAMAGE


Edge-lit image of an polished 14 cm optic with SSD

Edge-lit image of same optic after SSD removal

5. Showed link between sub-surface fracture removal & improved laser resistance

# HF:$NH_4F$ etching of fused silica glass allows for removing the Bielby layer and visually observing surface cracks

## Cross section view of cracks *before* etching

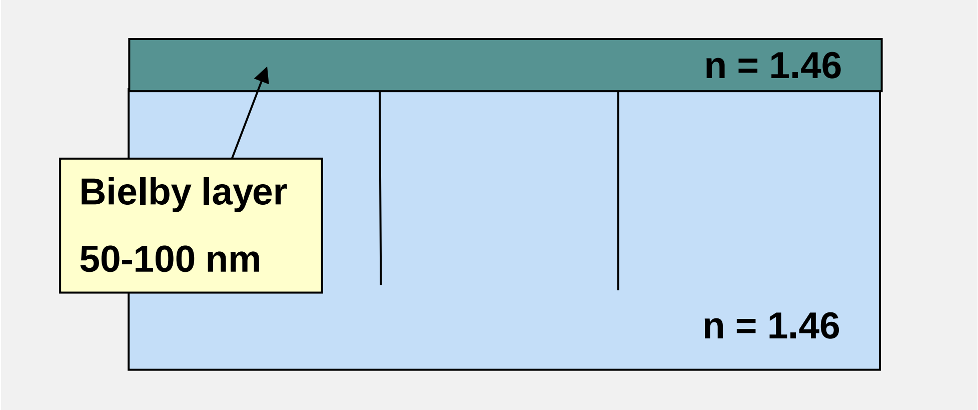

## Sleek on fused silica optic (before etch)

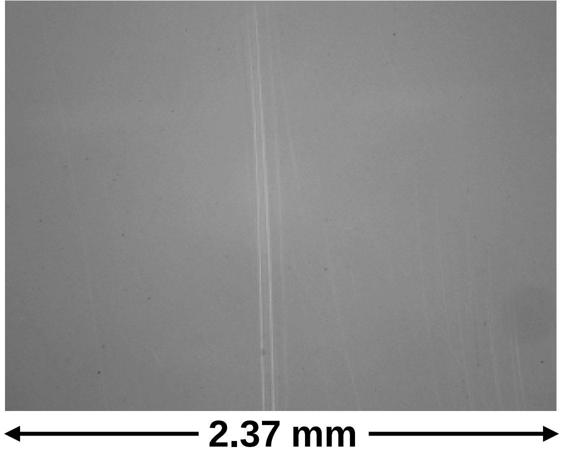

## Cross section view of cracks *after* etching

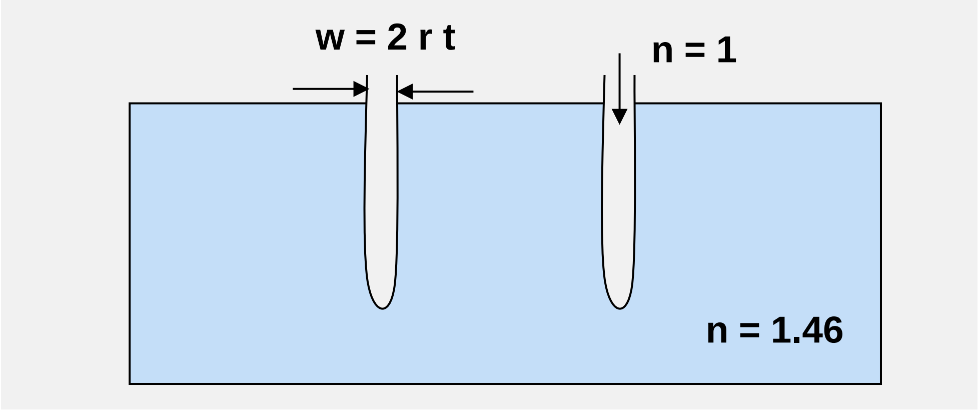

## Sleek on fused silica optic (after etch)

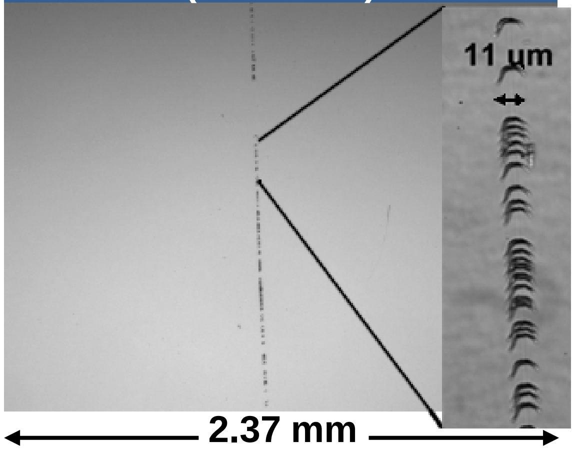

L. Wong, JNCS 355 (2009) 797

# HF Etching exposes sub-surface fractures allowing detection

- **Polished Optic (14 cm x 14 cm) viewed off axis by side lighting**

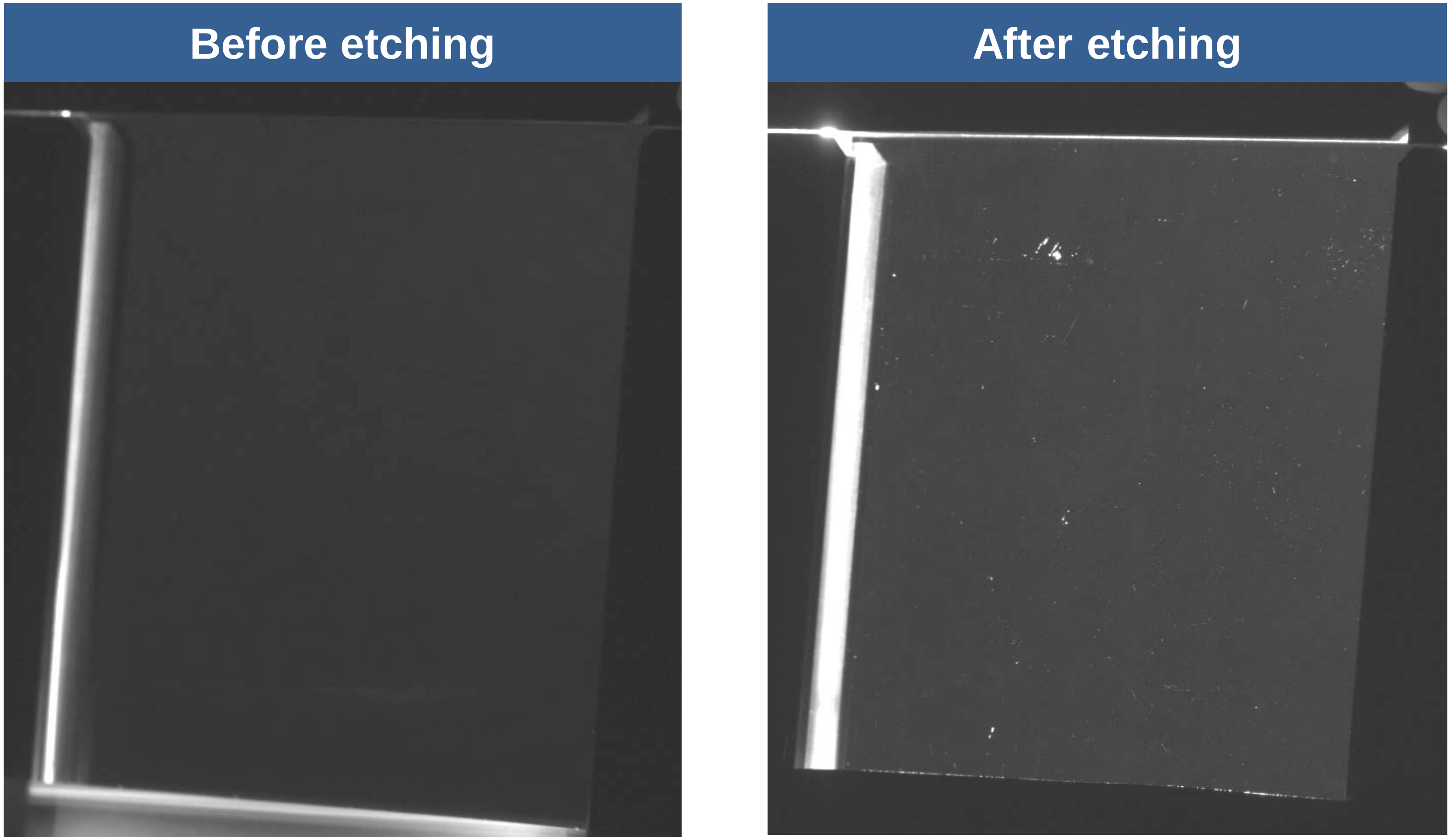
Before etching

After etching

**Preston reported this behavior in 1921**

L. Wong, JNCS 355 (2009) 797

# HF etching can be used after grinding to remove subsurface fracture because it annihilates neighboring cracks

## Etching a scratch

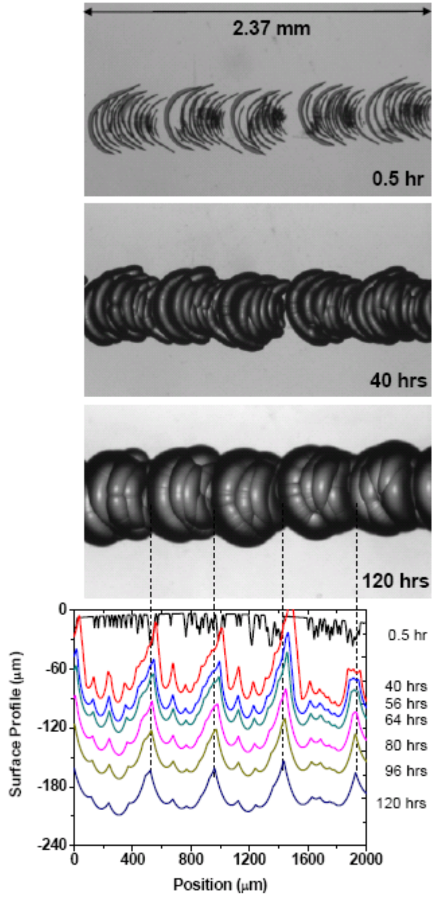

## Etching ground surface

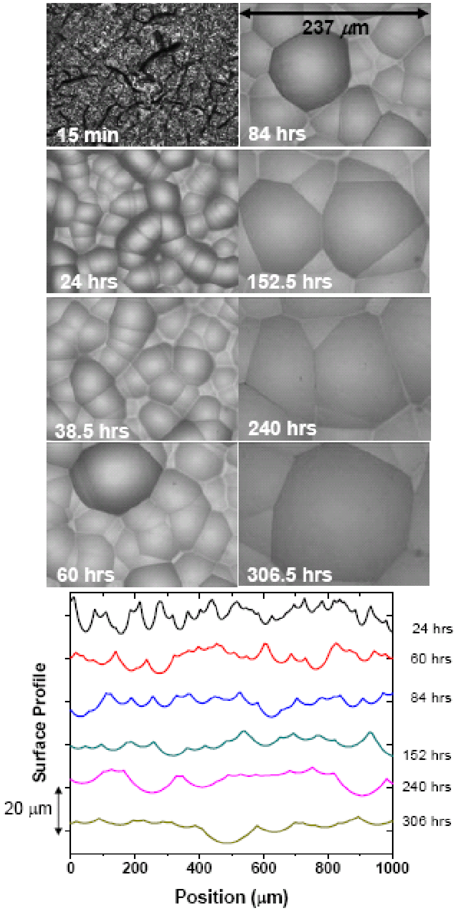

## Simple Geometric Model

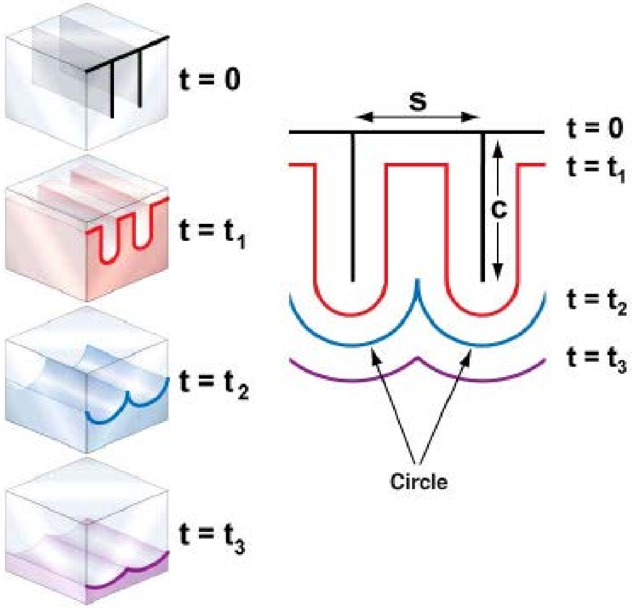

L. Wong, JNCS 355 (2009) 797

# There are five major areas of effort that have aided in managing sub-surface fractures

## GRINDING

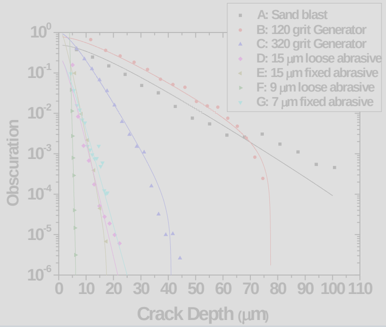

1. Developed fracture mechanics understanding of sub-surface fracture distributions

## POLISHING

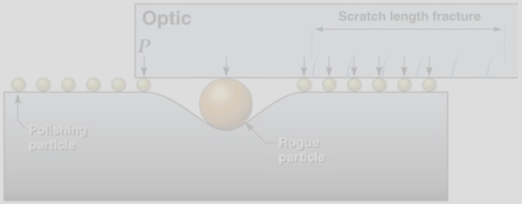

2. Identified/characterized behavior of rogue particles causing sub-surface fractures

## CHEMICAL ETCHING

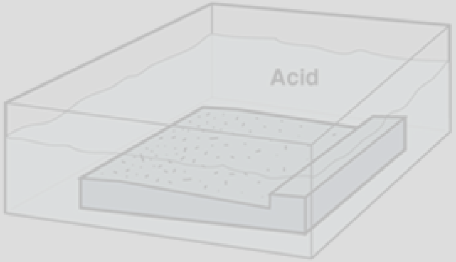

3. Established techniques using etching to reveal and remove subsurface fractures

## SCRATCH FORENSICS

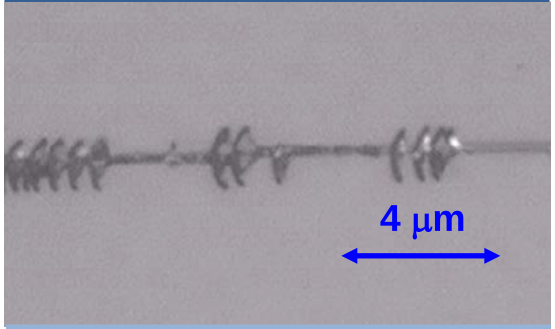

4. Developed quantitative rules for post-diagnosis of cause of surface fractures

## LASER DAMAGE


Edge-lit image of an polished 14 cm optic with SSD

Edge-lit image of same optic after SSD removal

5. Showed link between sub-surface fracture removal & improved laser resistance

# Our studies have provided new rules that Opticians use to diagnose the cause of or to mitigate scratches

| Property of scratch | What can it tell you? |
|---|---|
| 1. Scratch width or trailing indent length (L) | - Size of rogue particle (d)<br>- Size distribution of Rogue Particles<br>- Process step<br>- Depth of fracture ($c_{90}$ or $c_{max}$) |
| 2. Number density | - Rogue particle concentration |
| 3. Scratch length ($L_{scratch}$) | - Lap properties and rogue particle size |
| 4. Scratch type (plastic, brittle, mixed) | - Load during fracture<br>- Sharpness of particle |
| 5. Orientation and pattern of trailing indent | - Particle movement direction<br>- Particle rotation<br>- Stick slip behavior |
| 6. Curvature or scratch pattern | - Pathway of indenting particle<br>- Shape of tool<br>- Handling vs polishing |
| 7. Location on optic | - Material removal and surface figure |

**Rule / Example**

For grinding

$$0.15\ d \le\ L\ \le 0.3\ d$$

For polishing

$$0.3\,d \le L \le\ 0.5\ d$$

| Sample | <L> |
|---|---|
| A: Sandblast | 27.1 μm |
| B: 120 grit | 28.3 μm |
| C: 320 grit | 14.9 μm |
| D: 15 μm loose | 4.6 μm |
| E: 15 μm fixed | 4.5 μm |
| F: 9 μm loose | 1.9 μm |
| G: 7 μm fixed | 8.4 μm |

$$c_{90} = 0.9 < L > \quad c_{\max} = 2.8 < L >$$

$$P \approx 0.001 - 0.1\,N \quad \textit{Plastic only}$$
$$P \approx 0.1 - 5\,N \quad \textit{Plastic \& Brittle}$$
$$P > 5N \quad \textit{Plastic \& rubble}$$

$$L_{scratch} = 8.9\frac{v_{ave}\eta R^2}{P}$$

T. Suratwala, JNCS 354 (2006) 2023; T. Suratwala OPN (Sep 2008) 12

# Example of scratch forensics

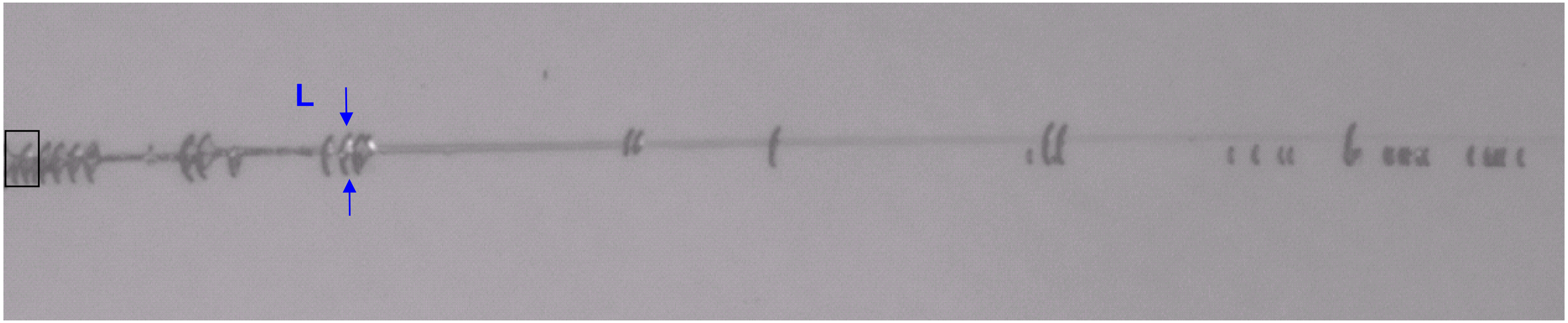

T. Suratwala OPN (Sep 2008) 12

# Example of scratch forensics

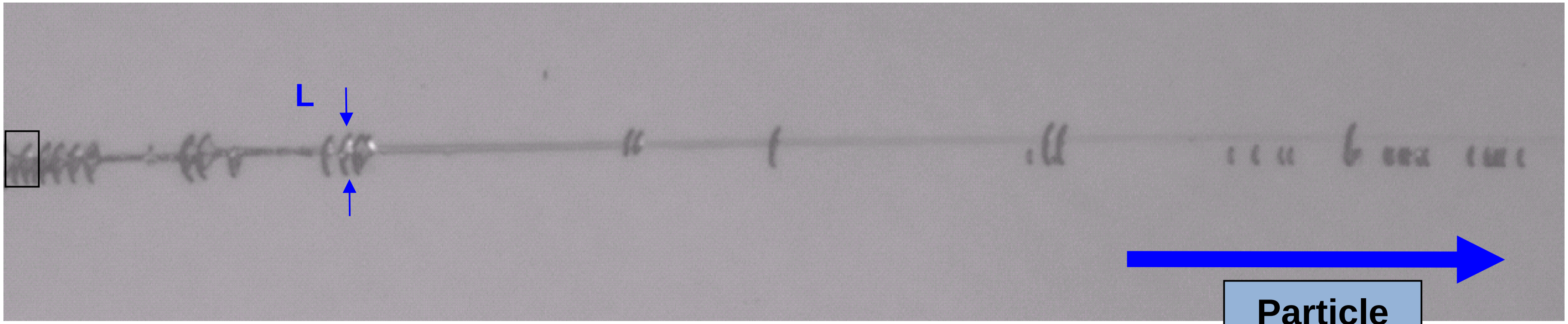

Particle Sliding Direction

**Scratch Type = Plastic + Brittle: trailing indent**

**Trailing Indent length: L= 1.9 μm**

**Rogue Particle ~ 3.8 – 5.7 μm**

**$c_{90}$= 1.8 μm**

**Scratch Length ~130 μm**

**Scratch time ~0.16 msec**

T. Suratwala OPN (Sep 2008) 12

# Strategy for reducing the scratch density on optical surfaces

1. Measure the SSD at each step
2. Define proper removal rate at each step such that all the SSD from previous step is removed
3. Can use etching as a means to remove SSD just after grinding
4. Ensure handling and cleaning at each step does not let rogue particles make contact with surface
5. Remove all rogue particles in polishers; Use scratch forensics to determine source
6. Use etched scratch dig inspections between steps and at end of process

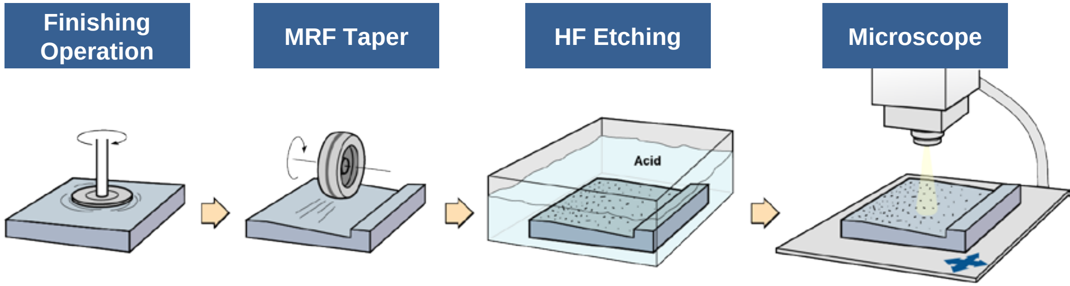

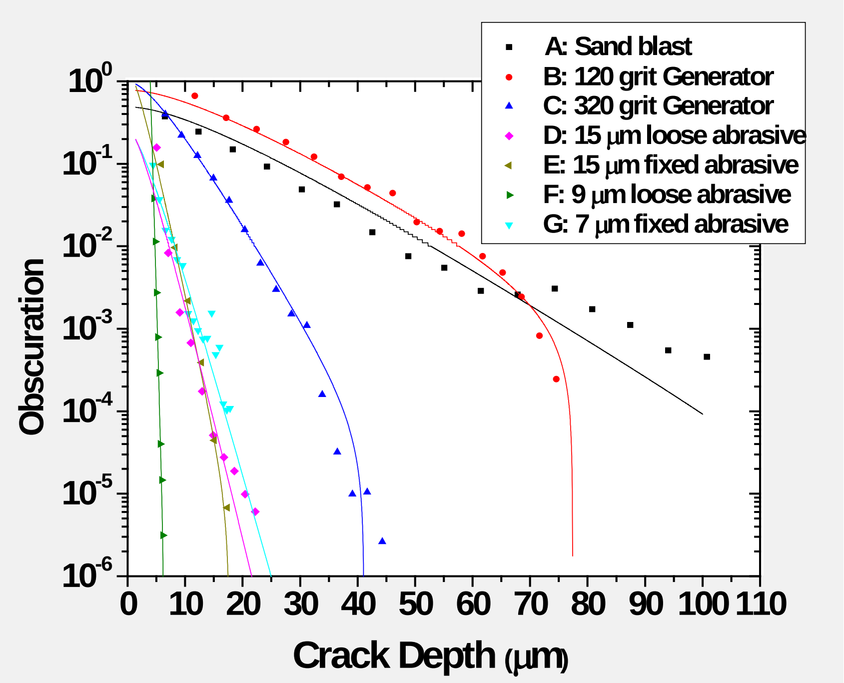

# Strategy for reducing the scratch density on optical surfaces

1. **Measure the SSD at each step**
2. **Define proper removal rate at each step such that all the SSD from previous step is removed**
3. **Can use etching as a means to remove SSD just after grinding**
4. **Ensure handling and cleaning at each step does not let rogue particles make contact with surface**
5. **Remove all rogue particles in polishers; Use scratch forensics to determine source**
6. **Use etched scratch dig inspections between steps and at end of process**

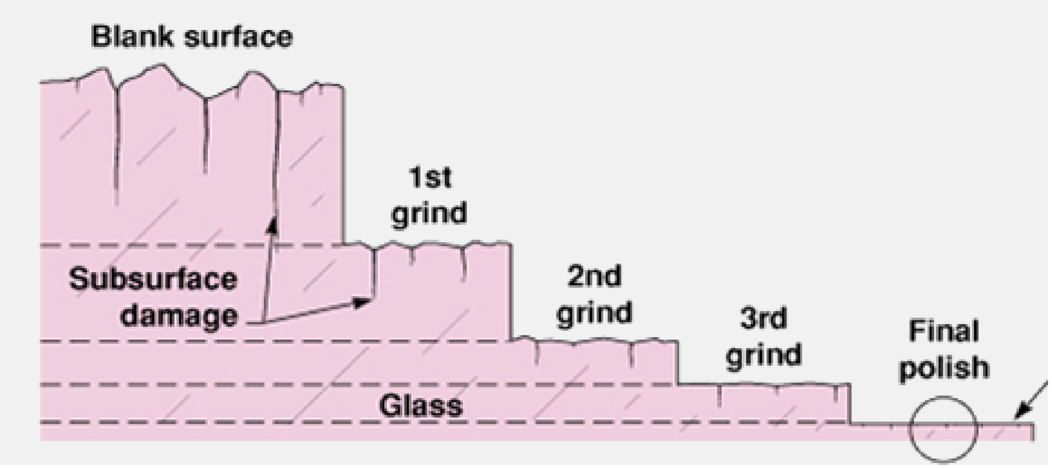

# Strategy for reducing the scratch density on optical surfaces

1. Measure the SSD at each step
2. Define proper removal rate at each step such that all the SSD from previous step is removed
3. Can use etching as a means to remove SSD just after grinding
4. Ensure handling and cleaning at each step does not let rogue particles make contact with surface
5. Remove all rogue particles in polishers; Use scratch forensics to determine source
6. Use etched scratch dig inspections between steps and at end of process

**Schematic**

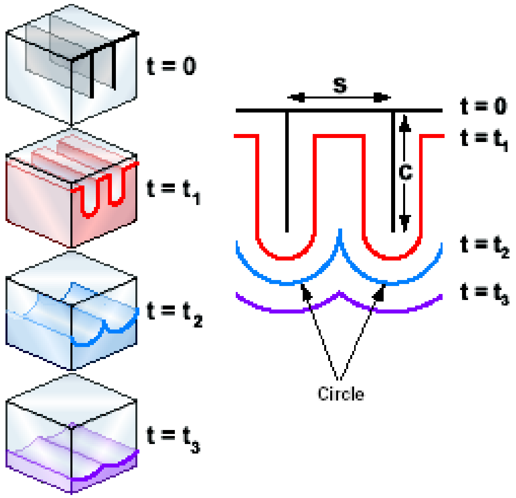

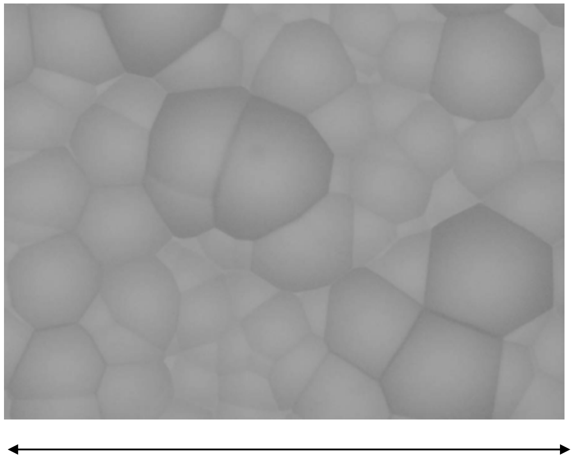

237 μm

# Strategy for reducing the scratch density on optical surfaces

1. **Measure the SSD at each step**
2. **Define proper removal rate at each step such that all the SSD from previous step is removed**
3. **Can use etching as a means to remove SSD just after grinding**
4. **Ensure handling and cleaning at each step does not let rogue particles make contact with surface**
5. **Remove all rogue particles in polishers; Use scratch forensics to determine source**
6. **Use etched scratch dig inspections between steps and at end of process**

**Crack *depth* distributions:**
**Loose abrasive grinding with addition of rogue particles**

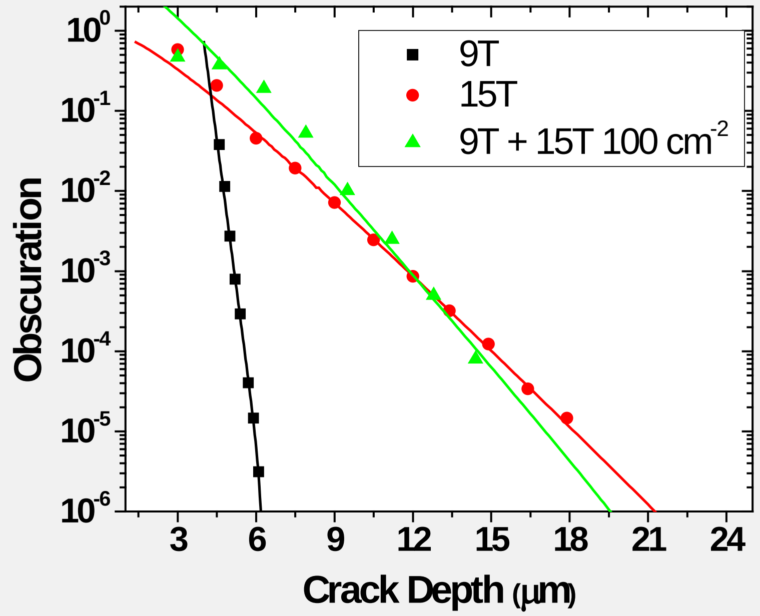

## Rogue particle sources

1) In slurry from foreign particle or agglomerates
2) Dried slurry on components falling in
3) Contamination from polisher exterior

# Strategy for reducing the scratch density on optical surfaces

1. Measure the SSD at each step
2. Define proper removal rate at each step such that all the SSD from previous step is removed
3. Can use etching as a means to remove SSD just after grinding
4. Ensure handling and cleaning at each step does not let rogue particles make contact with surface
5. Remove all rogue particles in polishers; Use scratch forensics to determine source
6. Use etched scratch dig inspections between steps and at end of process

**Etching provides a means of revealing subsurface damage masked by hydrated silica**

# There are five major areas of effort that have aided in managing sub-surface fractures

## GRINDING

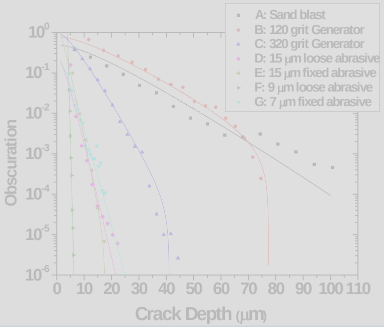

1. Developed fracture mechanics understanding of sub-surface fracture distributions

## POLISHING

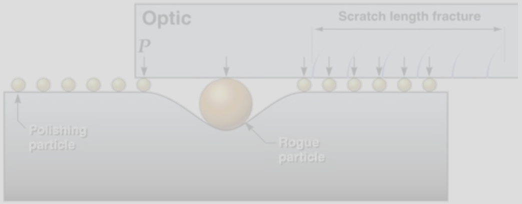

2. Identified/characterized behavior of rogue particles causing sub-surface fractures

## CHEMICAL ETCHING

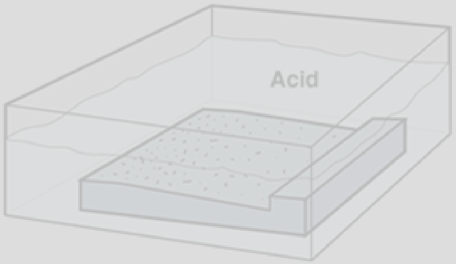

3. Established techniques using etching to reveal and remove subsurface fractures

## SCRATCH FORENSICS

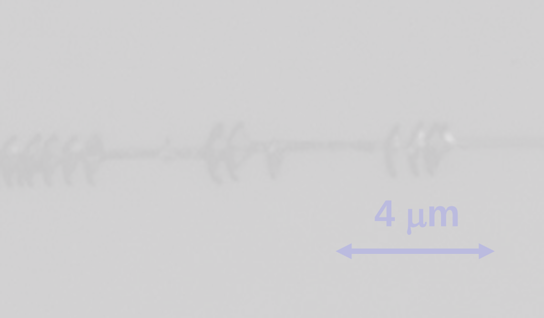

4. Developed quantitative rules for post-diagnosis of cause of surface fractures

## LASER DAMAGE

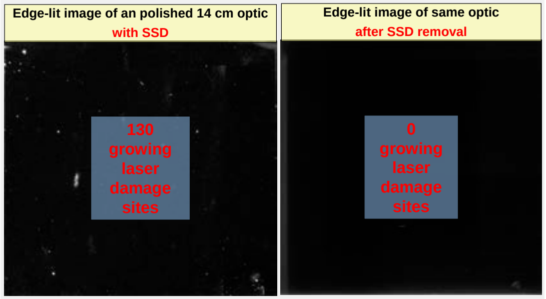
Edge-lit image of an polished 14 cm optic with SSD

Edge-lit image of same optic after SSD removal

5. Showed link between sub-surface fracture removal & improved laser resistance

# SSD-free test optics have been fabricated such it does not laser damage, supporting the “absorber-in-a-crack” theory

**Edge-lit image of an polished 14 cm optic with SSD**

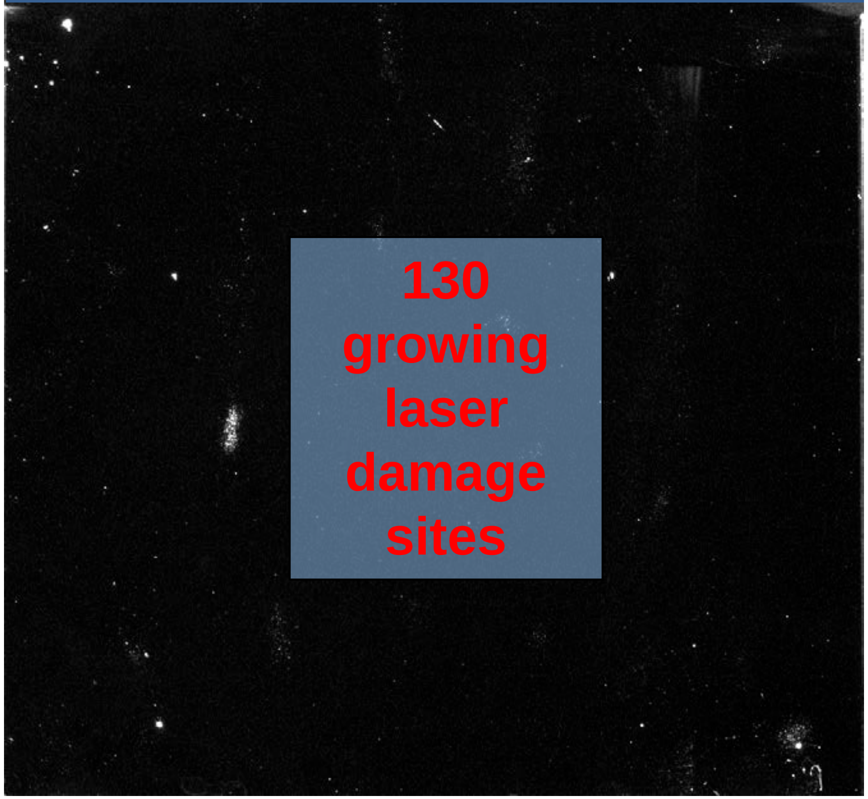

**130 growing laser damage sites**

**Edge-lit image of same optic after SSD removal**

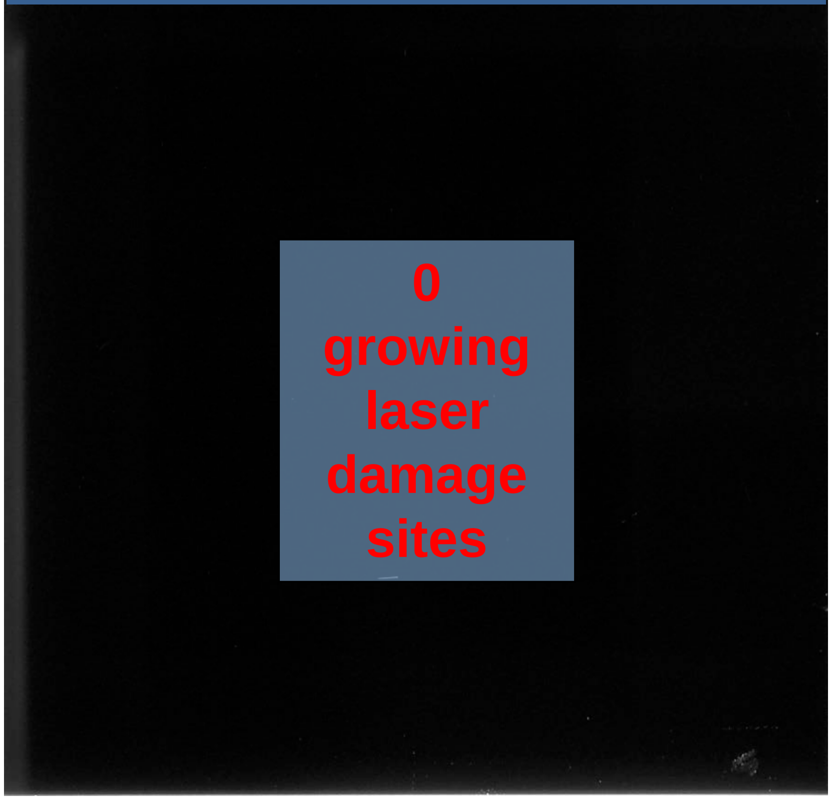

**0 growing laser damage sites**

**Laser testing on a 14 cm x 14 cm test optic to 14 J/cm$^2$ (351 nm, 3 ns equiv) resulted in the elimination of growing laser initiation site upon SSD removal**

# Advanced Mitigation Process dramatically improves laser damage resistance of fused silica optics

T. Suratwala JACS 94(2) (2010) 416; P. Miller US Patent 0079931 (2011)

# AMP process significantly reduces laser damage initiation per unit scratch length

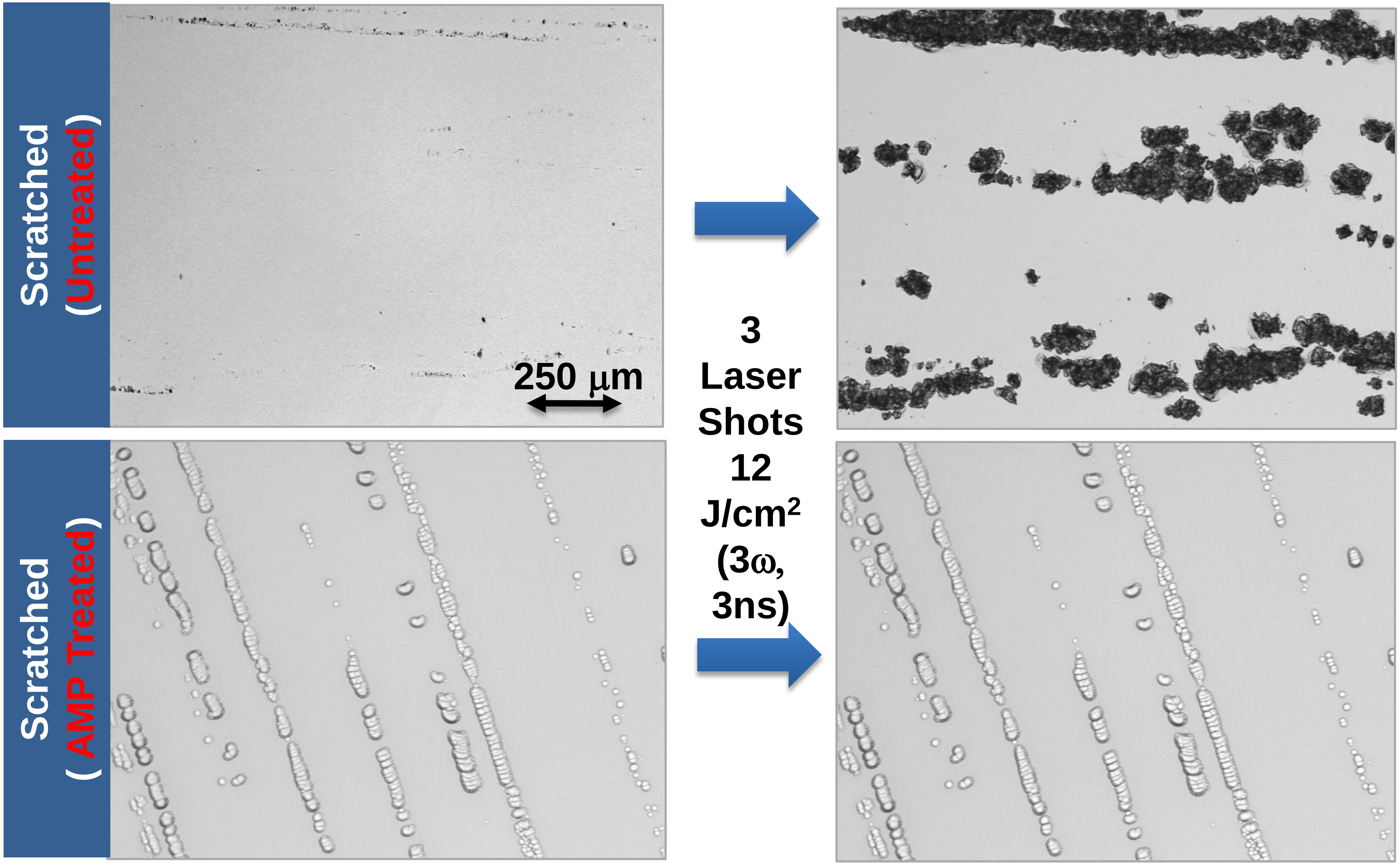

3 Laser Shots 12 J/cm$^2$ (3ω, 3ns)

T. Suratwala JACS 94(2) (2010) 416; P. Miller US Patent 0079931 (2011)

# The complexities of polishing has made is difficult to scientifically design, optimize a process for a given material

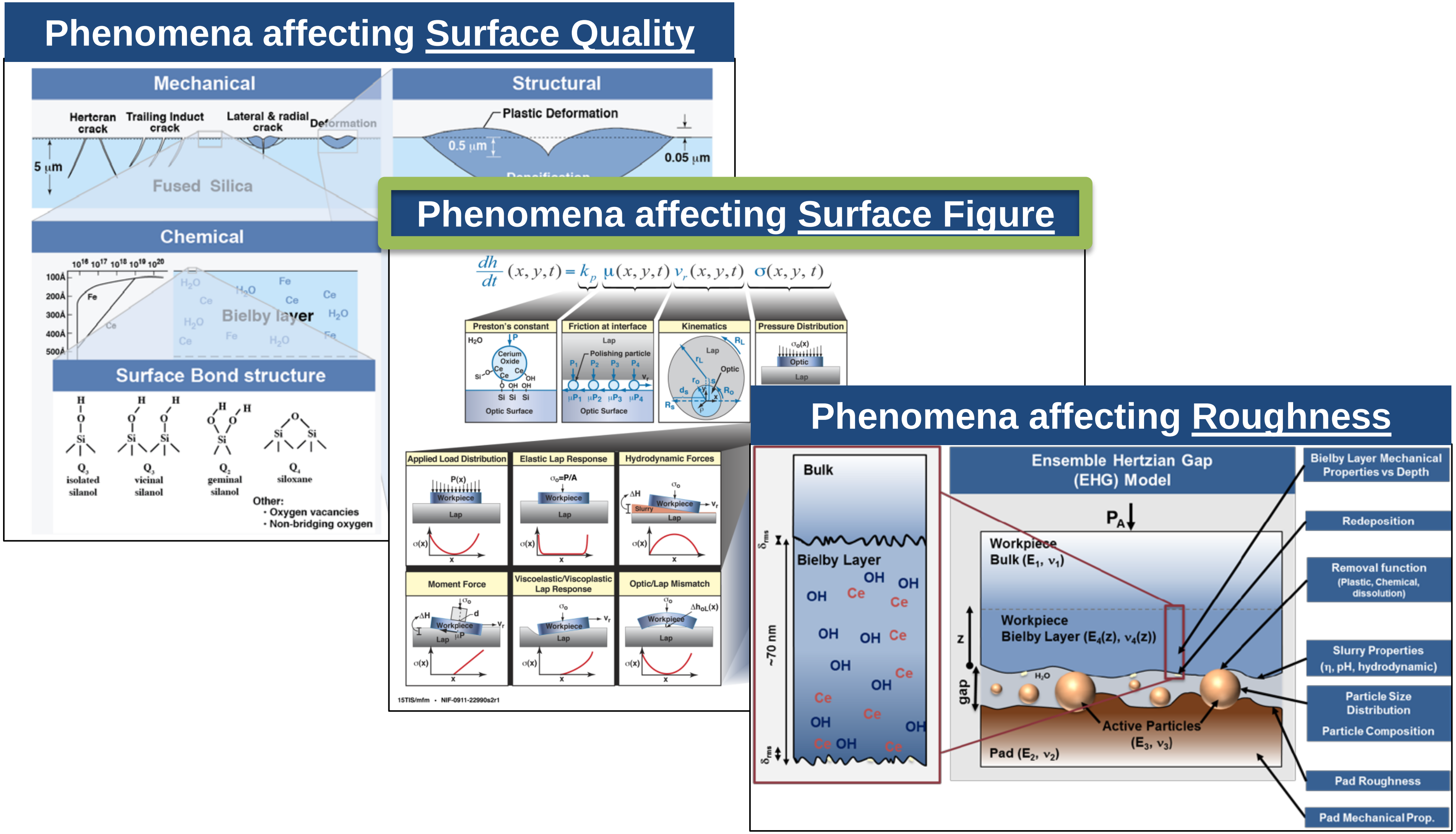

## Phenomena affecting Surface Quality

## Phenomena affecting Surface Figure

$$\frac{dh}{dt}(x,y,t) = \underbrace{k_p}\ \underbrace{\mu(x,y,t)}\ \underbrace{v_r(x,y,t)}\ \underbrace{\sigma(x,y,t)}$$

## Phenomena affecting Roughness

# The surface figure of an optic is typically measured by interferometry

**Fizeau Interferometer**

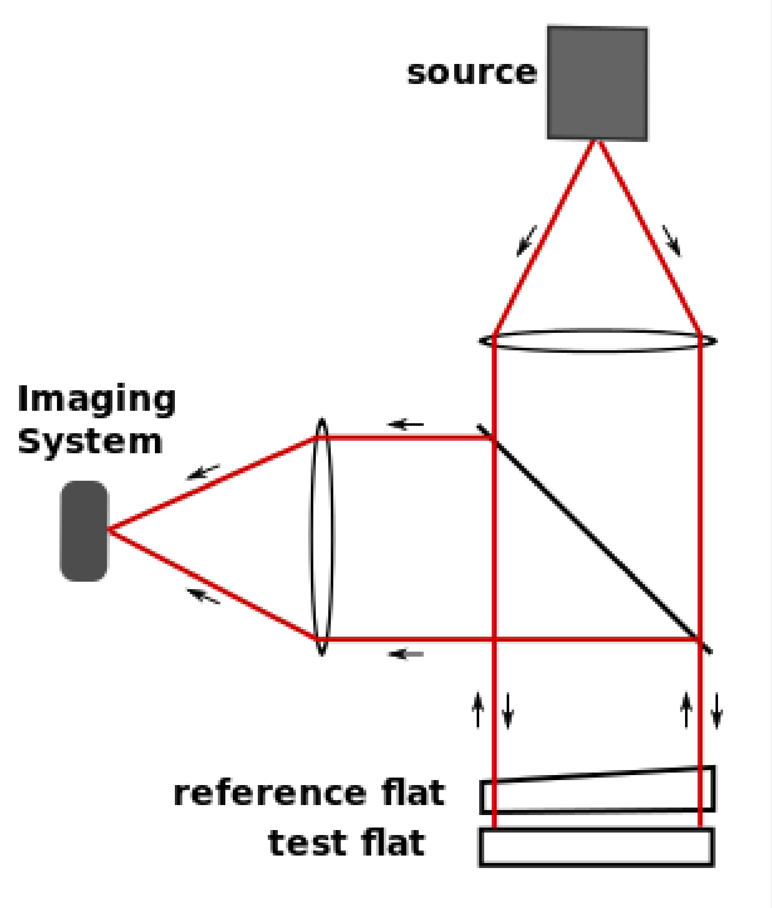

**Measured Surface Figure**

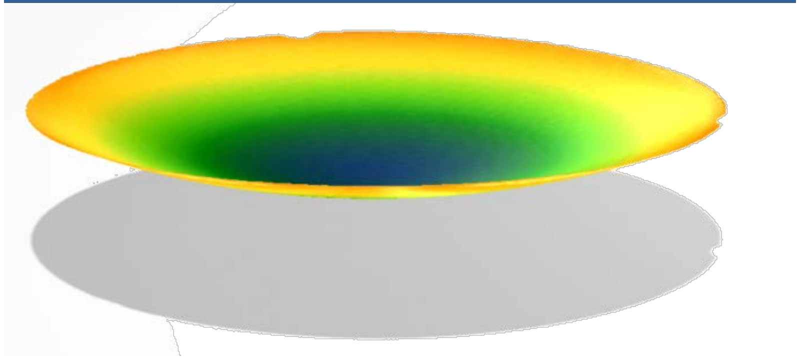

# Material removal on a workpiece is governed by a large number of phenomena

$$\frac{dh}{dt}(x,y,t) = \underbrace{k_p}\,\underbrace{\mu(x,y,t)}\,\underbrace{v_r(x,y,t)}\,\underbrace{\sigma(x,y,z,t)}$$

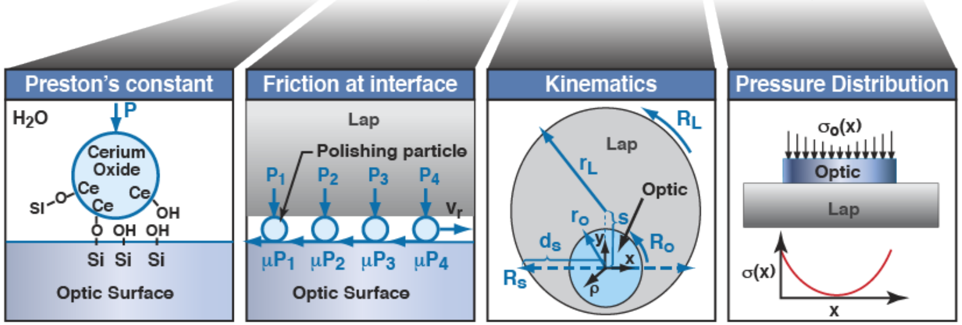

IJAGS 3(1) 14-28 (2012); J. Am. Ceram. Soc., 97 [6] 1720–1727 (2014); J. Am. Ceram. Soc., 93 [5] 1326–1340 (2010)

# Material removal on a workpiece is governed by a large number of phenomena

$$\frac{dh}{dt}(x,y,t) = \underbrace{k_p}\,\underbrace{\mu(x,y,t)}\,\underbrace{v_r(x,y,t)}\,\underbrace{\sigma(x,y,z,t)}$$

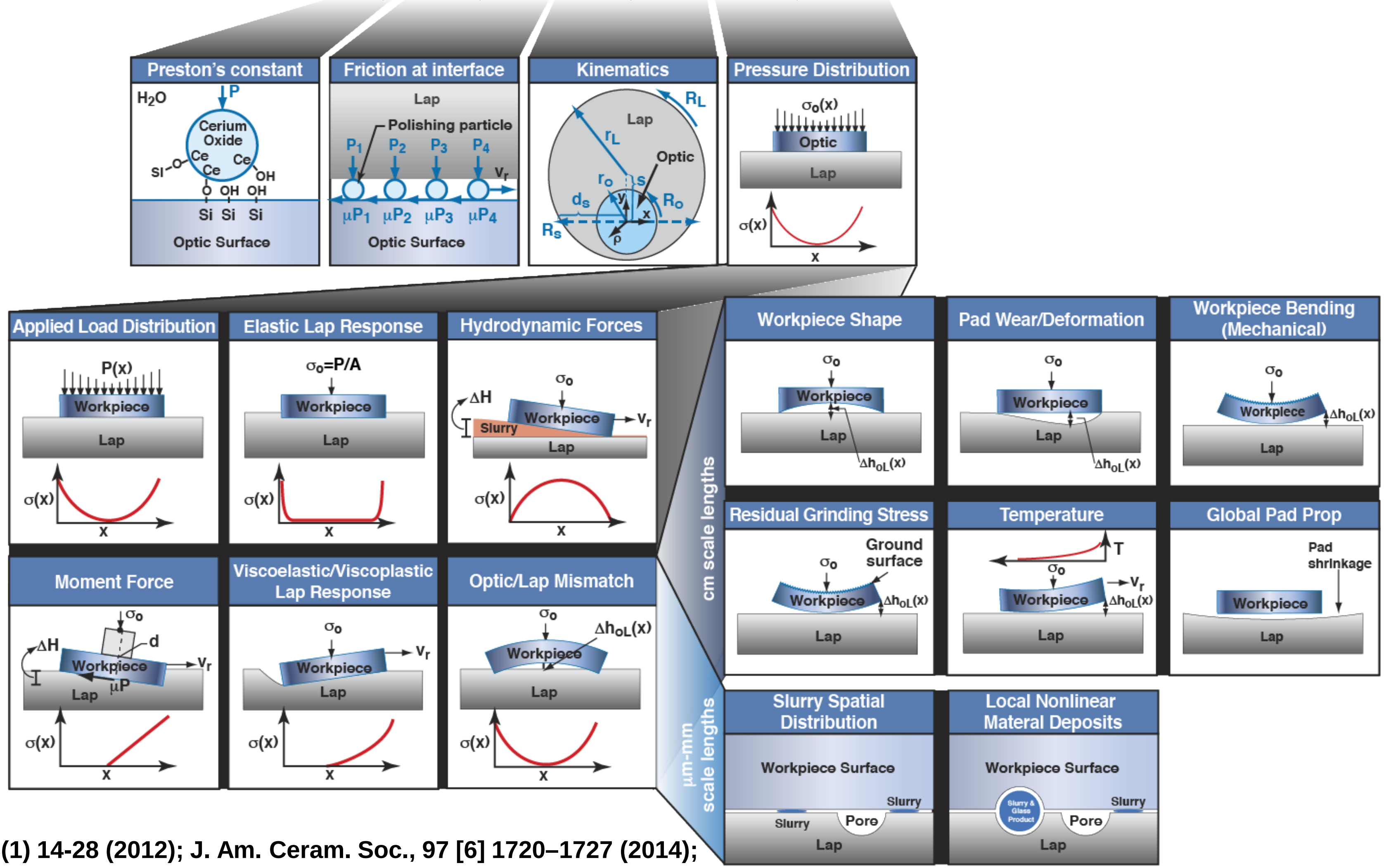

IJAGS 3(1) 14-28 (2012); J. Am. Ceram. Soc., 97 [6] 1720–1727 (2014); J. Am. Ceram. Soc., 93 [5] 1326–1340 (2010)

# The optic/lap can have different modes of contact which strongly influences the amount of material removal

## Contact Mode

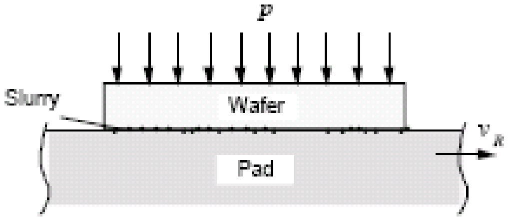

- **Friction μ>0.1**
- **Optic/pad mechanically make contact**
- **High pressure/low velocity**
- **Real contact area < nominal contact area**
- **Plastic deformation of optic/ pad occurs**
- **Fluid film is discontinuous**

## Mixed Mode

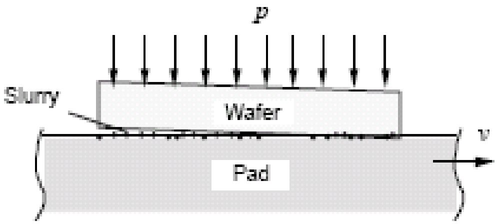

- **Friction μ~0.01 to 0.1**
- **Transition mode during pressure or velocity changes**
- **Contact is made between lap asperities and optic**

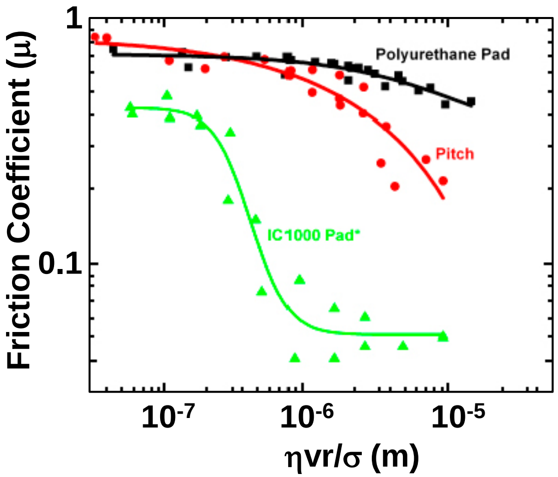

## Hydroplaning Mode

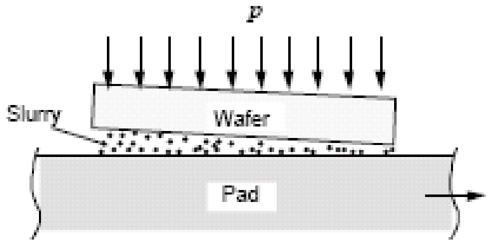

- **Friction μ~0.001 to 0.01 (due to shear of viscous fluid)**
- **Optic glides on fluid film without directly touching pad**
- **Low pressure/high velocity**
- **Pressure build-ups in fluid to support normal load of optic**
- **Pressure gradient is sensitive to wedge angle**

**J. Lai, Thesis (2001);**
**J. Am. Ceram. Soc., 93 [5] 1326–1340 (2010)**

# A geometric model is used to estimate the figure during conventional grinding/polishing

## Schematic of geometric model

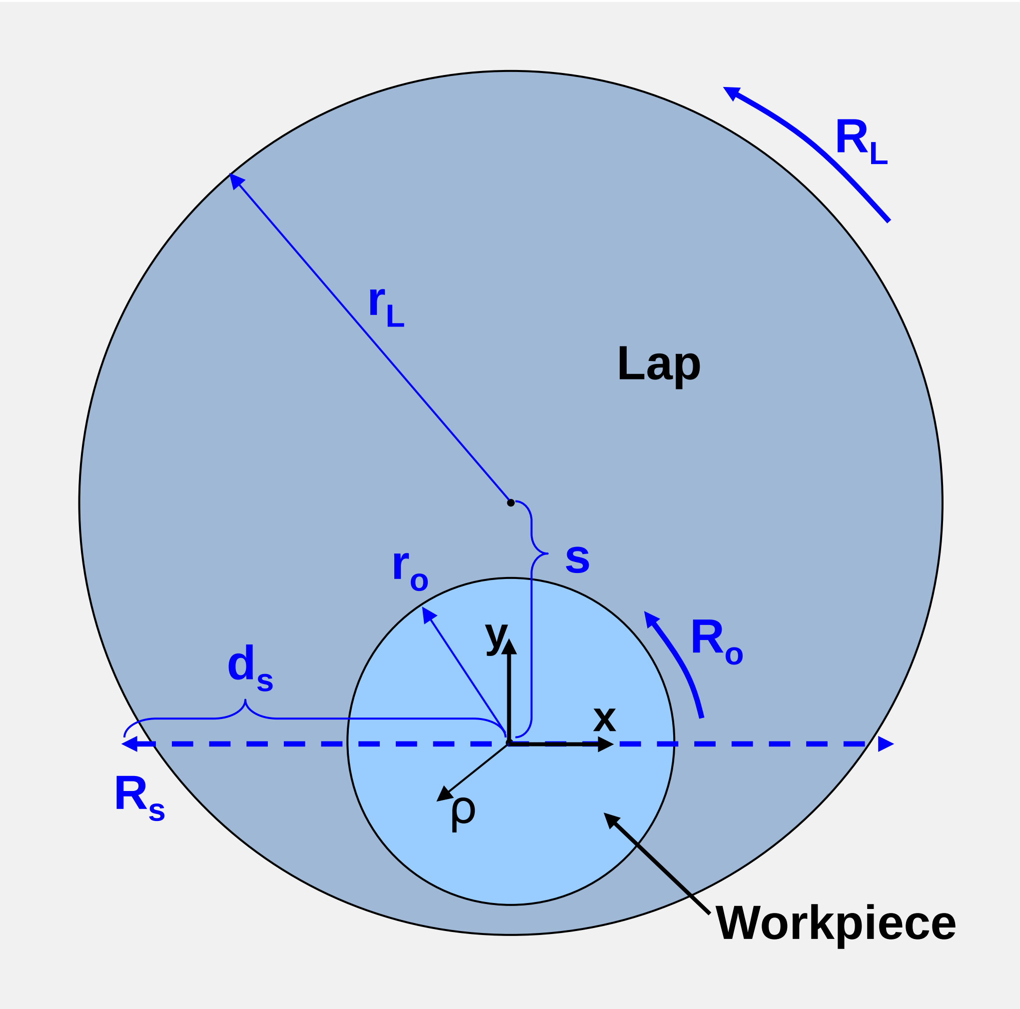

**The velocity vector at each point on the optic is the velocity relative to the optic rotation minus the velocity relative to the lap rotation**

$$\vec{V} = \left(\vec{R}_{optic} \times \vec{\rho}\right) - \left(\vec{R}_{Lap} \times \left(\vec{\rho} - \vec{S}\right)\right) + \vec{V}_s$$

**where the vectors are:**

$$\vec{R}_{optic} = \begin{pmatrix} 0 \\ 0 \\ R_{optic} \end{pmatrix} \qquad \vec{R}_{Lap} = \begin{pmatrix} 0 \\ 0 \\ R_{Lap} \end{pmatrix}$$

$$\vec{S} = \begin{pmatrix} d_s \sin\left(\dfrac{\pi v_s t}{d_s}\right) \\ s \\ 0 \end{pmatrix} \qquad \vec{V}_s = \begin{pmatrix} v_s \cos\left(\dfrac{\pi v_s t}{2 d_s}\right) \\ 0 \\ 0 \end{pmatrix}$$

$$\vec{\rho} = \begin{pmatrix} \sqrt{x^2 + y^2}\,\sin\left(a\tan(x/y) + 2\pi R_{optic} t\right) \\ \sqrt{x^2 + y^2}\,\cos\left(a\tan(x/y) + 2\pi R_{optic} t\right) \\ 0 \end{pmatrix}$$

**J. Am. Ceram. Soc., 93 [5] 1326–1340 (2010)**

# For a translating workpiece on a viscoelastic lap, stress is highest at leading edge and lowest at end

## Schematic of moving workpiece on a viscoelastic lap

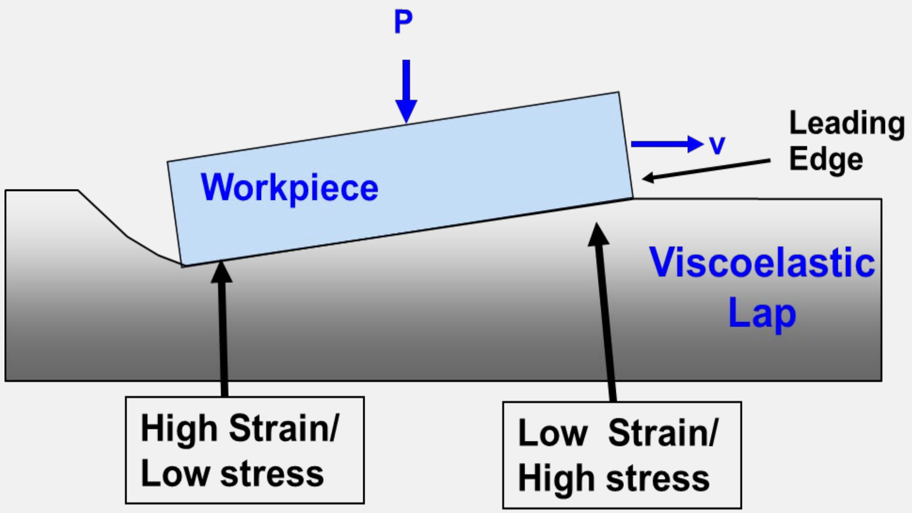

## Effect of moment on workpiece tilt

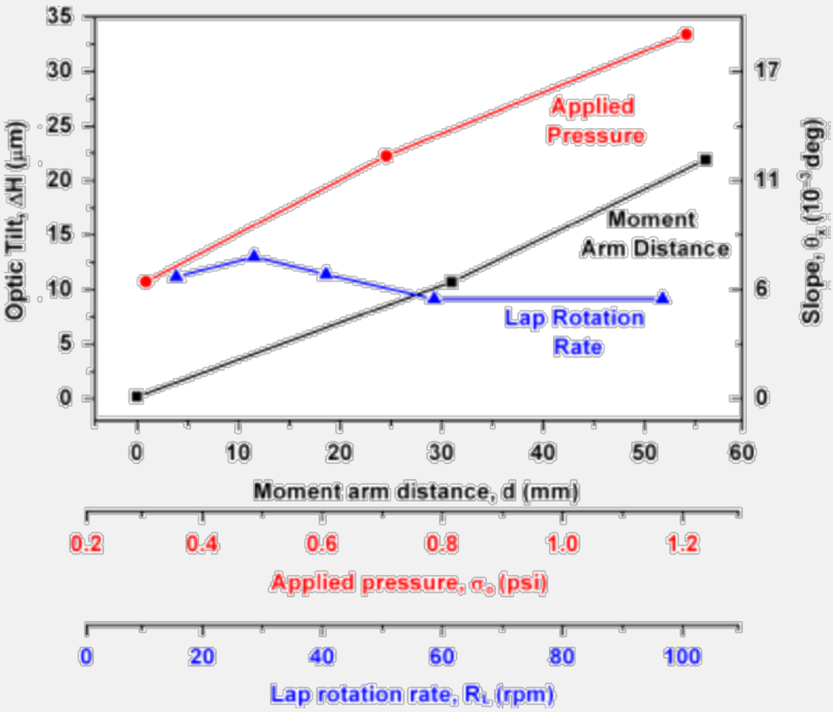

J. Am. Ceram. Soc., 93 [5] 1326–1340 (2010)

# Calculated instantaneous stress distribution is qualitatively similar to measured data

✦ **Leading edge**

## Calculated instantaneous Stress profile

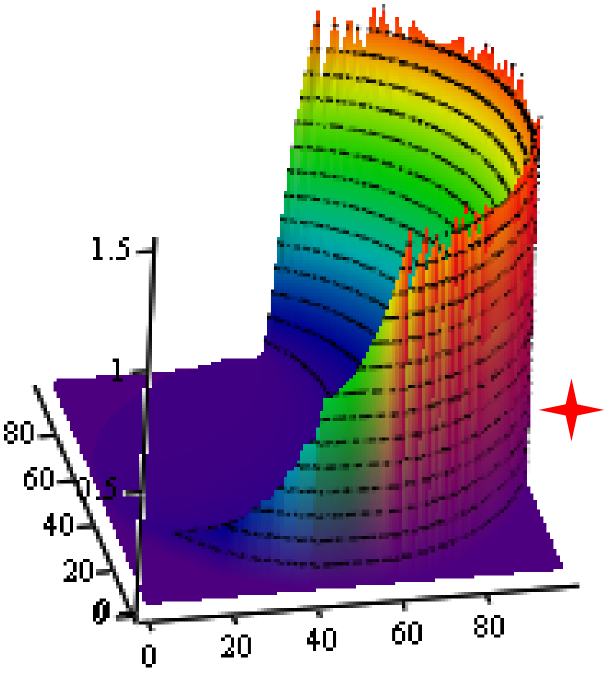

## Measured removal on optic when it is not rotated (Exp B)

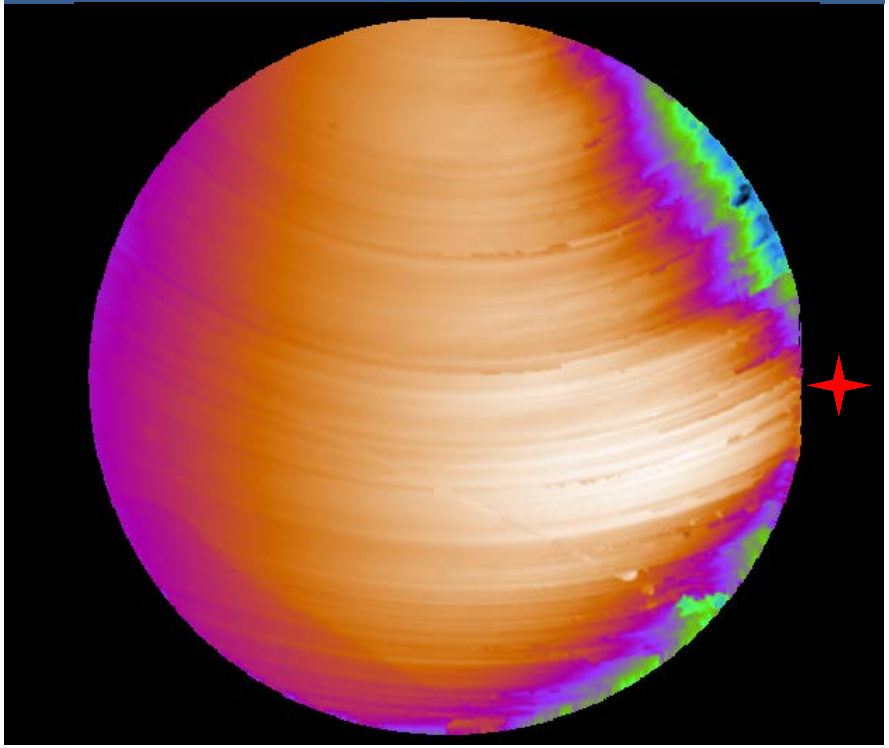

**High removal was observed at leading edge consistent with viscoelastic mechanism for causing pressure distribution**

J. Am. Ceram. Soc., 93 [5] 1326–1340 (2010)

# The pressure distribution across the workpiece can be predicted using the rigid punch indentation model for contact mode

## Rigid Flat Punch Model

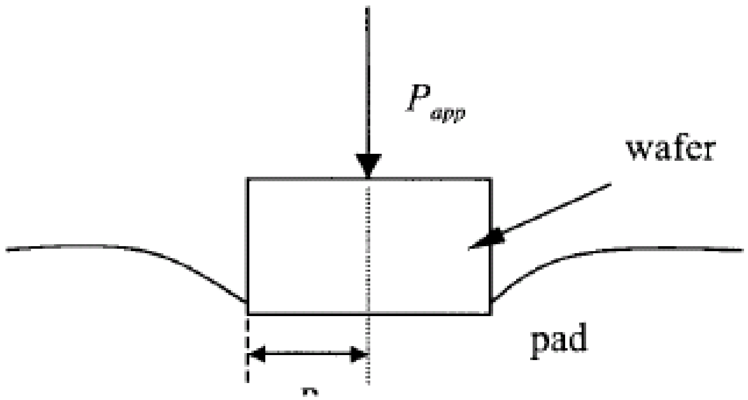

## Calculated pressure/load distribution

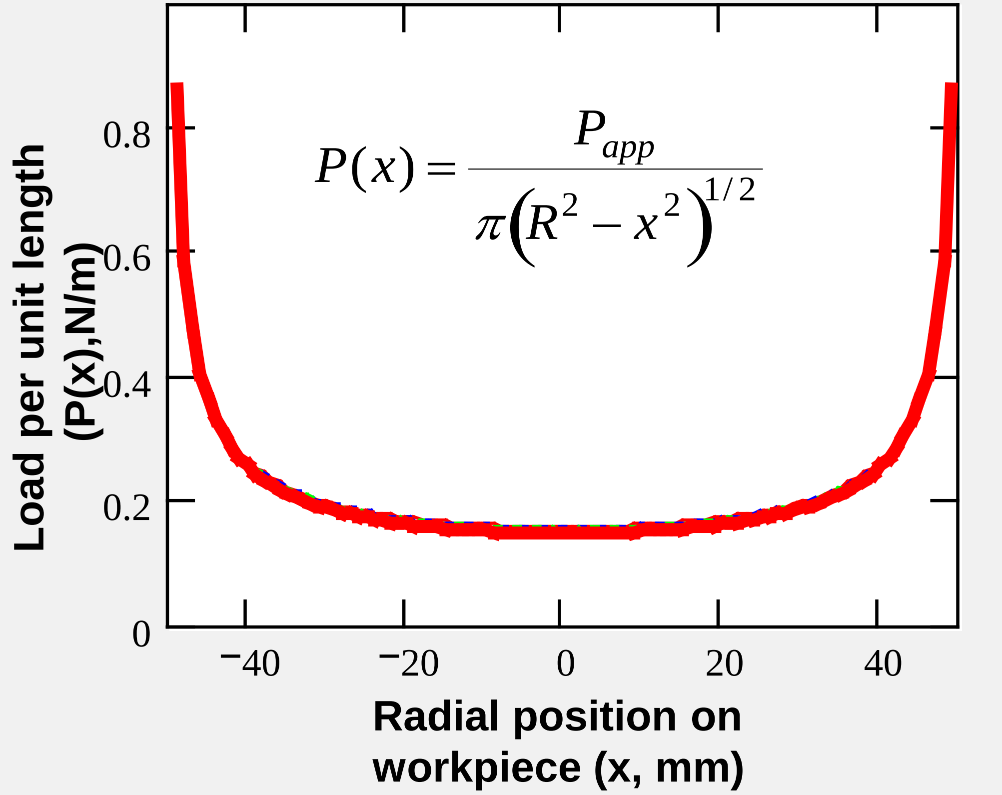

**Papp= 25 N; f=0.1; $\nu$=0.1**

# Our code SurF incorporates these phenomena & does a good job at predicting surface

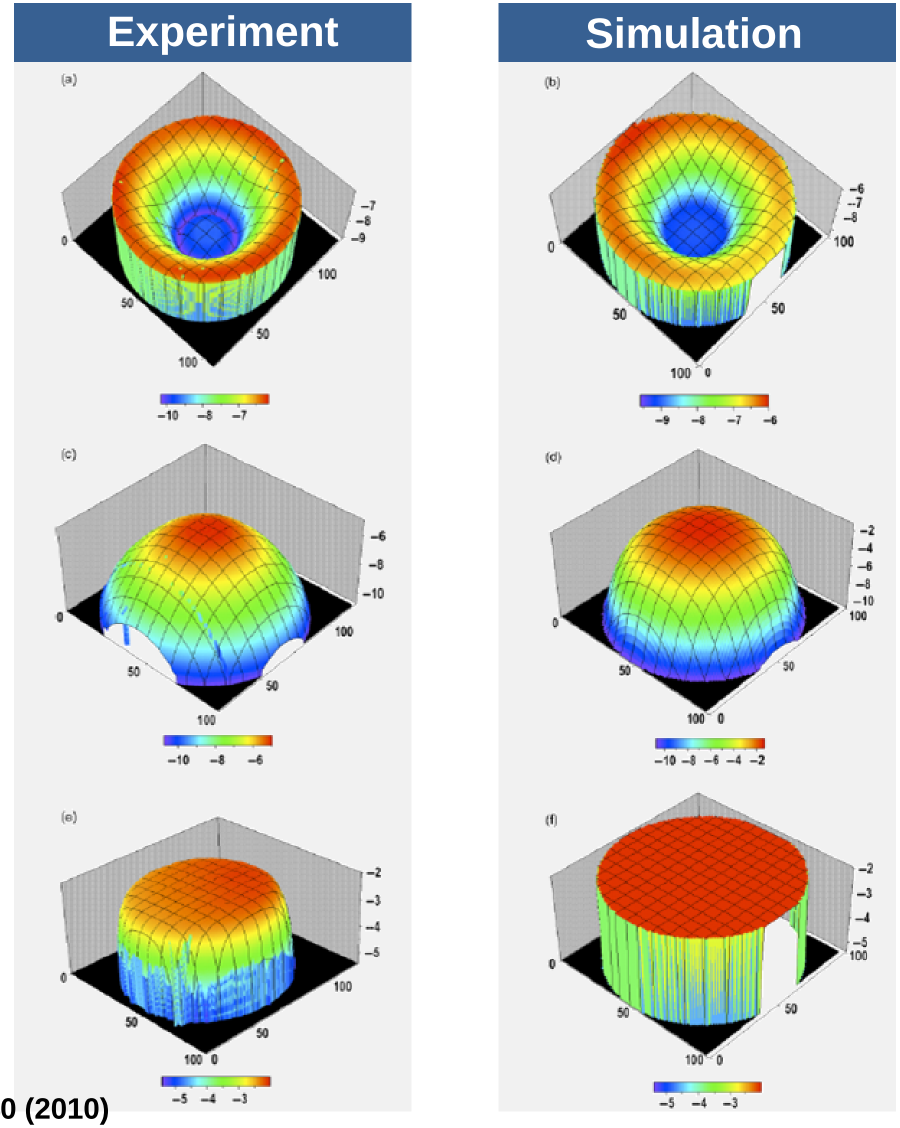
**Experiment**

**Simulation**

J. Am. Ceram. Soc., 93 [5] 1326–1340 (2010)

# Workpiece polishing can cause non-uniform wear of the lap

## Shape of lap after polishing workpiece

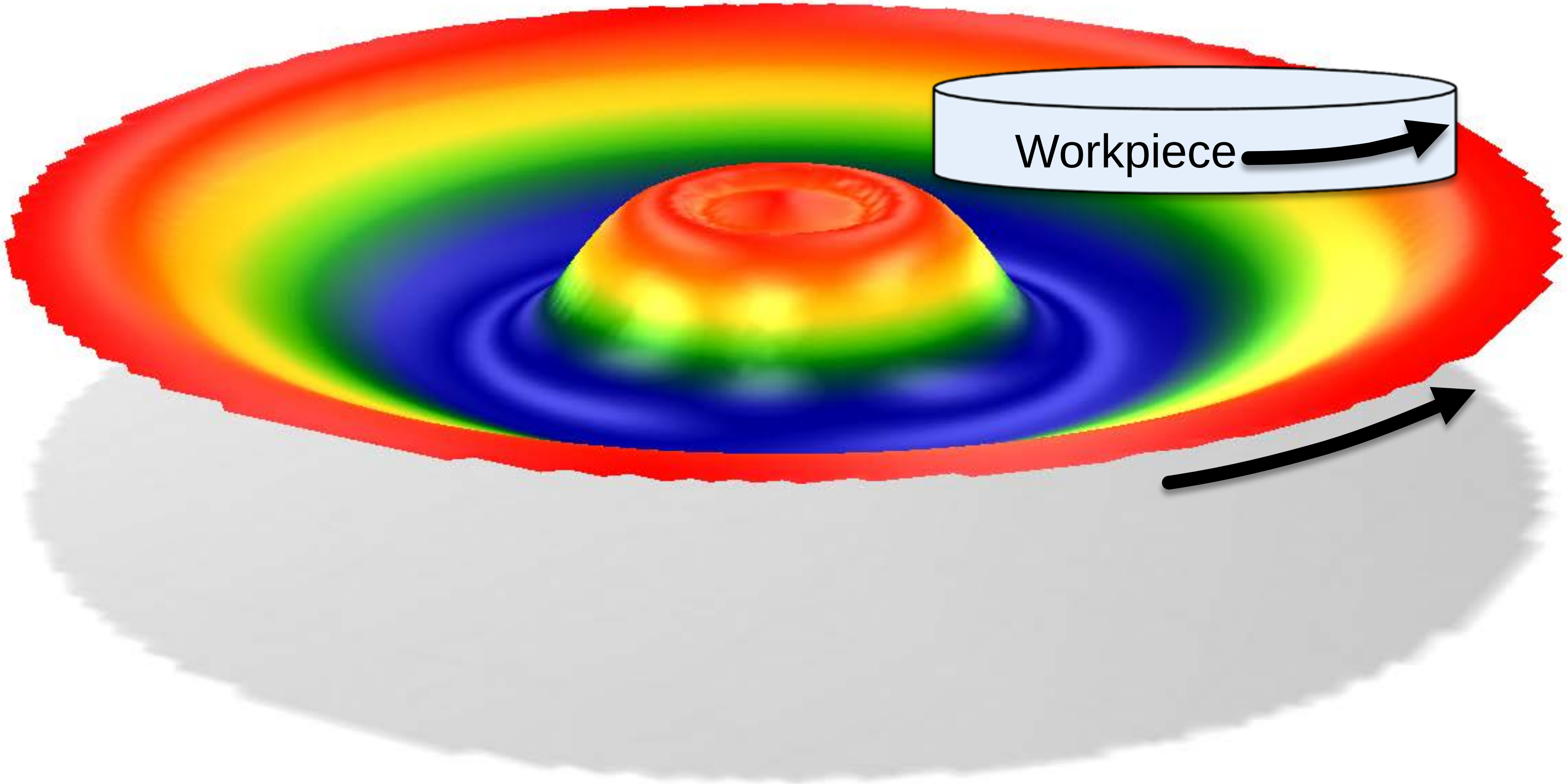

T. Suratwala et. al., IJAGS 3(1) 14-28 (2012).

# A novel septum has been designed to counteract non-uniform wear on the pad

## Pad wear vs lap radius due to workpiece and engineered septum

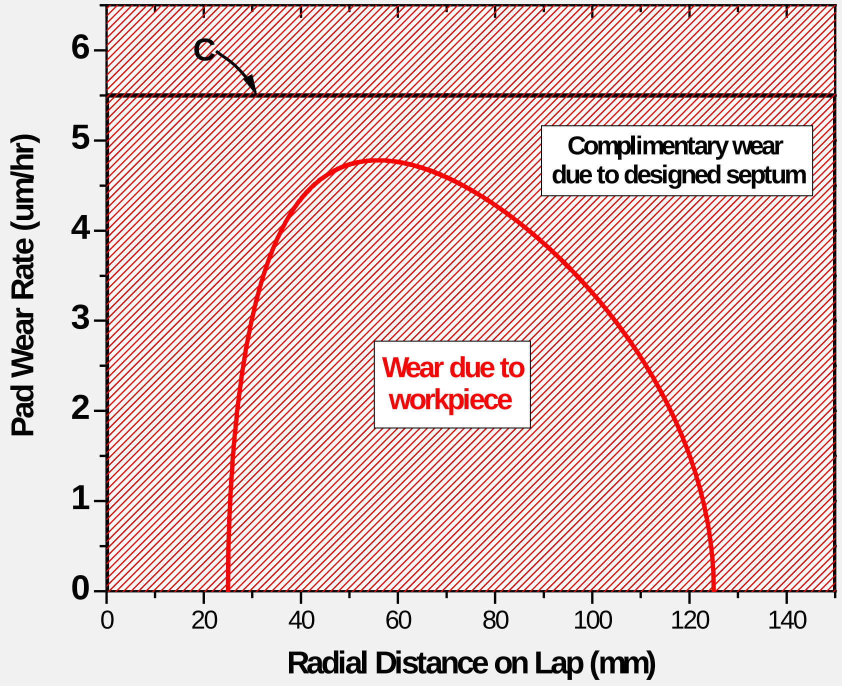

## Determined shape of Septum

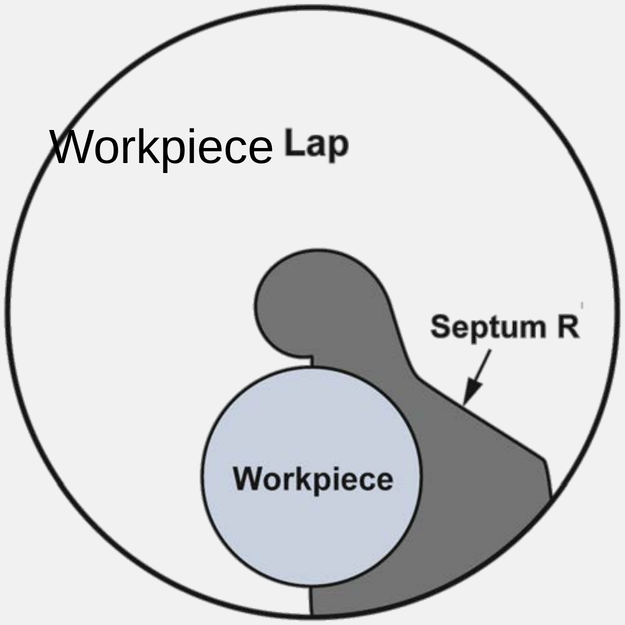

T. Suratwala et. al., IJAGS 3(1) 14-28 (2012).

# Temperature variations across workpiece can be minimized using rotated workpiece and septum

## Temperature on non-rotated workpiece

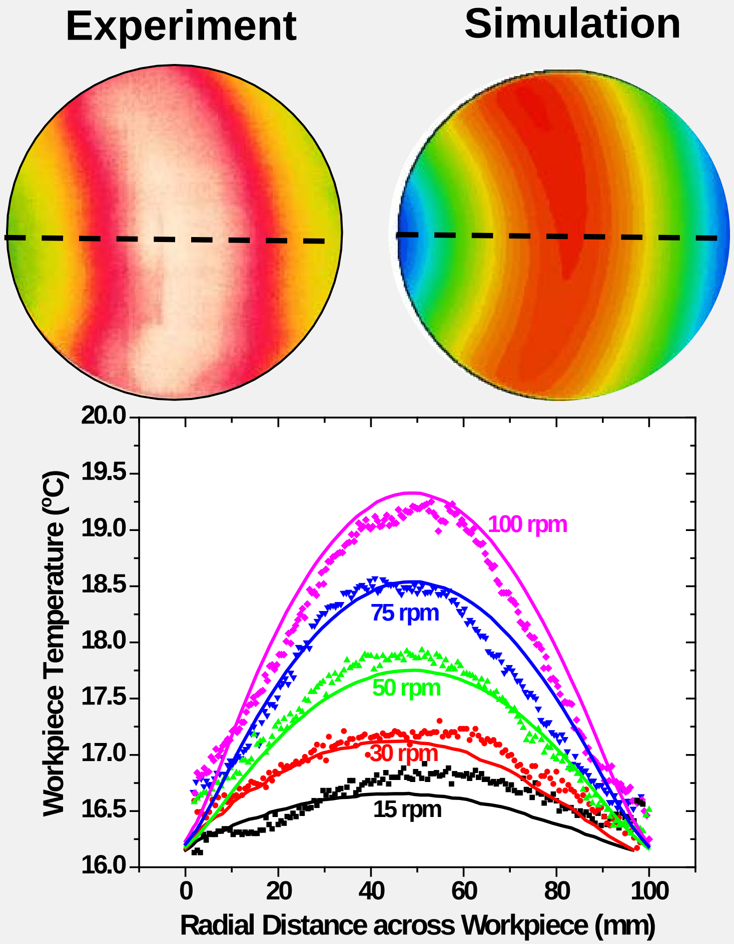

## Temperature variations vs polishing configuration

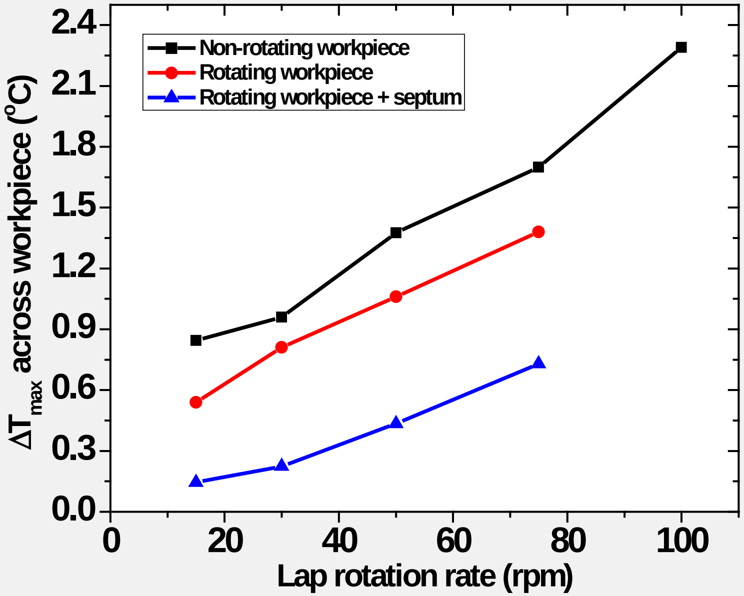

T. Suratwala et al *JACS* 97(6) (2014) 1720.

# Pitch (Stiff) Button Blocking (PBB) and Foam (Compliant) Button Blocking (FBB) allows different workpiece response during polishing for High AR workpieces

## Pitch Button Blocking (PBB)

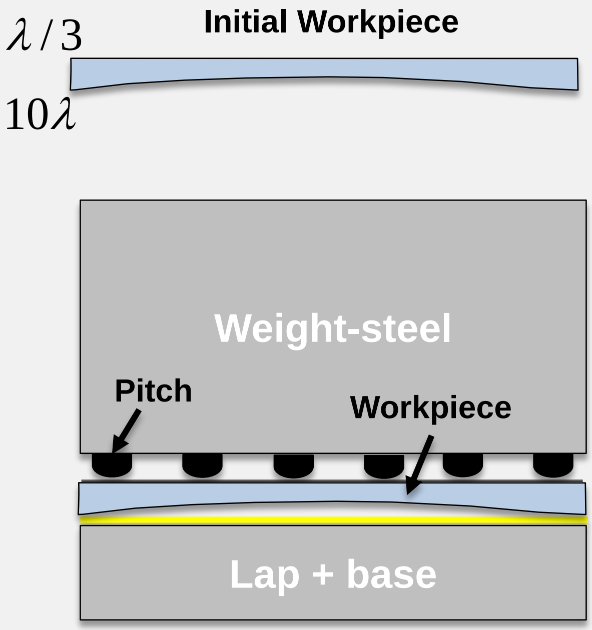

- Workpiece does <u>not conform</u> to lap upon loading
- Allows for surface figure to match lap figure

## Foam Button Blocking (FBB)

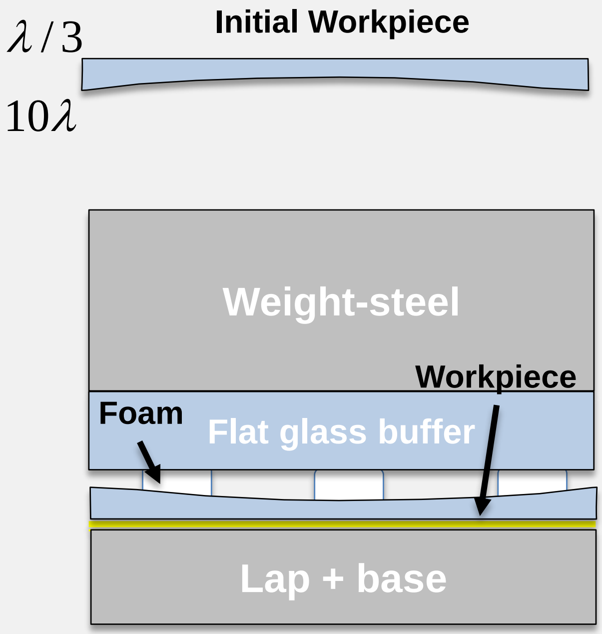

- Workpiece conforms to lap deform upon loading
- Allows for uniform removal on workpiece

# Without stiff blocking, thin workpiece deflects during polishing

**Thick Workpiece (26 x 26 x 4 $cm^3$)**
**FBB (Exp 1034)**

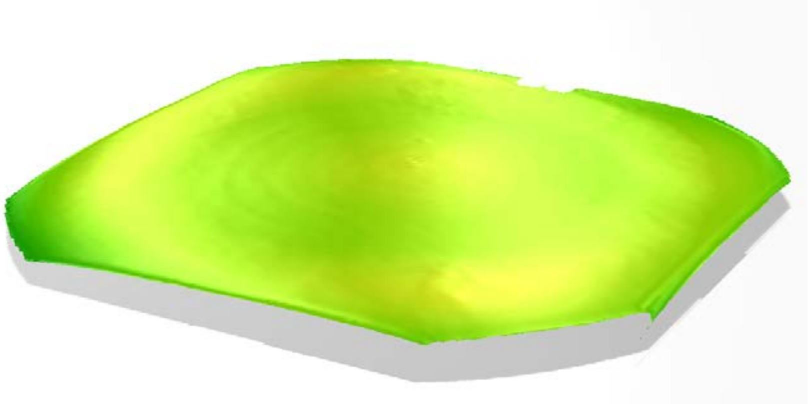

$PV_q$=0.42 um

**Thin Workpiece (26 x 26 x 0.8 $cm^3$)**
**FBB (E1019)**

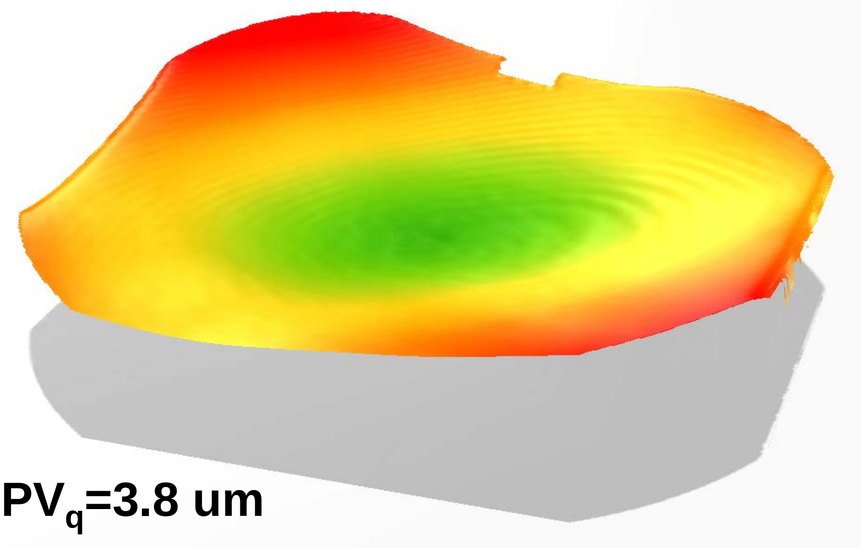

$PV_q$=3.8 um

# Pitch button blocking (PBB) technique prevents workpiece from bending during polishing

## 265 mm (side) x 8 mm (thick) Fused Silica PBB

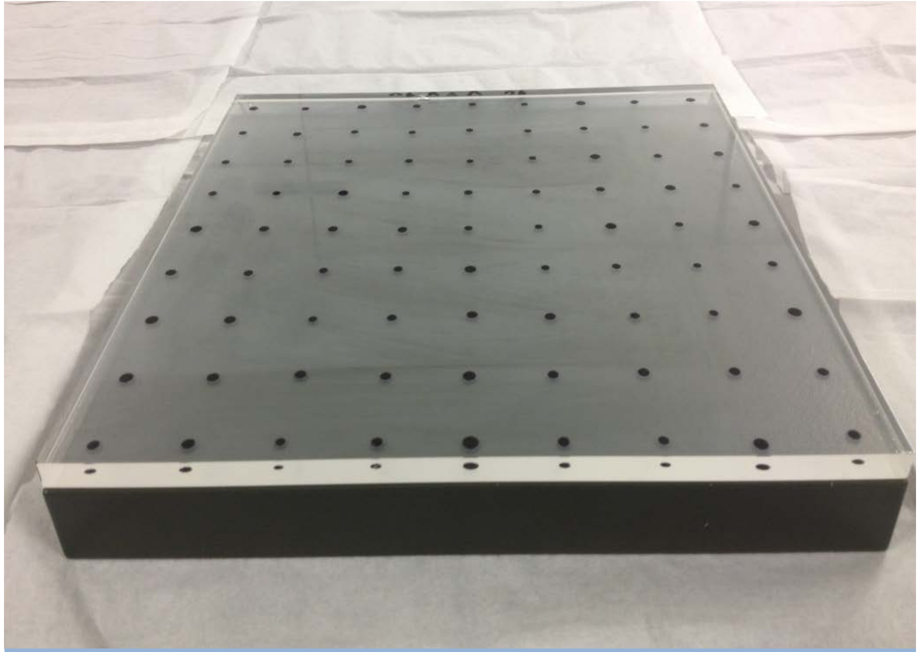

| | |
|---|---|
| **FS** | **ΔPV=0.003 μm** |
| **Phosphate** | **ΔPV=0.035 μm** |

## Model vs Experiment: ΔPV as fn of pitch button area fraction

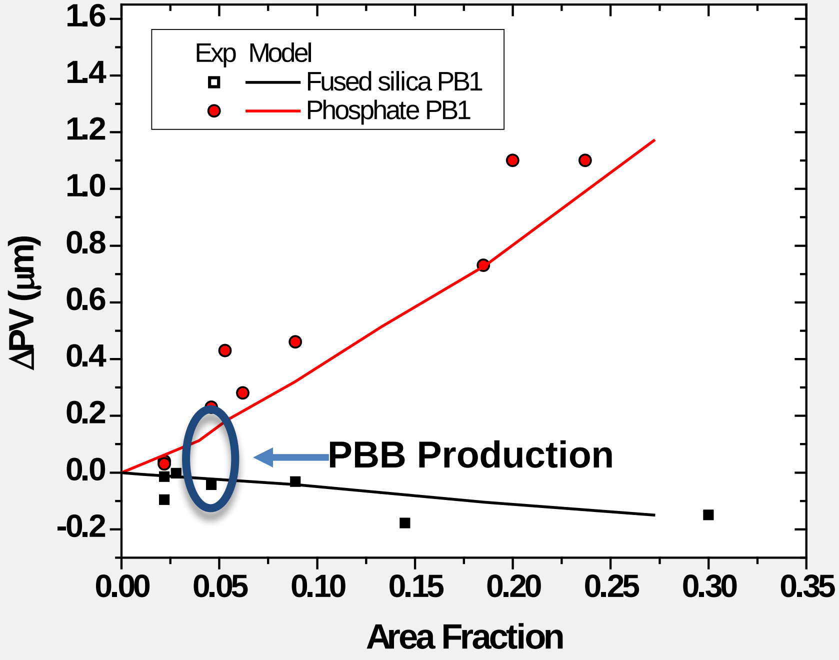

M. Feit et. al., *Applied Optics* 51(35) (2012) 8350-59

# Fine scale radial material non-uniformity is caused by local islands of slurry on the pad

**Schematic representation of islands of slurry on pad**

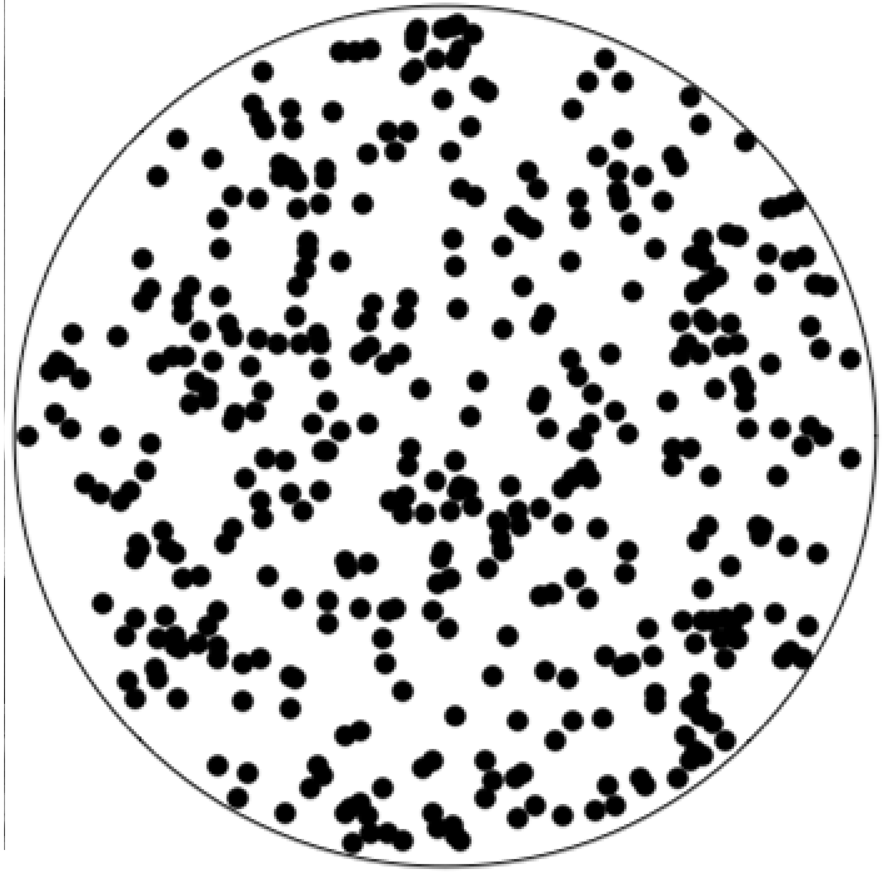

**Optical micrograph of grooves observed on non-rotated workpiece**

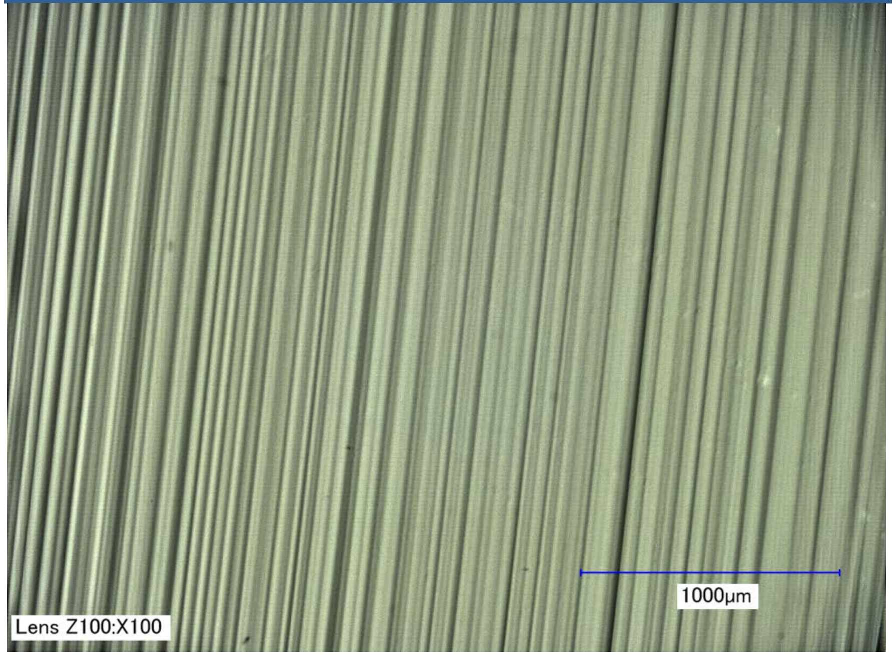

J. Am. Ceram. Soc., 97 [6] 1720–1727 (2014)

# Fine scale radial material non-uniformity is caused by local islands of slurry on the pad

**Schematic representation of islands of slurry on pad**

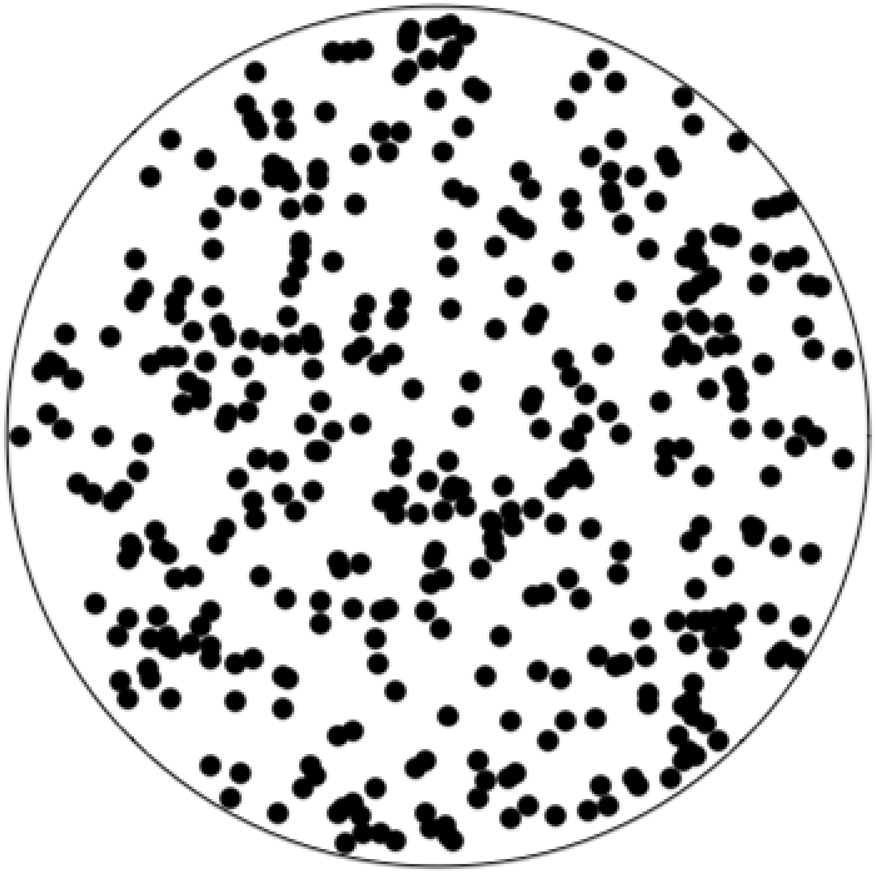

**Optical micrograph of grooves observed on non-rotated workpiece**

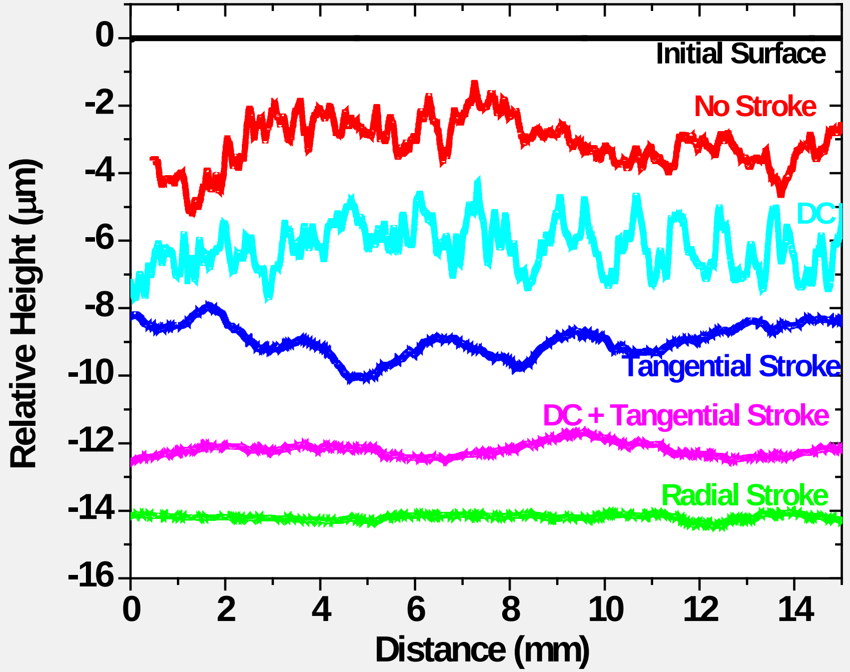

**Radial stroke motion dramatically reduces this non-uniformity**

J. Am. Ceram. Soc., 97 [6] 1720–1727 (2014)

# Residual grinding stress causes a high aspect ratio workpiece to bend

**Surface Figure of S2 (Initial)**

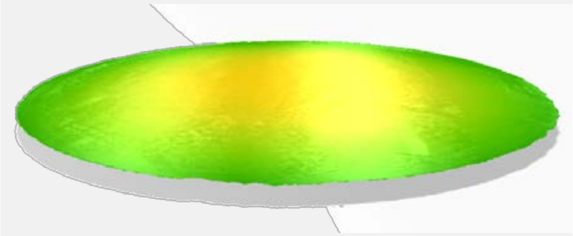

$PV_q = -1.29\ \mu m$

**Surface Figure of S2 (After Grinding S1)**

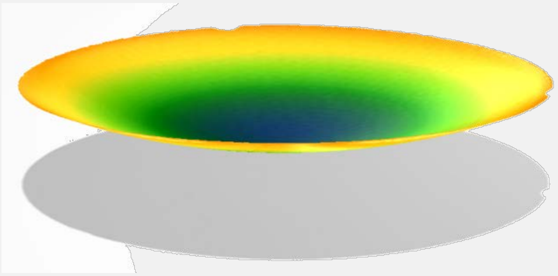

$PV_q = 3.65\ \mu m$

**Surface Figure of S2 (After Grinding/Etching*)**

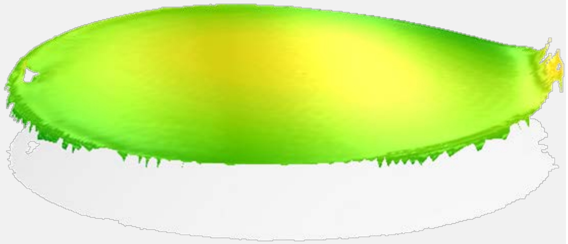

$PV_q = -1.16 \mu m$

**Chemical etching can effectively remove the residual stress and any complications to workpiece-lap mismatch**

T. Suratwala, IJAGS 3(1) 14-28 (2012)

# Convergent Polishing machine (CISR2) is ready for process trials for reducing GDS finishing cost

# Material removal on a workpiece is governed by a large number of phenomena

$$\frac{dh}{dt}(x,y,t)=\underbrace{k_p}\,\underbrace{\mu(x,y,t)}\,\underbrace{v_r(x,y,t)}\,\underbrace{\sigma(x,y,z,t)}$$

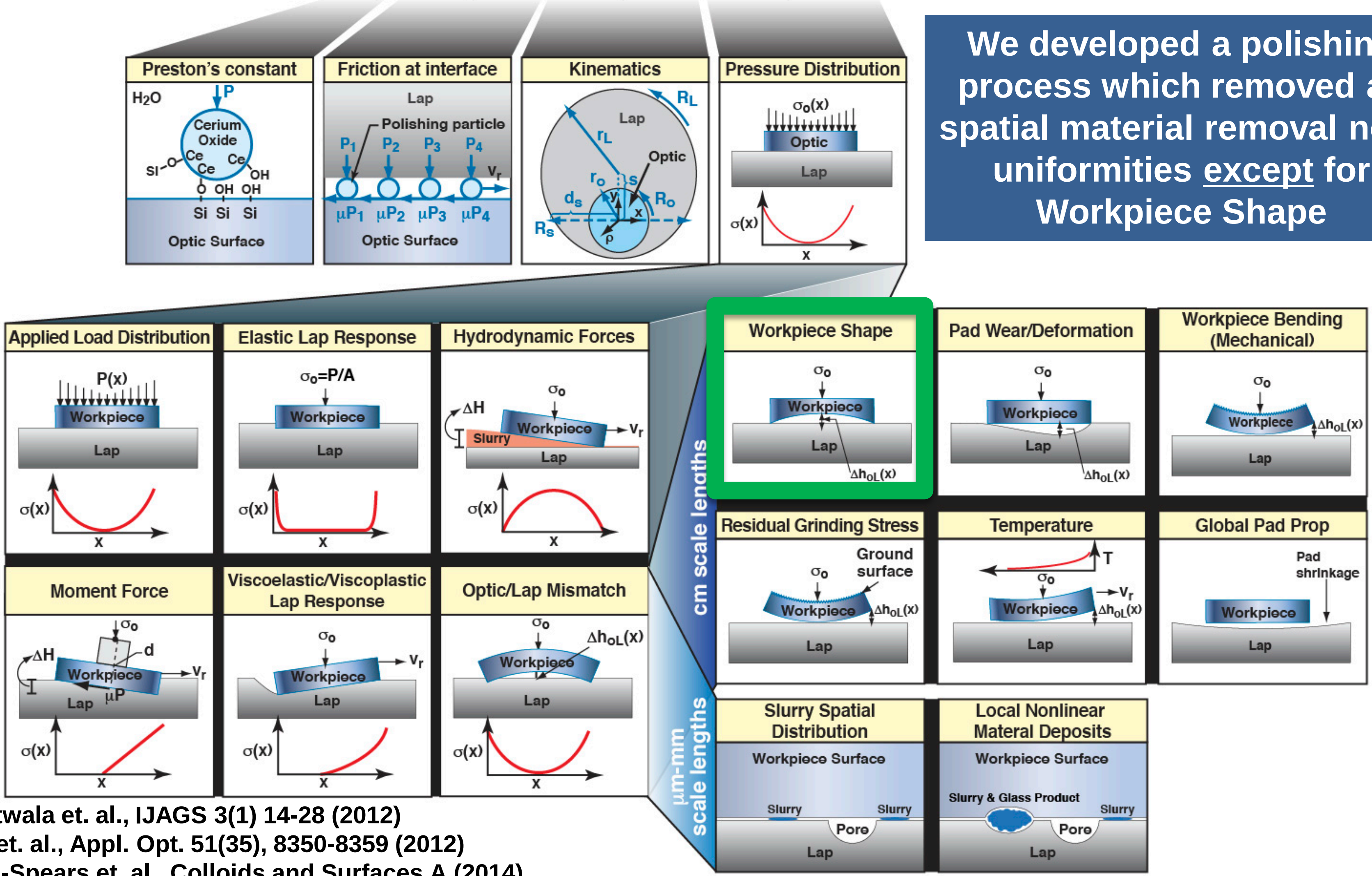

**We developed a polishing process which removed all spatial material removal non-uniformities except for Workpiece Shape**

**T. Suratwala et. al., IJAGS 3(1) 14-28 (2012)**
**M. Feit et. al., Appl. Opt. 51(35), 8350-8359 (2012)**
**R. Dylla-Spears et. al., Colloids and Surfaces A (2014)**

# Convergent Polishing works on the principle of time varying pressure distribution due to workpiece-lap mismatch of workpiece shape

**Workpiece shape**

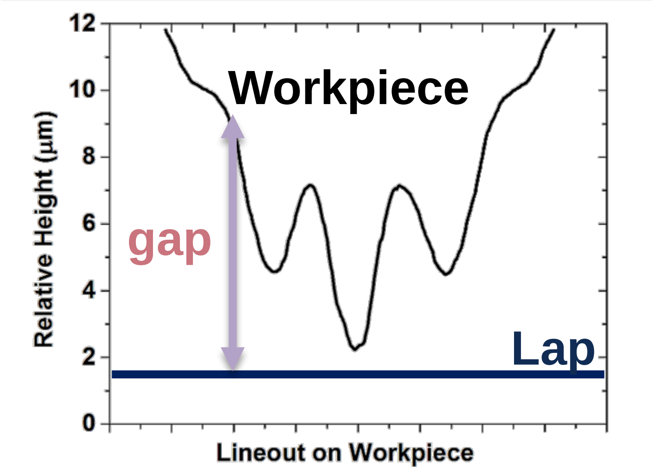

**Pressure Distribution**

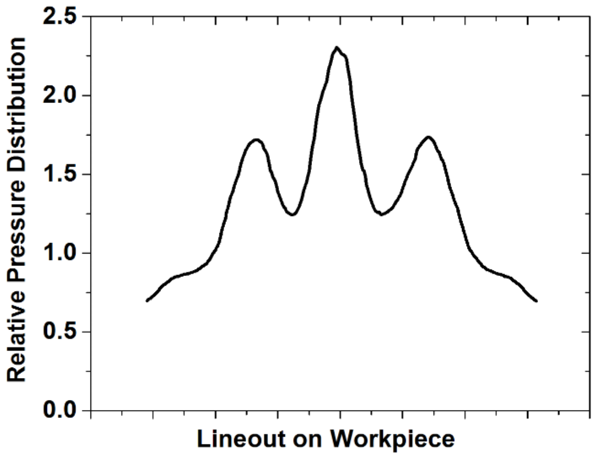

## Convergent Polishing Concept

- Material removal non-uniformity is due only to workpiece-lap mismatch (i.e. gap) due to workpiece shape
- Higher pressures where gap is smallest, leading to greater removal rate
- Removal changes gap, reducing pressure
- Convergence reached when pressure is uniform (workpiece & lap will have same shape)

# A novel septum has been designed to counteract non-uniform wear on the pad

## Pad wear vs lap radius due to workpiece and engineered septum

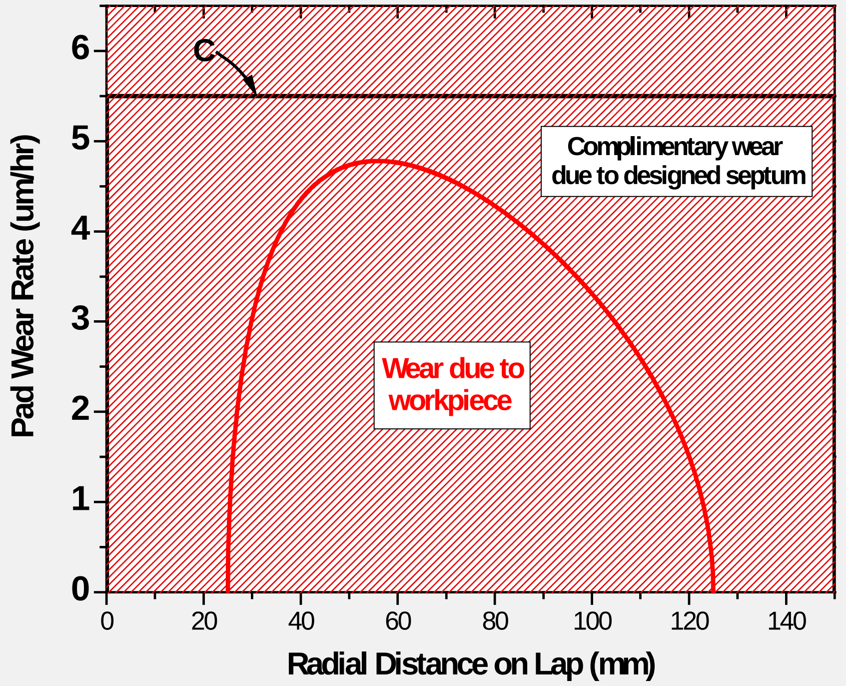

## Determined shape of Septum

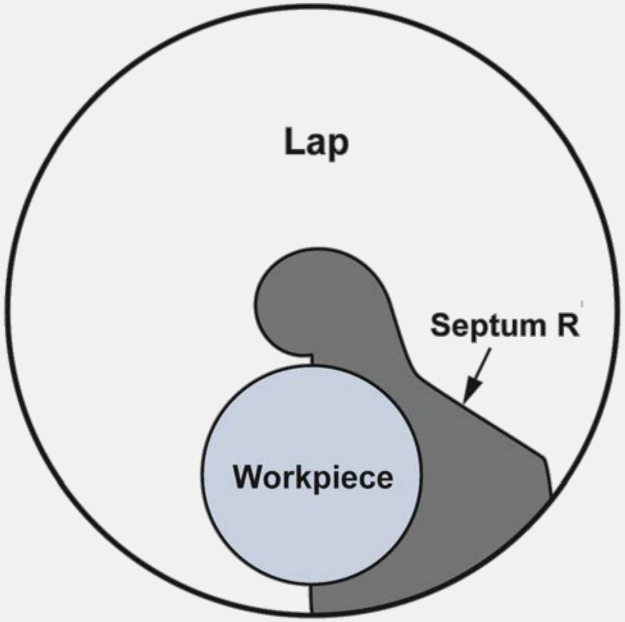

T. Suratwala et. al., IJAGS 3(1) 14-28 (2012).

# Convergent Polishing converges workpiece (regardless of its initial shape) to final shape in a single iteration without process changes

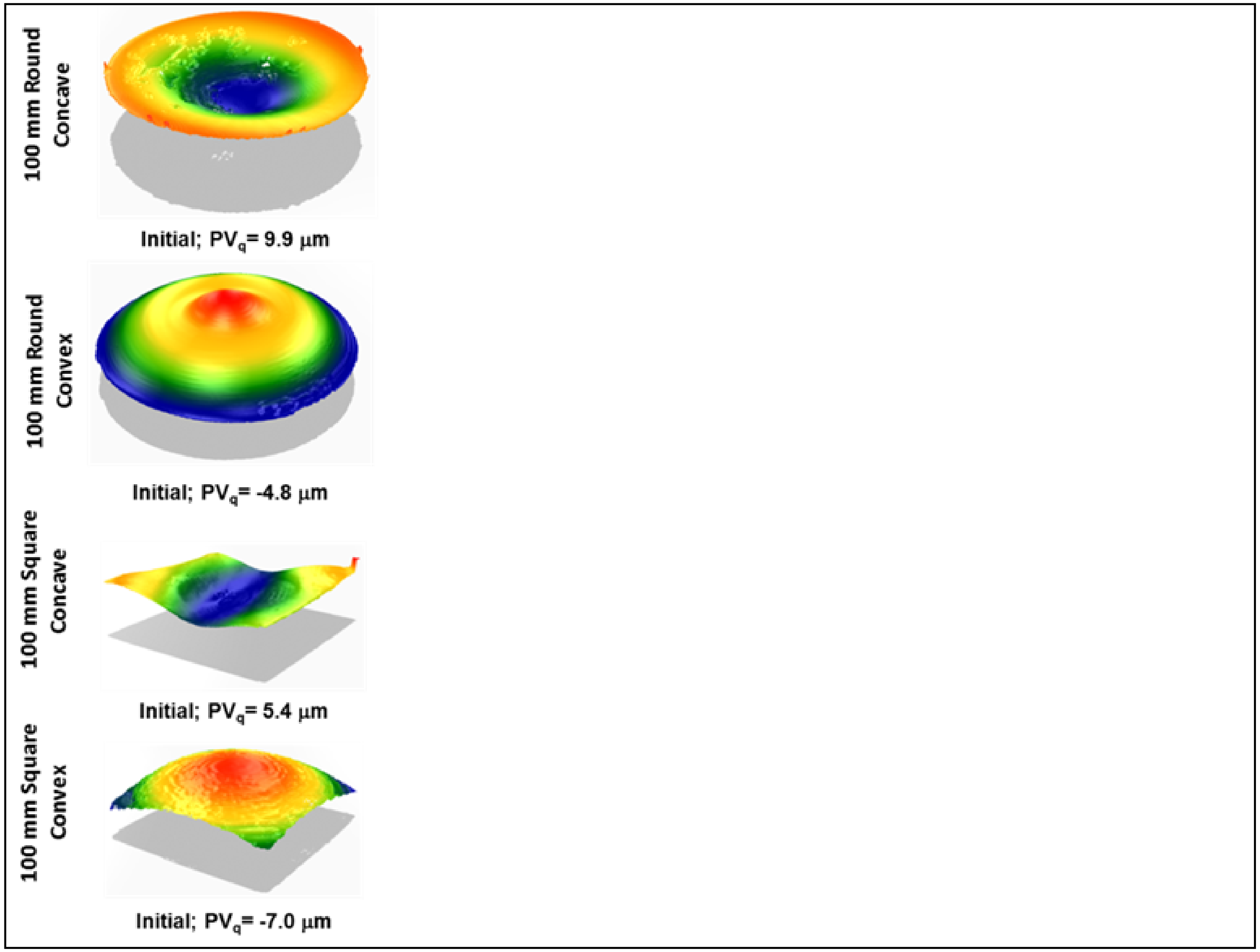

**US Patent Application, T.Suratwala et. al. "Method and system for convergent polishing"**
**WO 2012129244 A1 (September 27, 2012)**

# Convergent Polishing can and has been applied to numerous optic shapes, materials & sizes

**Flats**

**Spheres**

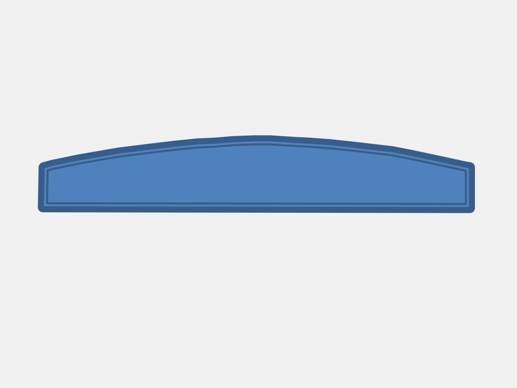

**Symmetric Asphere**

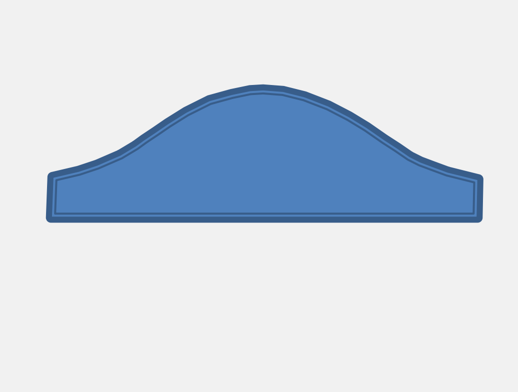

| | |
|---|---|
| **Shape** | Round, square, rectangular |
| **Sizes** | 10 cm →26 cm → 43 cm |
| **Aspect ratios (AR)** | 10 cm >50 AR with PBB/EBB, 26.5 cm >50 AR with PBB/EBB |
| **Materials** | Fused silica, Phosphate, Borosilicate |
| **Stability** | λ/2 for 100+ Workpieces (>800 hrs) |

# The complexities of polishing has made is difficult to scientifically design, optimize a process for a given material

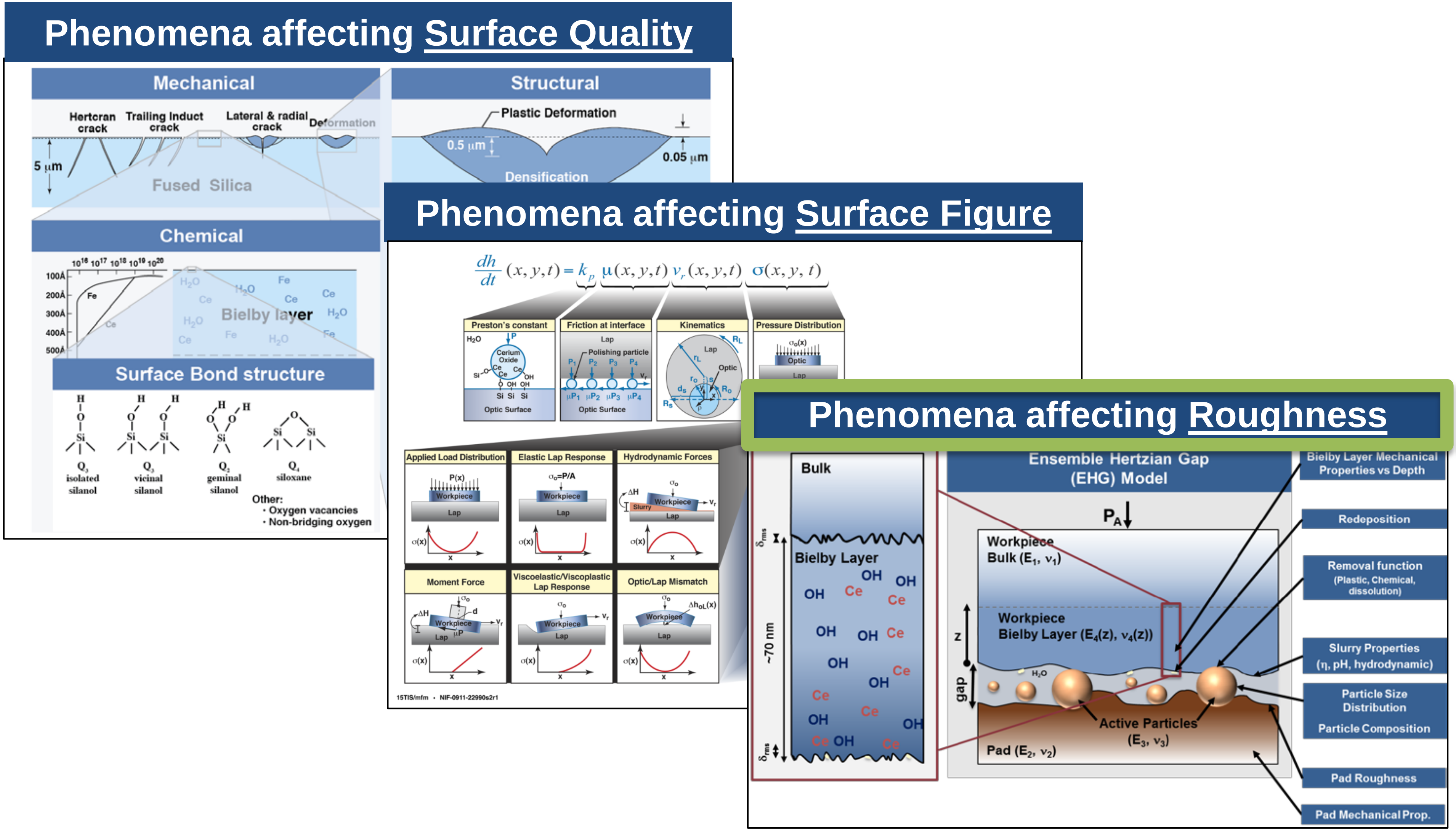

## Phenomena affecting Surface Quality

## Phenomena affecting Surface Figure

$$\frac{dh}{dt}(x,y,t) = \underbrace{k_p}\ \underbrace{\mu(x,y,t)}\ \underbrace{v_r(x,y,t)}\ \underbrace{\sigma(x,y,t)}$$

## Phenomena affecting Roughness

# Schematic model of the parameters that affect roughness during polishing

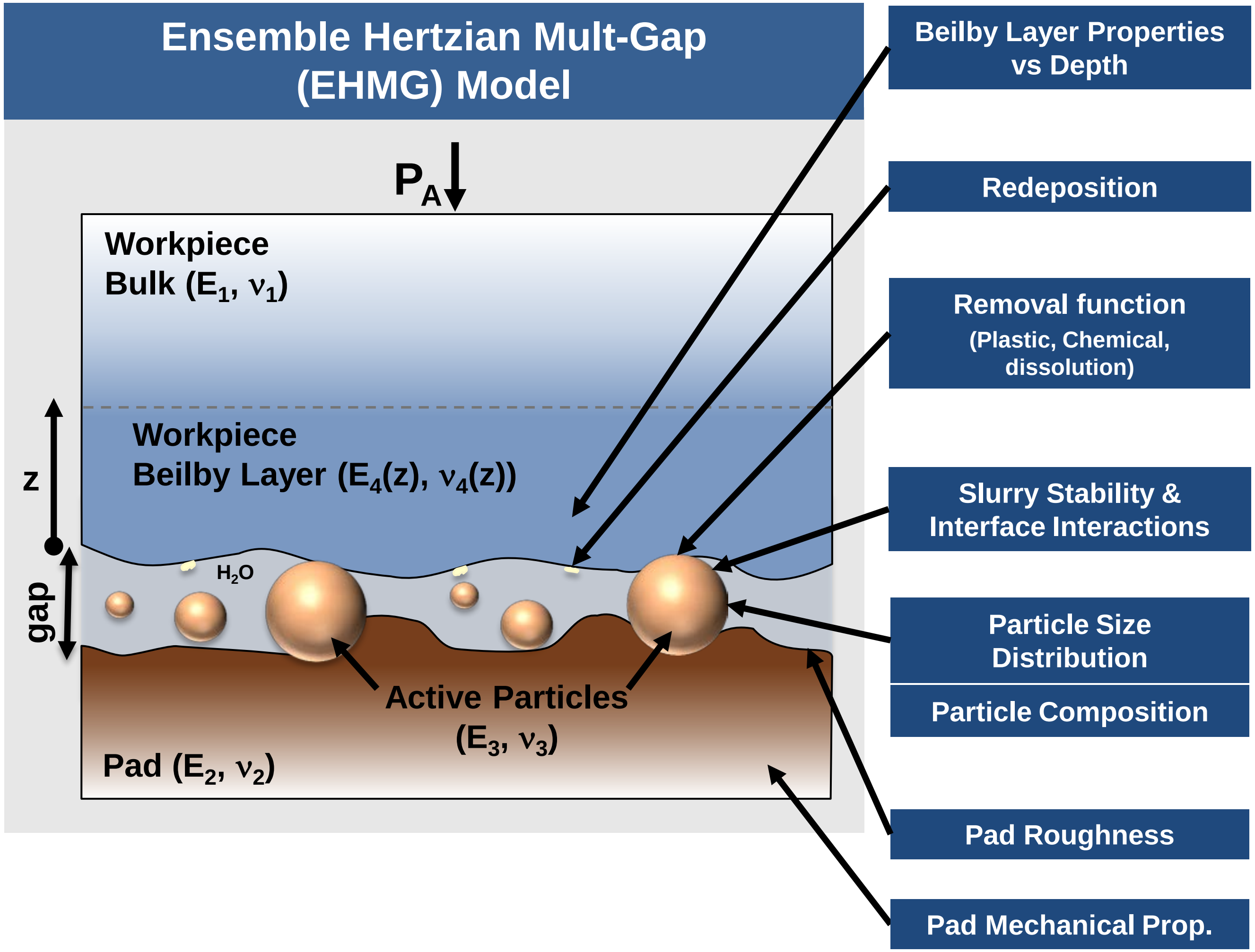

**Ensemble Hertzian Mult-Gap (EHMG) Model**

Beilby Layer Properties vs Depth

Redeposition

Removal function
(Plastic, Chemical, dissolution)

Slurry Stability & Interface Interactions

Particle Size Distribution

Particle Composition

Pad Roughness

Pad Mechanical Prop.

# Polishing was conducted using the Convergent Polishing Method (ceria or silica slurry on various glasses using a polyurathane pad)

**CISR0 polisher**

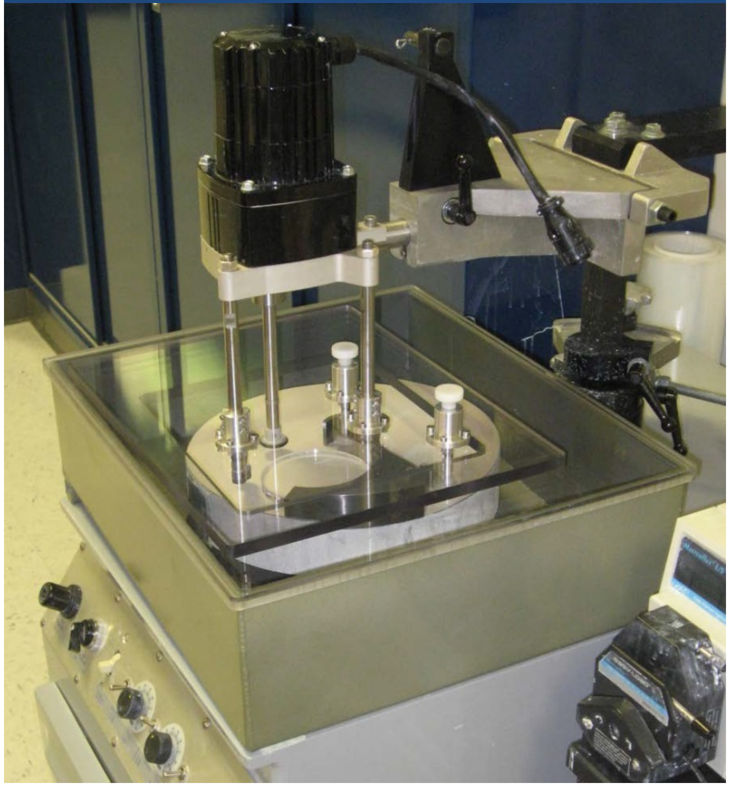

**CISR1 polisher**

# SIMS measurements show Ce penetration into polished surface is not due to diffusion & K penetration is consistent with diffusion

**[Ce] profile on polished fused silica surface as fn of polishing velocity**

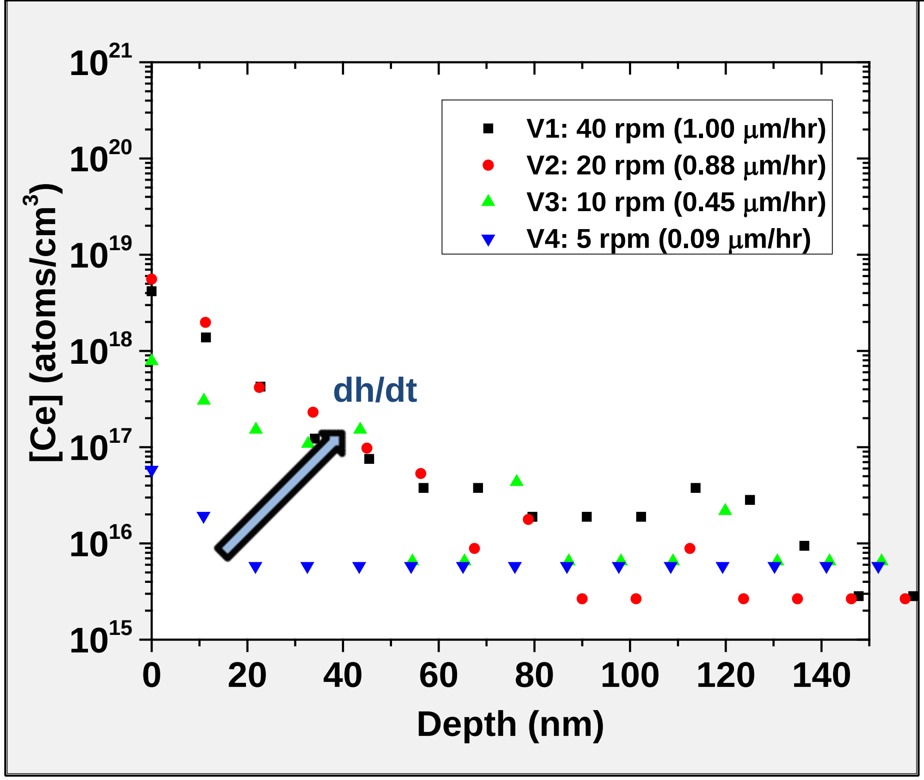

**[K] profile on polished fused silica surface as fn of polishing velocity**

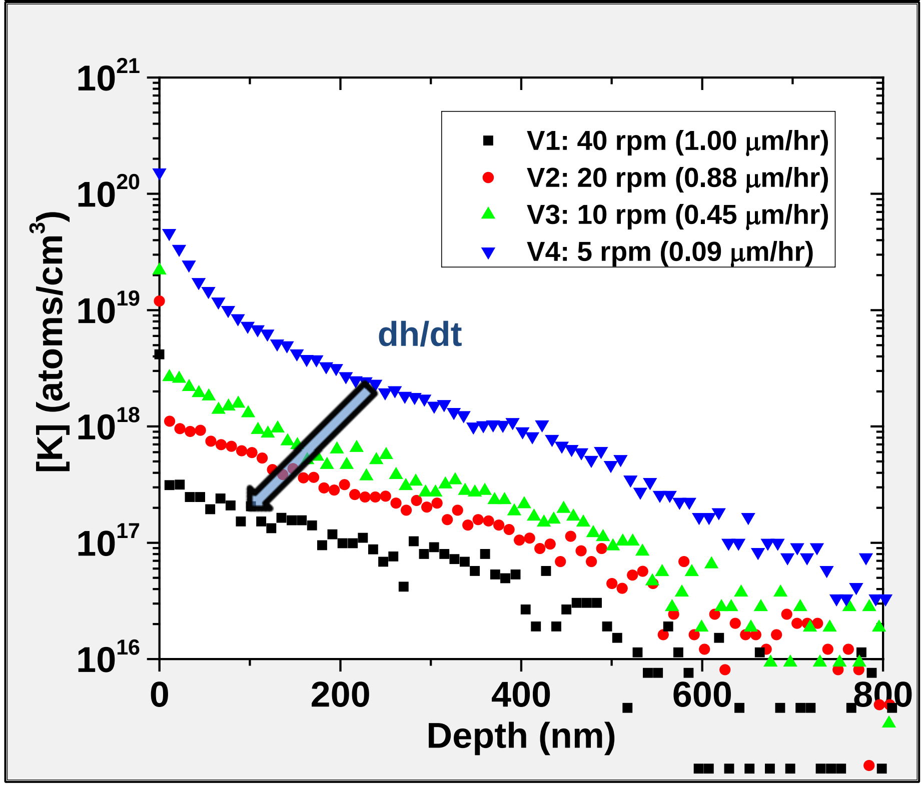

SIMS (note Si $2\times10^{22}$ atom/cm$^3$)

# $[Ce]_s$ increases with polishing removal rate & is weakly dependent on other polishing parameters

## [Ce] of polished surface layer for variety of polishing conditions

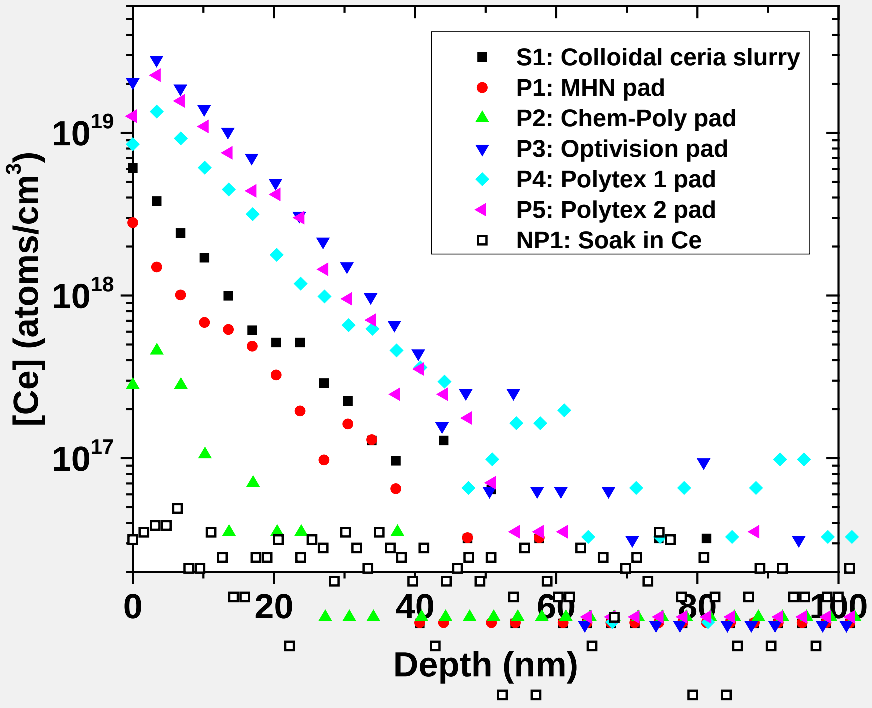

T. Suratwala et. al., *J. Am. Cer. Soc* 98(8) (2015) 2396

## Correlation between $[Ce]_s$ and removal rate (dh/dt)

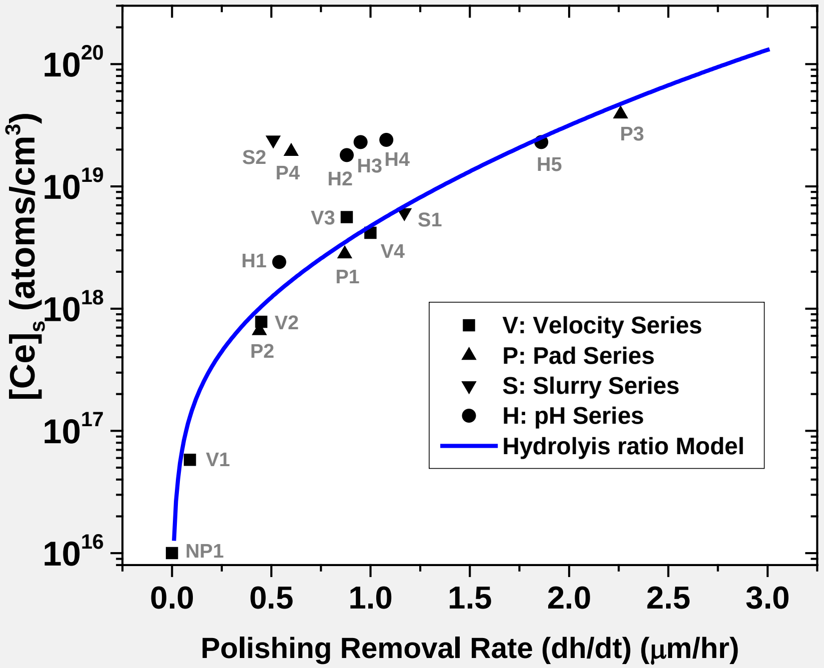

# The penetration of Ce into silica surface during polishing is proposed to be a competition of hydrolysis reactions

**Mechanism**

1) Removal rate increases
2) Interface temperature increases
3) Arrhenius increase to r
4) Greater Ce surface deposition

**Condensation**

$$\underset{\text{glass}}{\equiv \mathrm{Si\text{-}OH}} + \underset{\text{particle}}{\mathrm{HO\text{-}Ce} \equiv} \rightarrow \equiv \mathrm{Si\text{-}O\text{-}Ce} \equiv + \mathrm{H_2O}$$

**Silica Hydrolysis**

$$\equiv \mathrm{Si\text{-}O\text{-}Si\text{-}O\text{-}Ce\text{-}O\text{-}Ce} \equiv + \mathrm{H_2O} \rightarrow \equiv \mathrm{Si\text{-}OH} + \mathrm{HO\text{-}Si\text{-}O\text{-}Ce\text{-}O\text{-}Ce} \equiv$$

**Ceria Hydrolysis**

$$\equiv \mathrm{Si\text{-}O\text{-}Si\text{-}O\text{-}Ce\text{-}O\text{-}Ce} \equiv + \mathrm{H_2O} \rightarrow \equiv \mathrm{Si\text{-}O\text{-}Si\text{-}O\text{-}Ce\text{-}OH} + \mathrm{HO\text{-}Ce} \equiv$$

**r =Ceria Hydrolysis rate/ Silica Hydrolysis rate**

# K continues to diffuse into the workpiece even after polishing

## Proposed 2-step diffusion model

**Step 1: During polishing, K diffuses into surface via moving boundary diffusion**

$$C(x) = C_s exp\left(-\frac{\frac{dh}{dt}x}{D}\right)$$

**Step 2: After polishing, K continues to diffuse into fused silica surface (has initial condition from step 1 and no moving boundary)**

$$\frac{d}{dx}\left(D\frac{dC}{dx}\right) = \frac{dC}{dt}$$

## Simulation vs Experiment

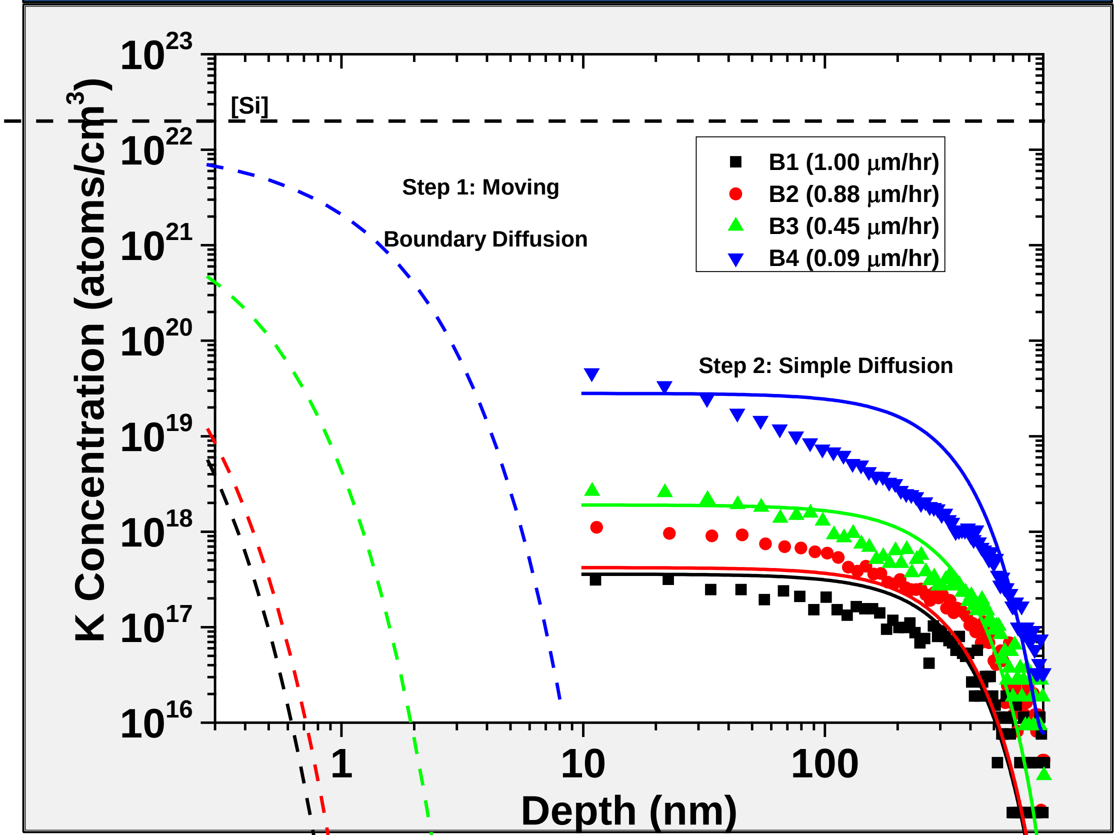

$D=1.5\times10^{-16}$ cm$^2$/sec $C_s=10^{21}$ cm$^{-3}$/$u_x$
$C_b=0$ atoms/cm$^3$ t=2 weeks

Suratwala et. al. *J. Am. Cer. Soc.* (5/2015)

# Schematic Model of the parameters that affect roughness during polishing

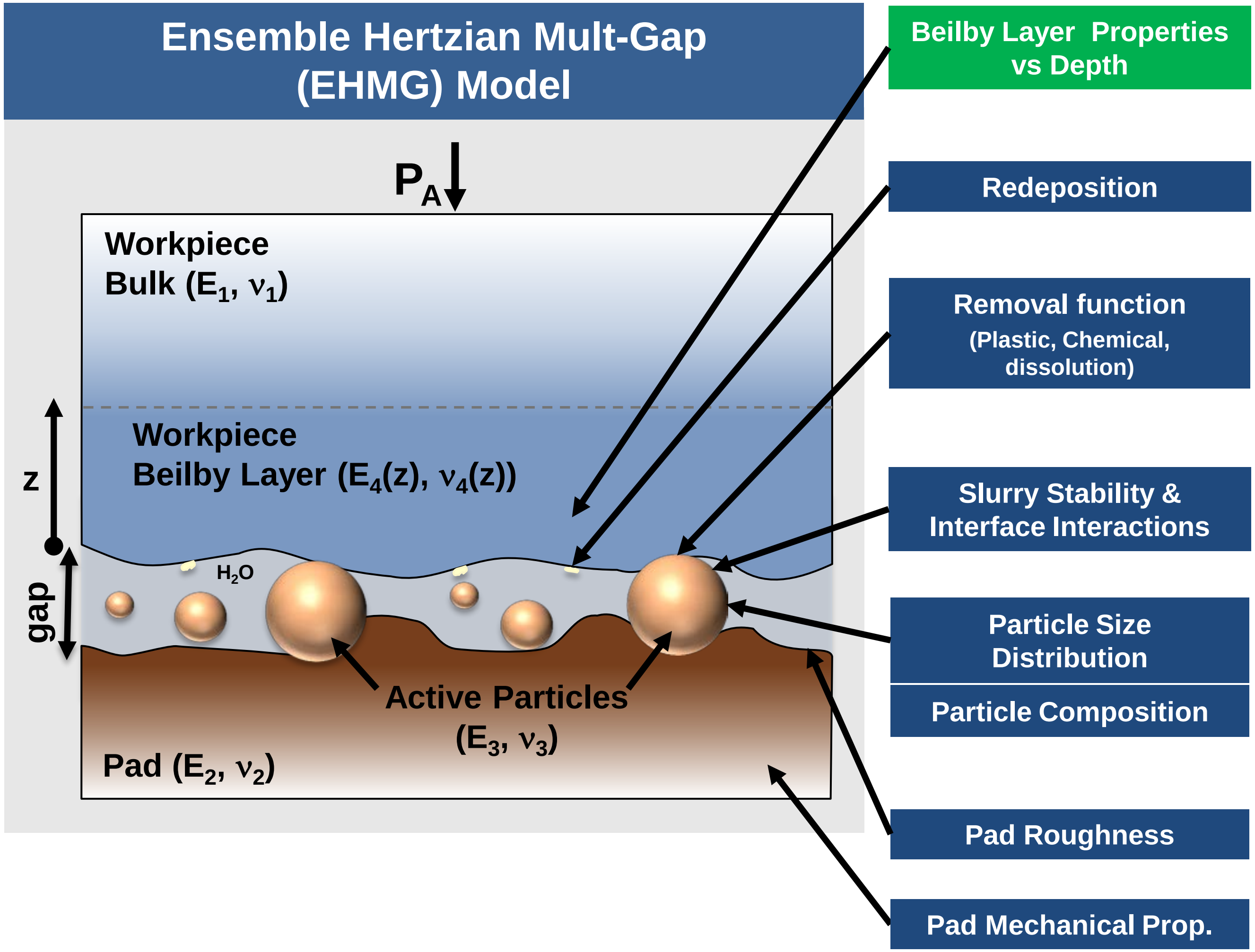

Beilby Layer Properties vs Depth

Redeposition

Removal function (Plastic, Chemical, dissolution)

Slurry Stability & Interface Interactions

Particle Size Distribution

Particle Composition

Pad Roughness

Pad Mechanical Prop.

# The removal volume for a single polishing particle was determined from multi-pass nanoscratching to account densification effects

## LHG-8 phosphate glass: scratches at 110 μN

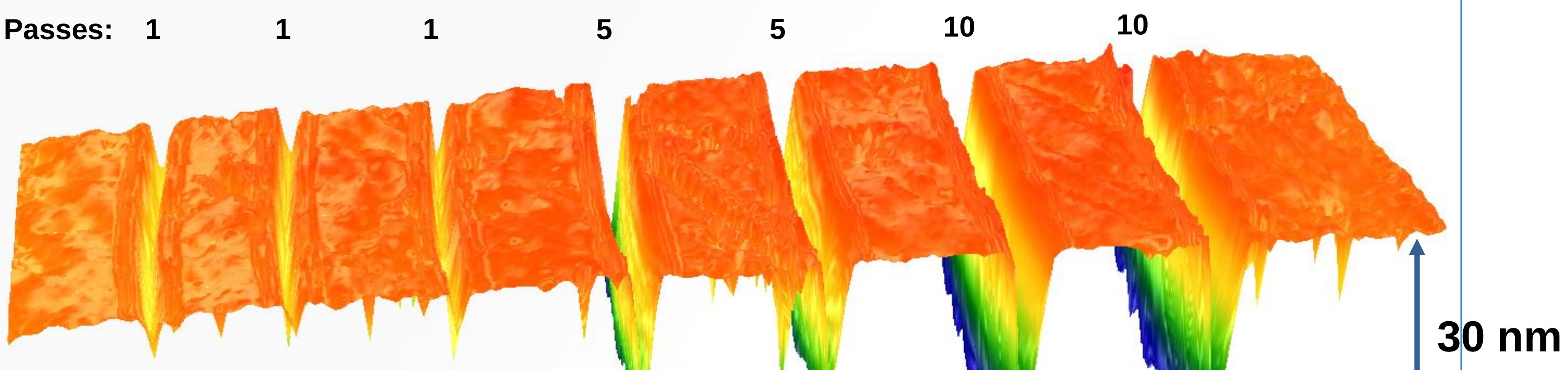

N. Shen et. al., *J. Am. Cer. Soc* (2016) 1-8

# Fused silica and BK7 show little load dependence on permanent deformation; changes in Bielby layer of fused silica influences depth

## AFM images of nanoscratches on different surfaces at various loads

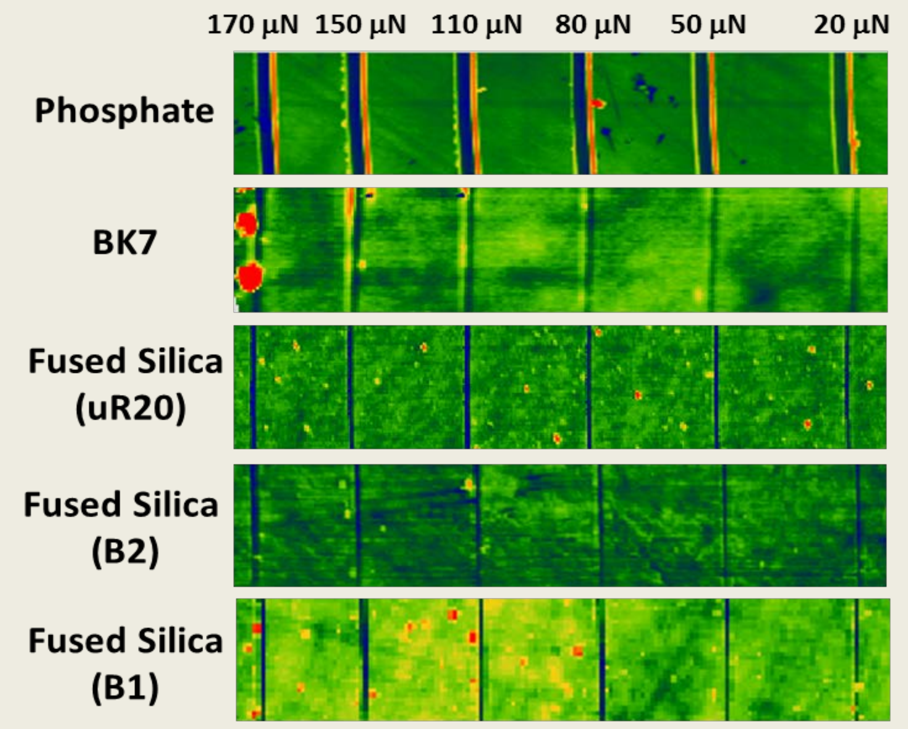

## Cross-section of nanoscratches at various loads on various substrates

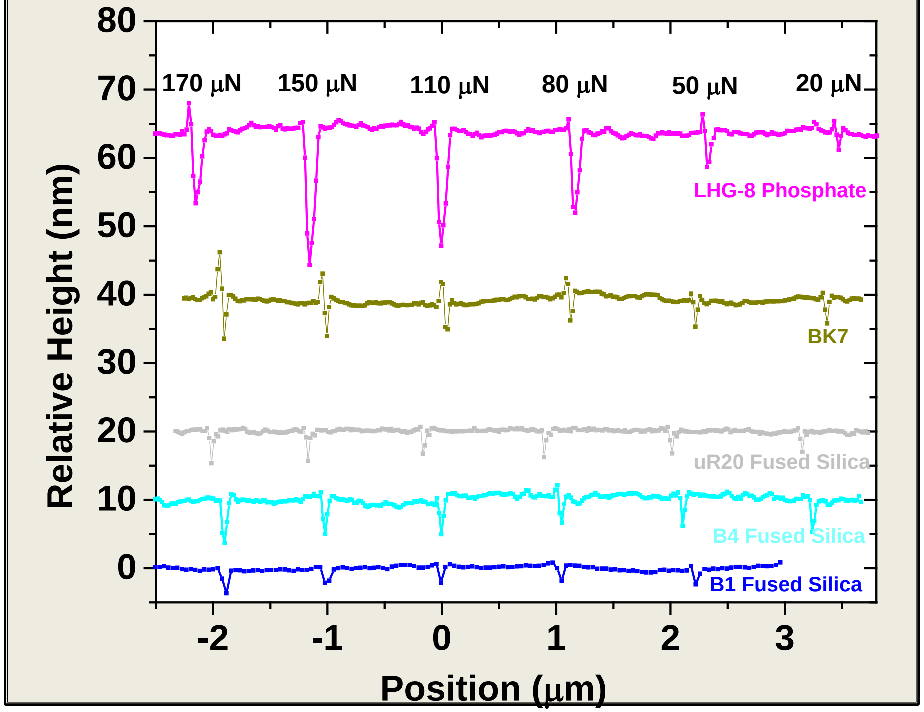

# A detailed description of the removal function has been determined for various glasses aiding to the prediction of roughness

## Determined removal function for single particle on various glasses

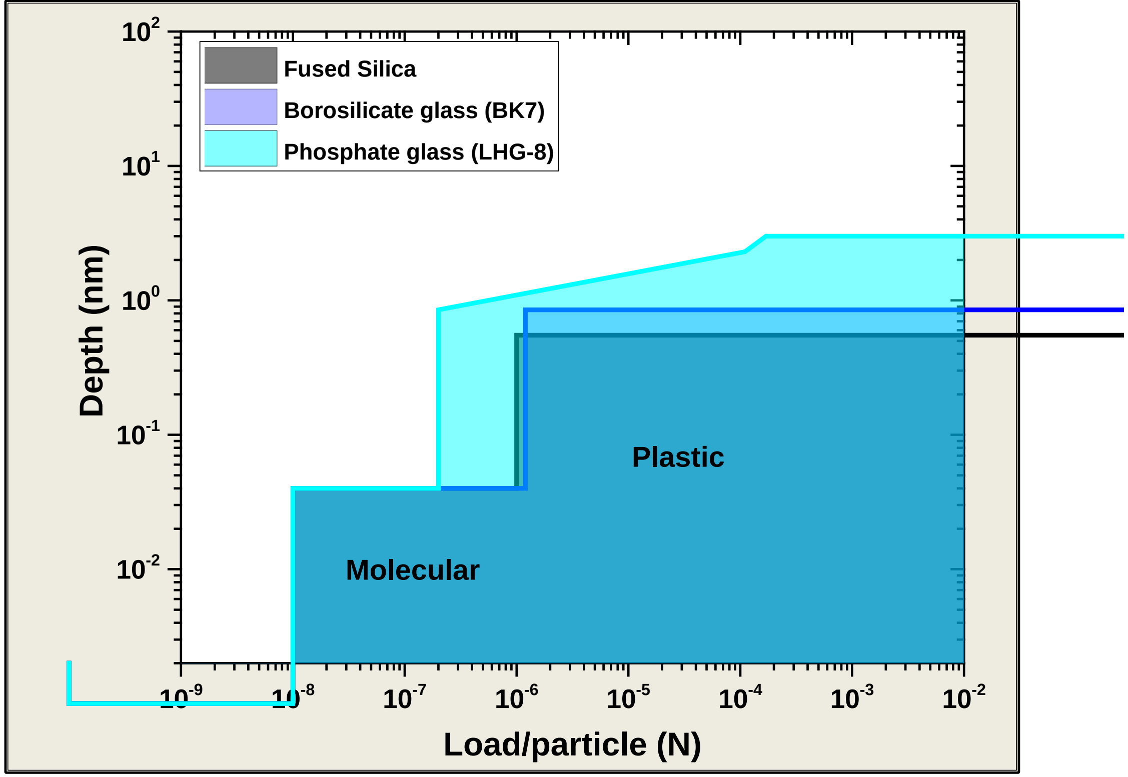

N. Shen et. al., *J. Am. Cer. Soc* (2016) 1-8

- **Removal occurs over two regimes during polishing (molecular and plastic)**
- **Fused silica and BK7 have similar removal functions**
- **Removal function for phosphate glass is higher**
- **Combining removal function with load/particle distribution allows for predicting roughness**

# Schematic model of the parameters that affect roughness during polishing

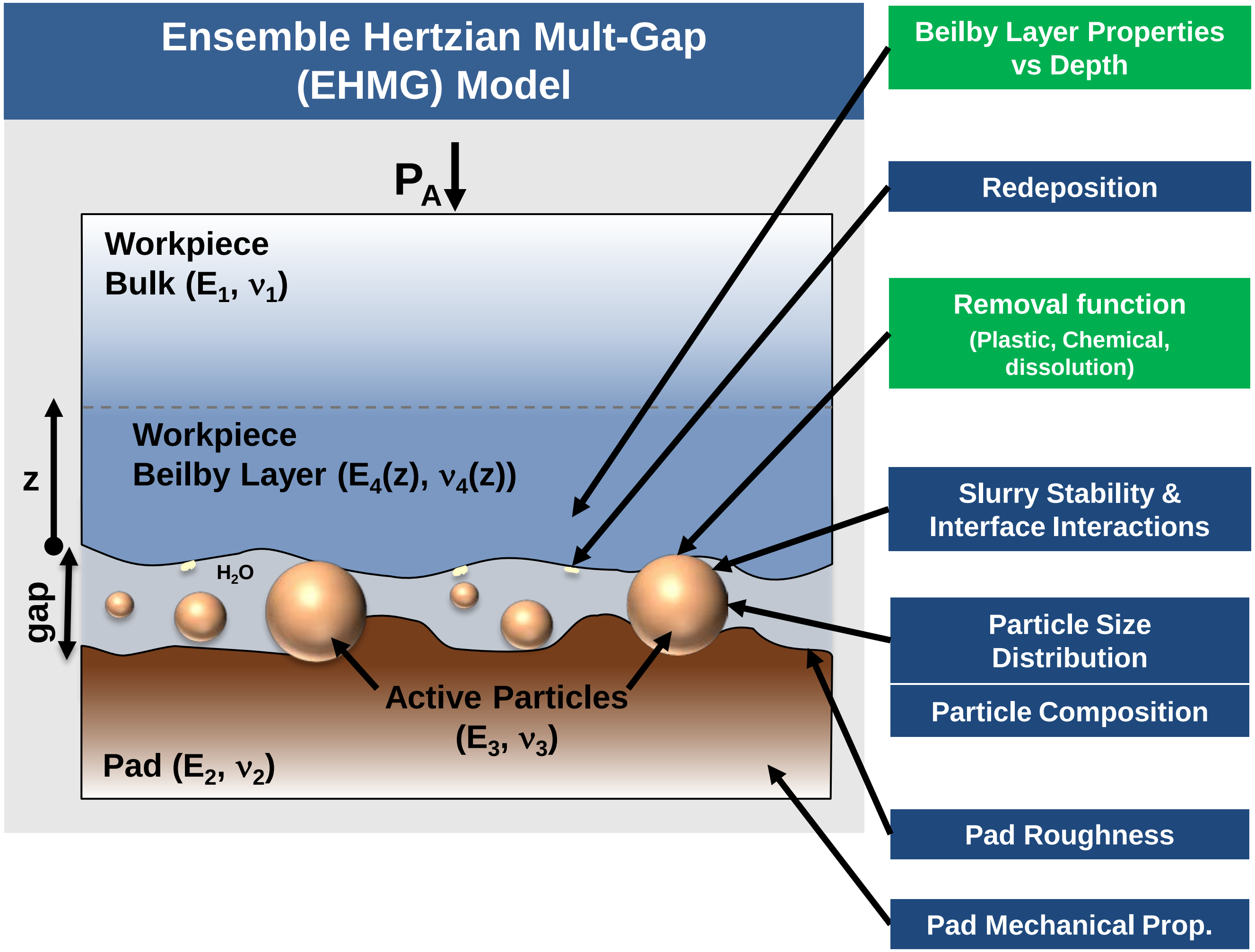

**Ensemble Hertzian Mult-Gap (EHMG) Model**

Beilby Layer Properties vs Depth

Redeposition

Removal function
(Plastic, Chemical, dissolution)

Slurry Stability & Interface Interactions

Particle Size Distribution

Particle Composition

Pad Roughness

Pad Mechanical Prop.

# Slurry's PSD* strongly correlates with workpiece roughness and removal rate

## Measured PSD of ceria slurries

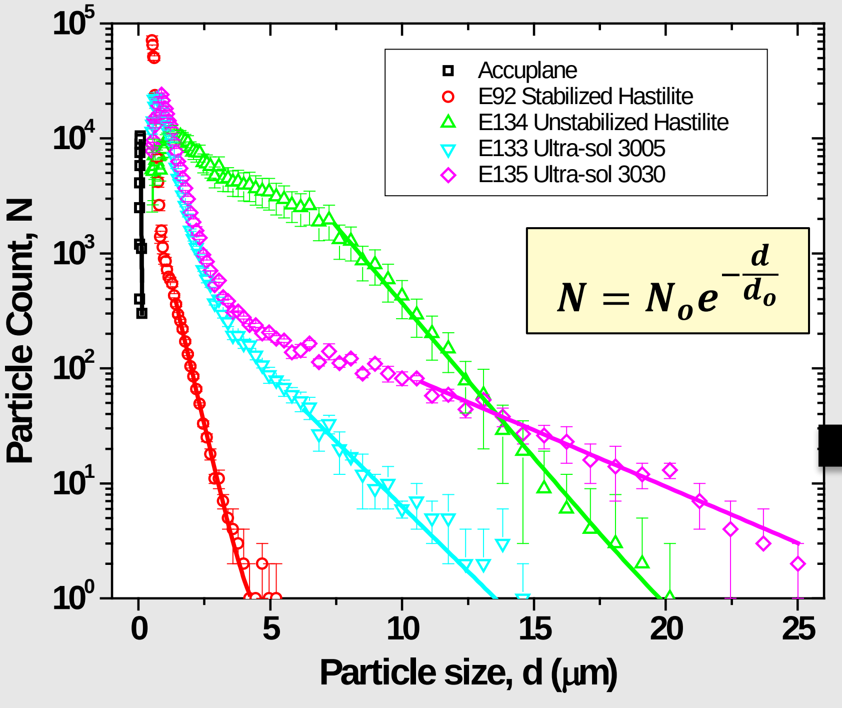

$$N = N_o e^{-\frac{d}{d_o}}$$

**The tail end of each slurry follows a single exponential distribution**

T. Suratwala et. al., *J. Am. Cer. Soc* 97(1) (2014) 81

## Exponent constant in PSD of slurry vs RMS roughness of polished surface

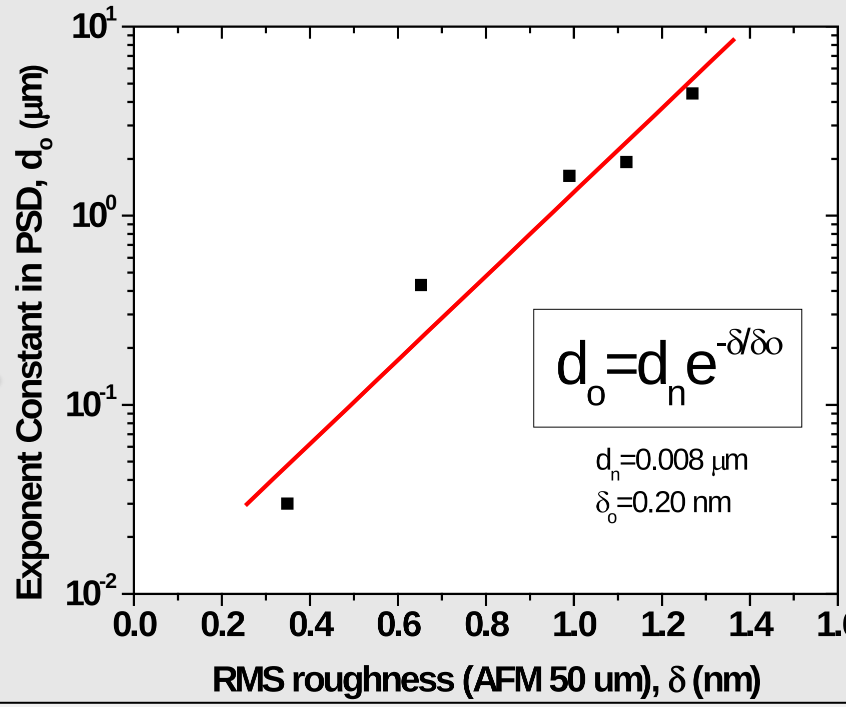

$$d_o = d_n e^{-\delta/\delta o}$$

$d_n$=0.008 μm
$\delta_o$=0.20 nm

**The slope of the slurry's PSD quantitatively scales with the rms roughness**

*Particle size distribution

# Pad topography during polishing strongly influences removal rate

**MHN Pad Surface Topology (Confocal Microscope Images) with various surface treatments**

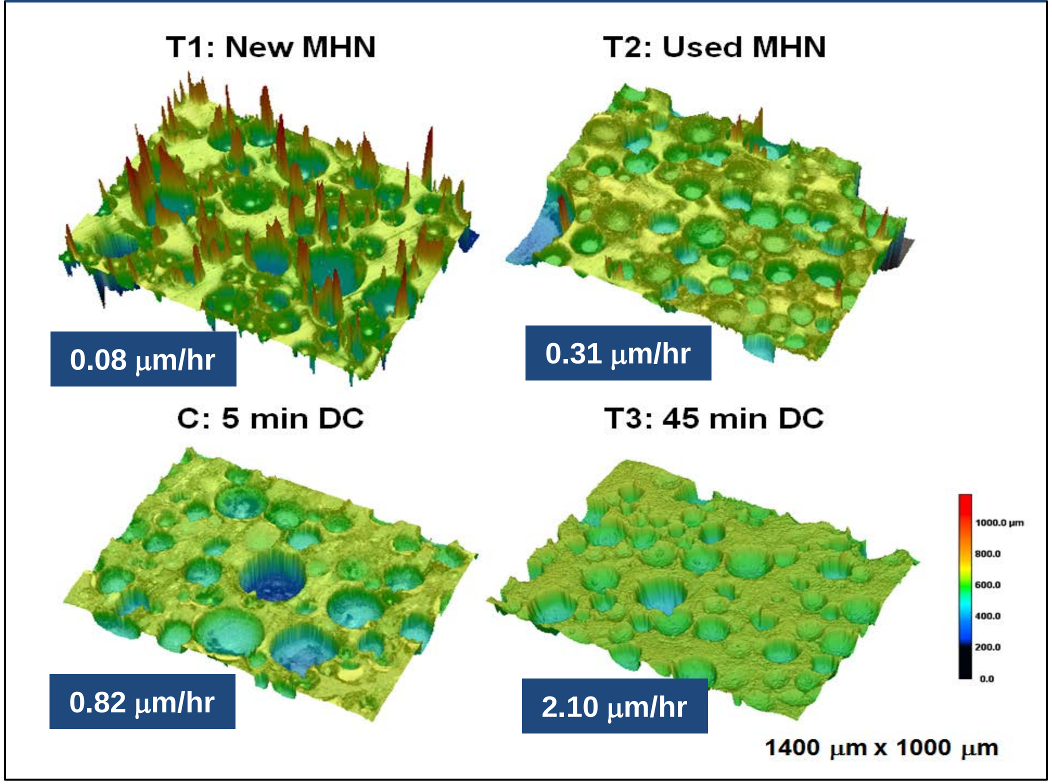

**Pad Height Histograms**

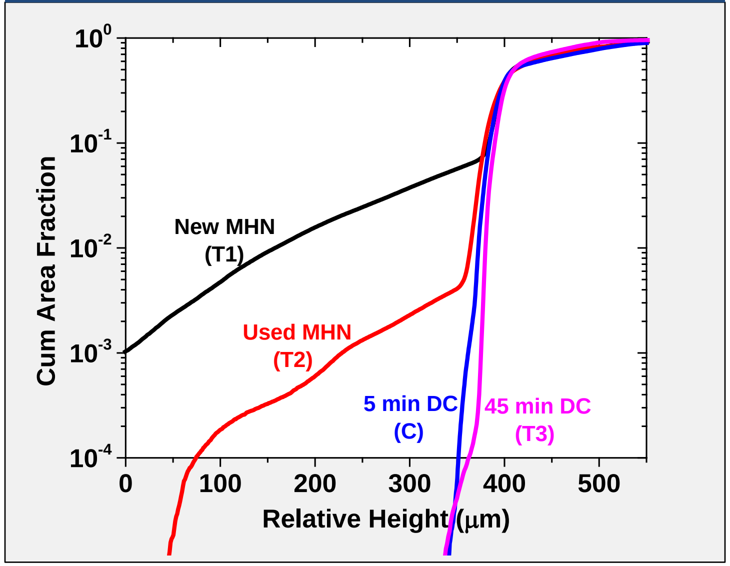

- Tall pad asperities (100’s μm) are removed with diamond conditioning pad treatment
- Removal rate increased from 0.08 μm/hr to 2.10 μm/hr; 26x increase

# EHMG (Esemble Hertzian Multi-Gap) polishing model accounts for both slurry PSD & pad topology to determine RR and roughness

**EHMG Model Setup**

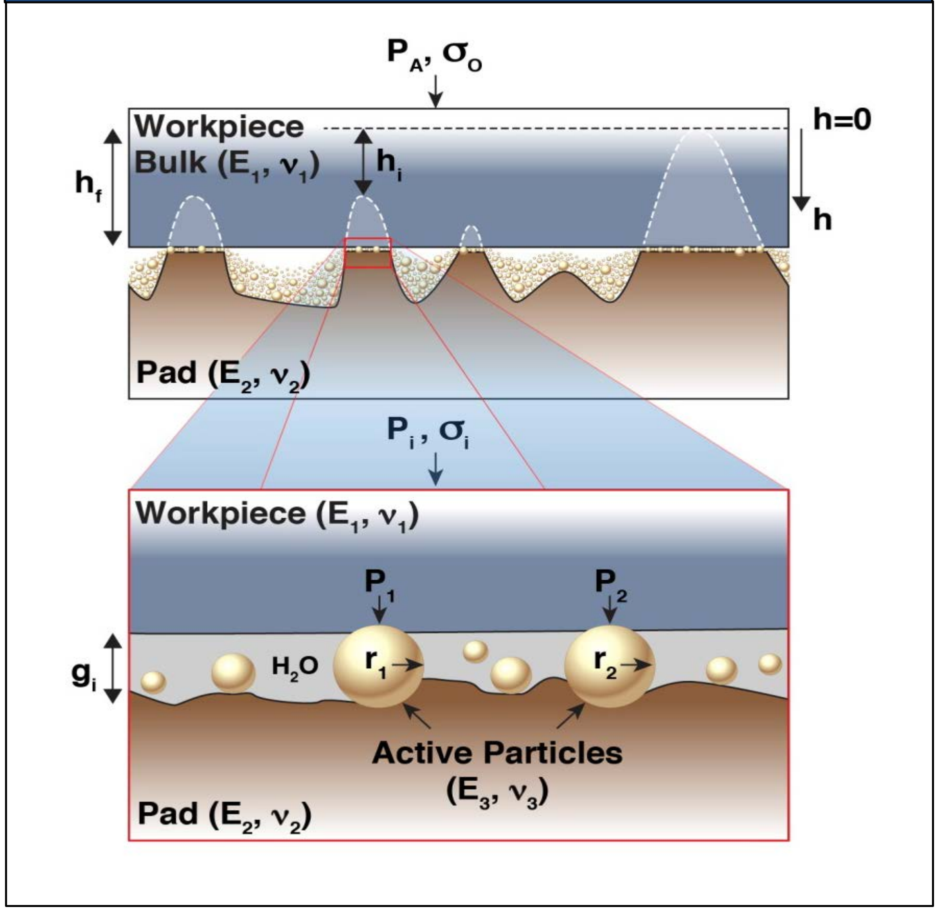

T. Suratwala et. al., *J. Am. Cer. Soc* (2016) accepted

- **<u>Key Inputs:</u> Slurry PSD & Pad Topology**
- **Using pad height histograms:**
  - **Pad asperities compress leading to single value gap of pad ($g_p$) based on load balance**
  - **Fraction of pad area making contact is calculated**
- **Each asperity compresses by height ($h_i$) resulting in stress ($\sigma_i$)**
- **Using slurry PSD at <u>each asperity</u> land–workpiece interface, slurry particles are loaded with a unique gap ($g_i$) following load balance**
- **Load/particle distribution is calculated from summing all pad asperities**

# EHMG model compared with experiments expands our insight to the diverse factors affecting material removal rate

## Measured removal rate & EHMG model Comparison

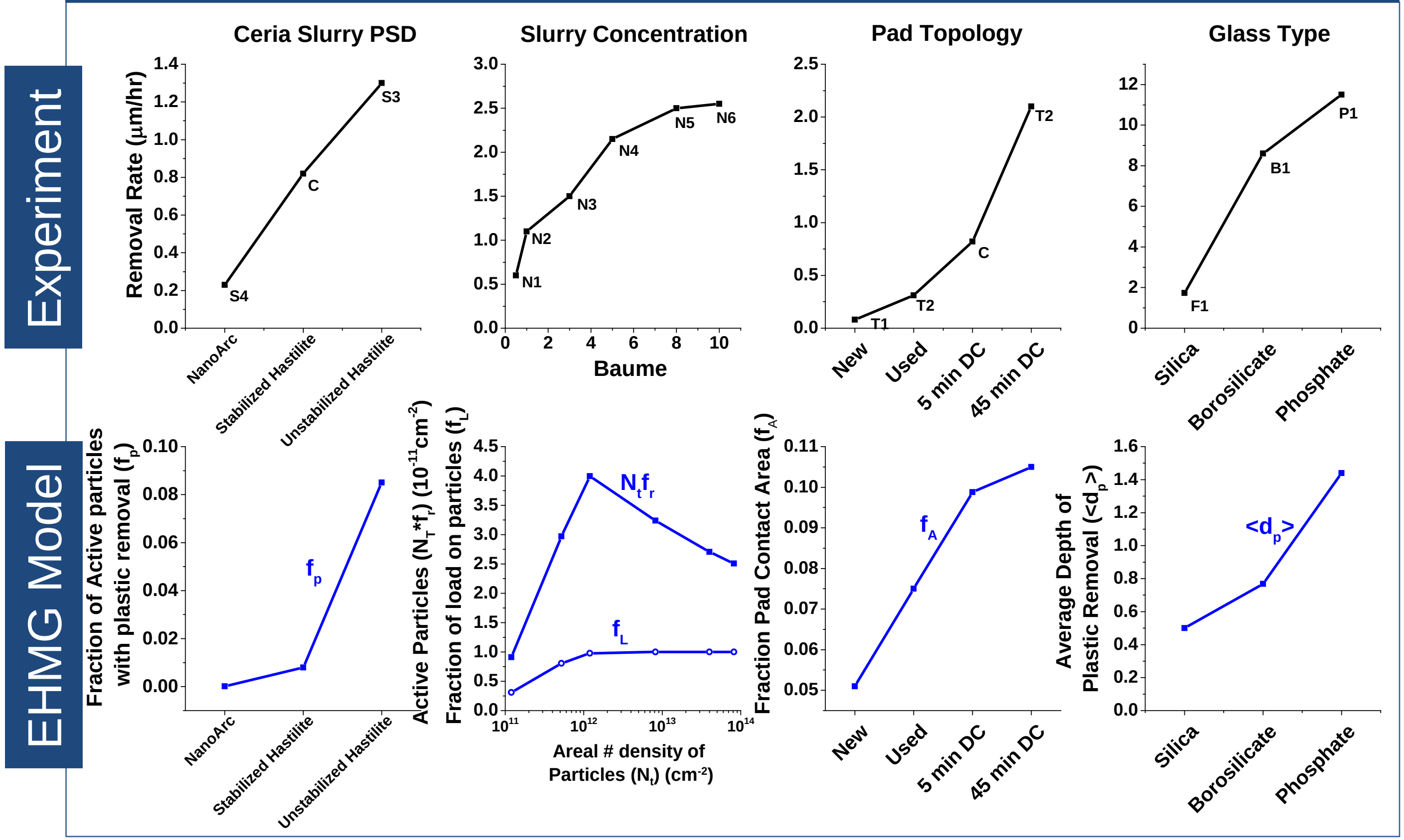

$$\frac{dh}{dt} \approx N_t \, f_A \, f_L \, f_r V_r \left( f_p \langle d_p \rangle \langle 2a_p \rangle + f_m \langle d_m \rangle \langle 2a_m \rangle \right)$$

- **Widening PSD increases load/particle & fraction of removal by plastic removal ($f_p$)**
- **Increasing slurry conc increases active particles density ($N_t f_r$) and fraction of load carried by particle ($f_L$)**
- **Increasing pad flatness increases fraction of pad area making contact ($f_A$)**
- **Change in glass type change removal depth by plastic removal ($d_p$)**

# Load/particle distribution calculated using EHMG model, combined with measured removal function, gives the removal amount for each slurry particle

**Single particle removal function & calculated load/particle distribution**

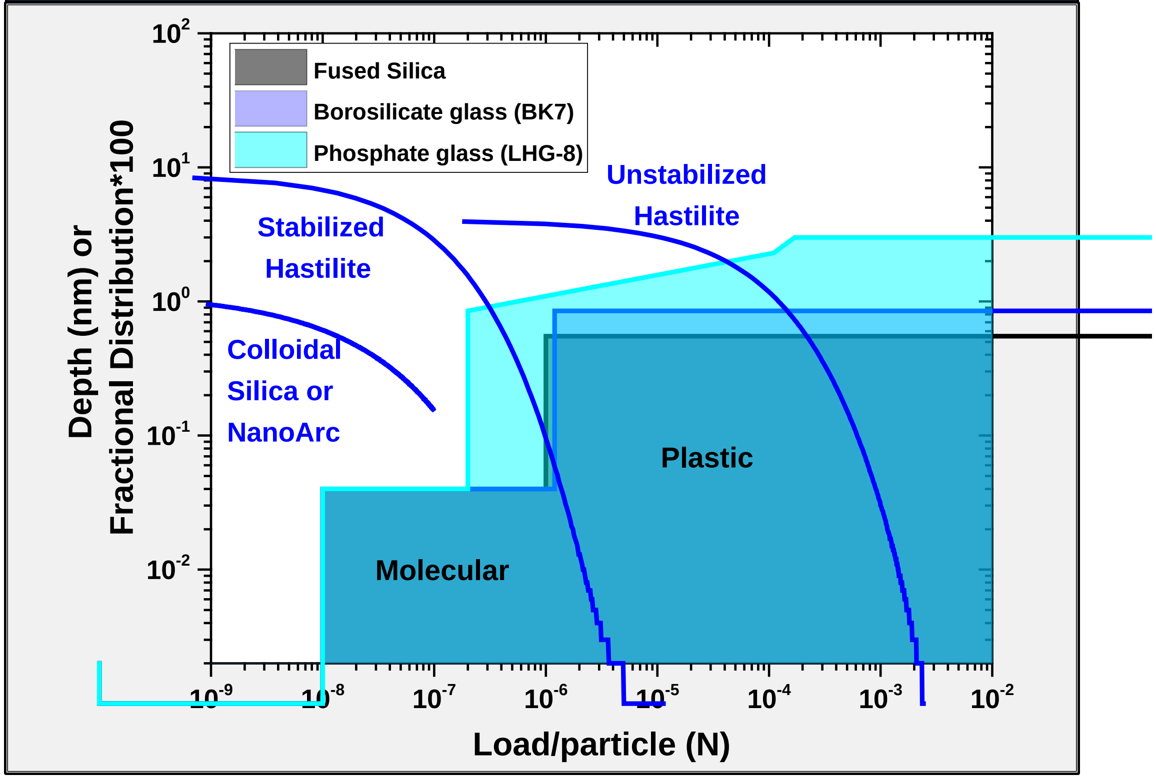

**This can be now used to calculate both removal rate and roughness during polishing**

# Using the EHG model, polished surfaces using different PSDs have been simulated over multiple spatial scale lengths

**Unstabilized Hastilite PO Polished Surface**

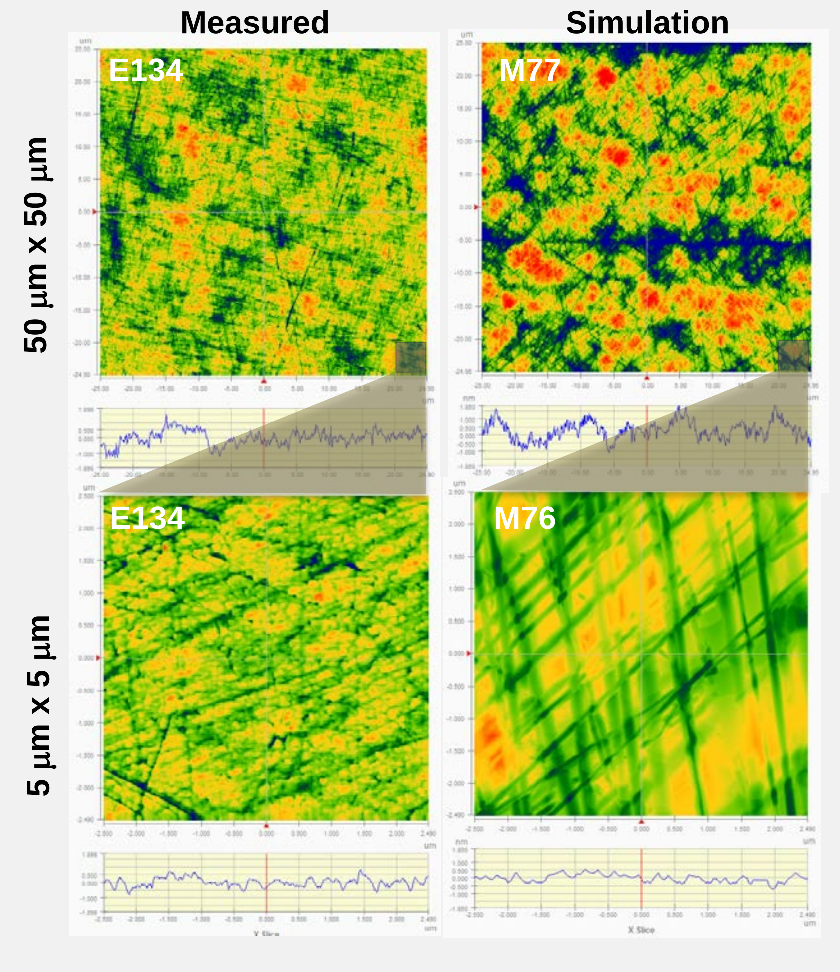

**Stabilized Hastilite PO Polished Surface**

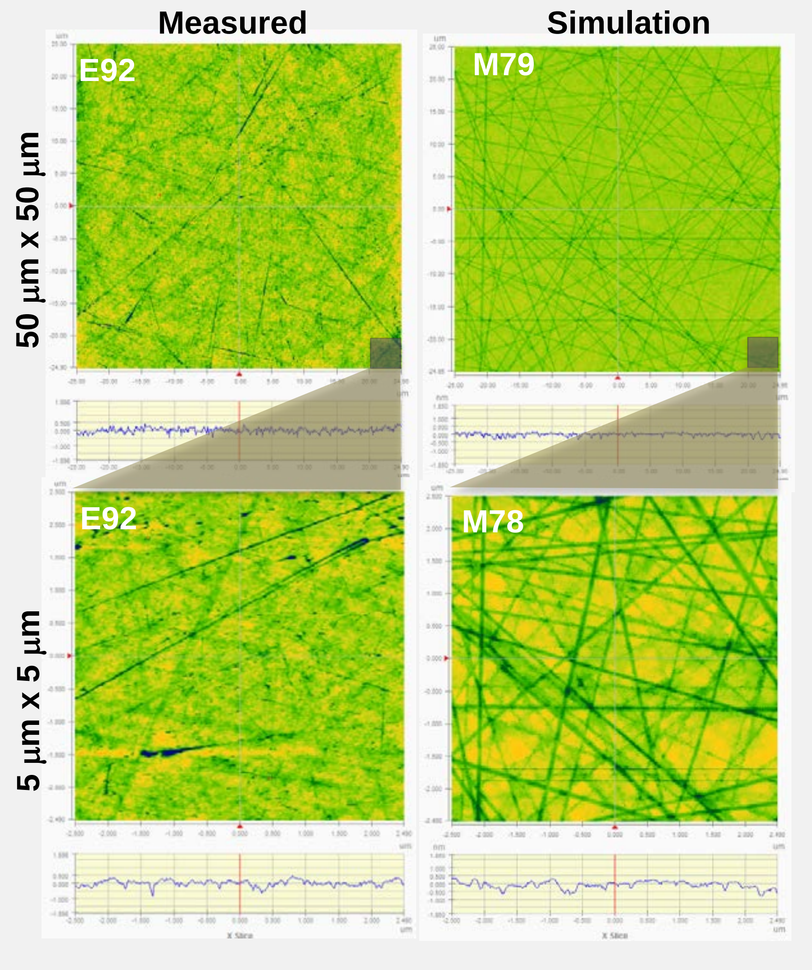

Suratwala et. al., *J. Am. Cer. Soc.* 97(1) 2014

# EHMG model also simultaneously simulates trends in observed AFM roughness over a variety of polishing parameters

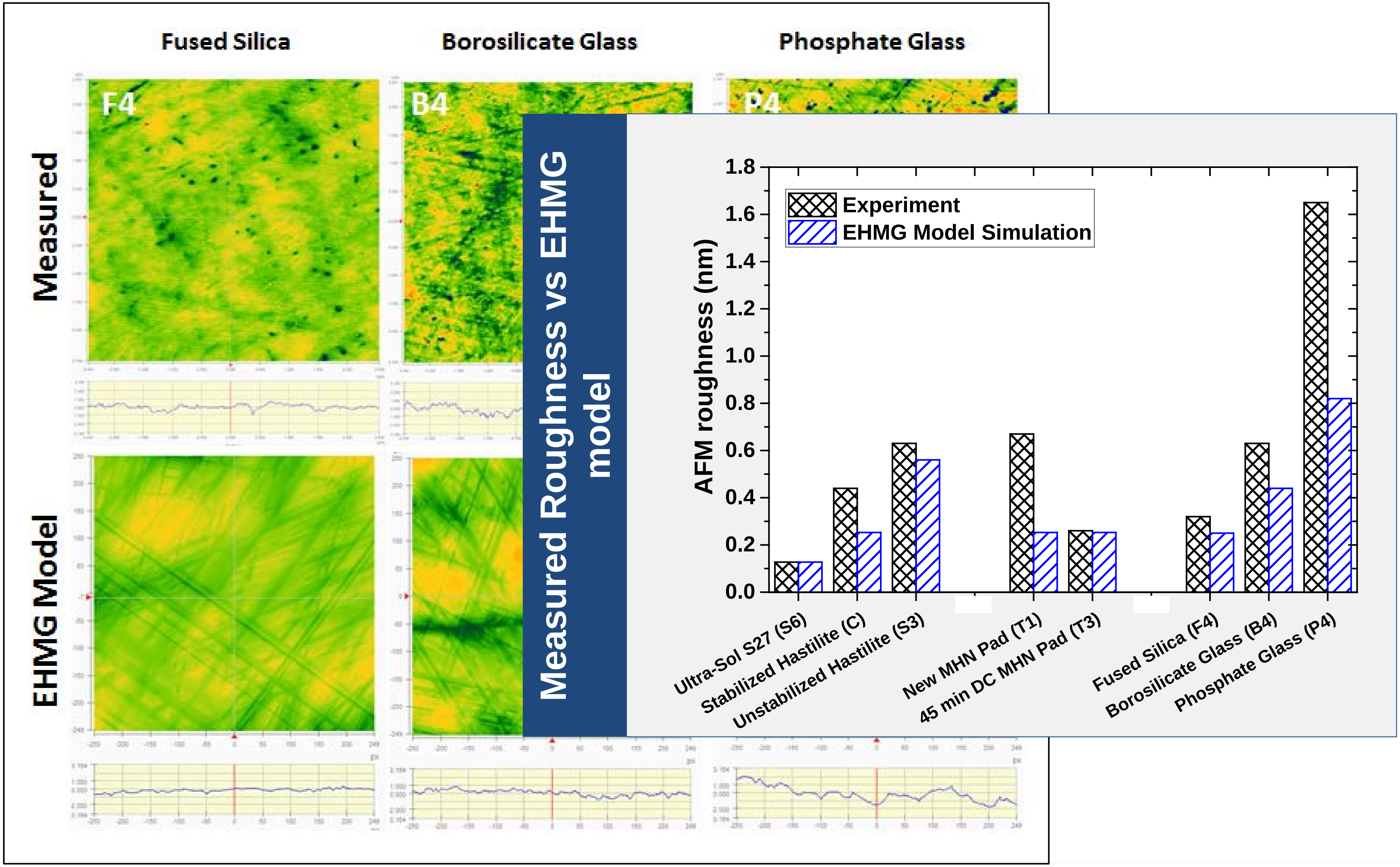

**Measured Roughness vs EHMG model**

T. Suratwala et. al., *J. Am. Cer. Soc* 97(1) (2016) 81

# Novel chemical slurry stabilization and engineered filtration has resulted in improve slurry PSD

## Chemical Stabilization

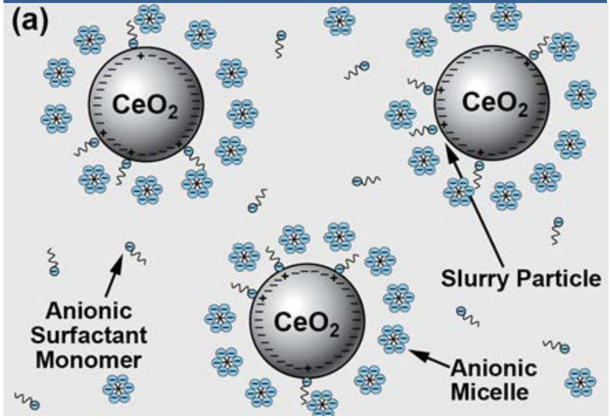

## Engineered Filtration

## Improved Particle Size Distributions

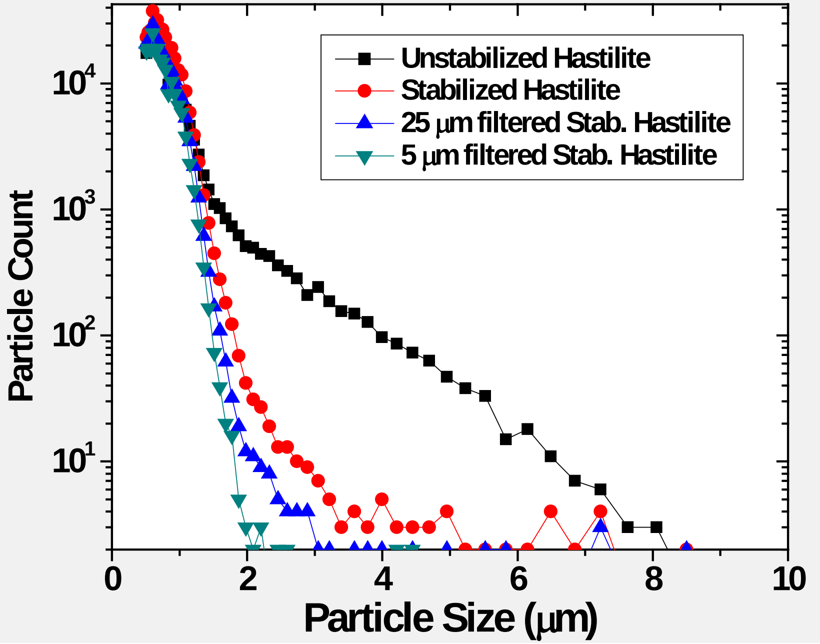

- **Surfactant dramatically reduces agglomeration without reducing removal rate**
- **Appropriate filtration further improves PSD**

**US Patent Application WO 2012129244 A1 (September 27, 2012)**
**R. Dylla-Spears, Colloids & Surfaces A 447 (2014) 32**
**T. Suratwala, JACS 97 (2014) 81**

# Schematic model of the parameters that affect roughness during polishing

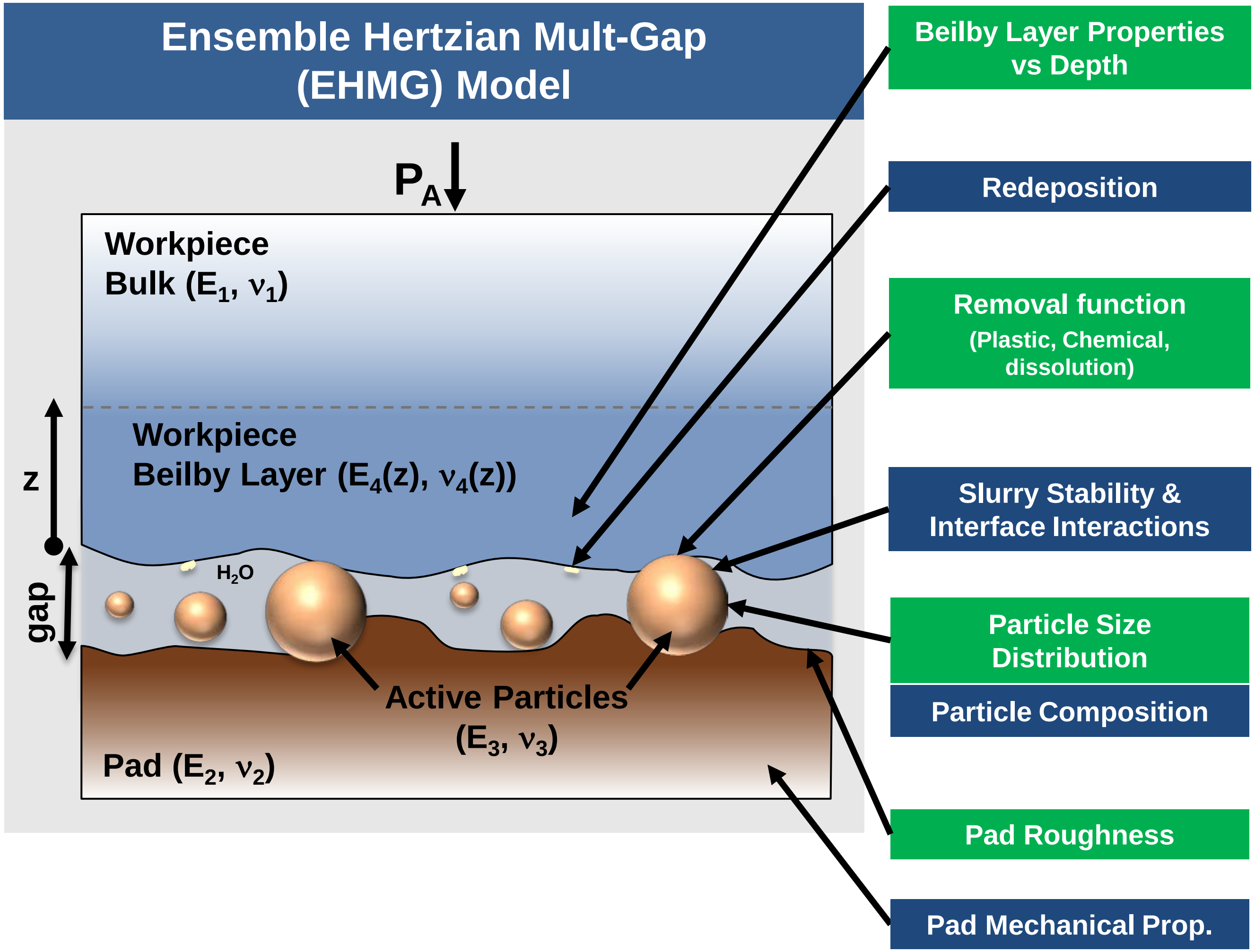

**Ensemble Hertzian Mult-Gap (EHMG) Model**

$P_A$

Workpiece
Bulk ($E_1$, $\nu_1$)

Workpiece
Beilby Layer ($E_4(z)$, $\nu_4(z)$)

z

gap

$H_2O$

Active Particles
($E_3$, $\nu_3$)

Pad ($E_2$, $\nu_2$)

Beilby Layer Properties vs Depth

Redeposition

Removal function
(Plastic, Chemical, dissolution)

Slurry Stability & Interface Interactions

Particle Size Distribution

Particle Composition

Pad Roughness

Pad Mechanical Prop.

# Probing roughness over different scale length: factors affecting u-roughness are not necessarily the same as those affecting AFM roughness

## Power Spectra for various spatial band on a typical fused silica optic

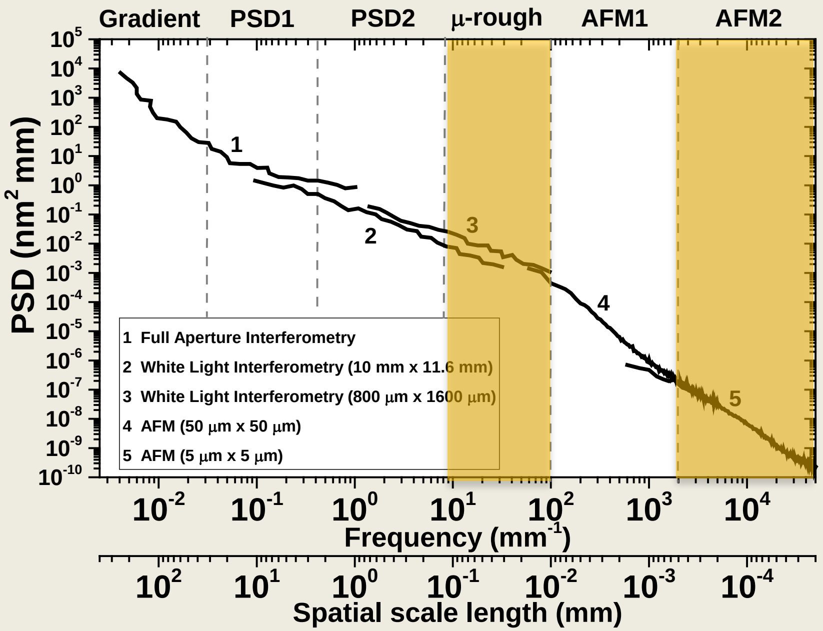

## μ-roughness vs AFM roughness

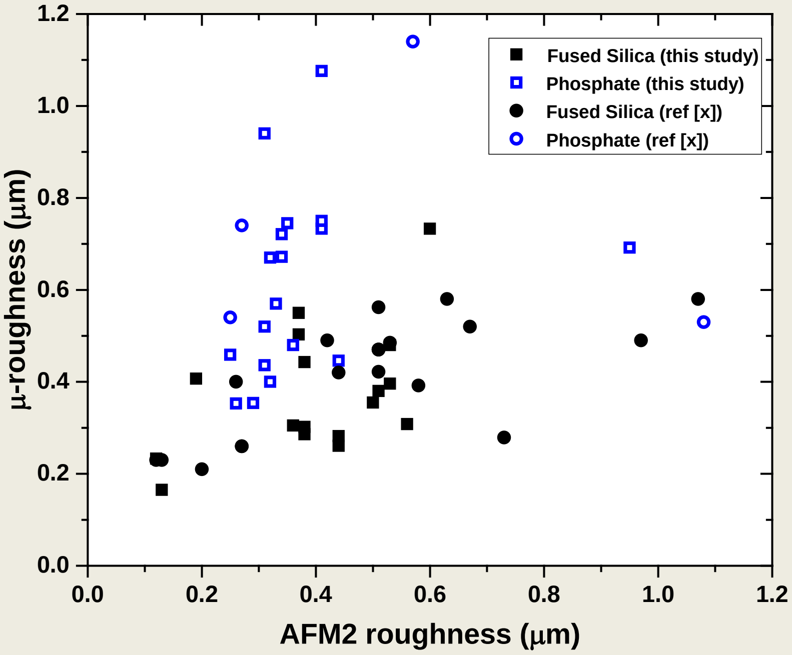

# Little change in AFM roughness suggests plastic removal function is unaffected by pH; Large change in μ-roughness suggest pH is influencing slurry agglomeration at larger scale lengths

**Surface roughness of Phosphate glass (LHG-8) polished with Stabilized Hastilite at different pHs**

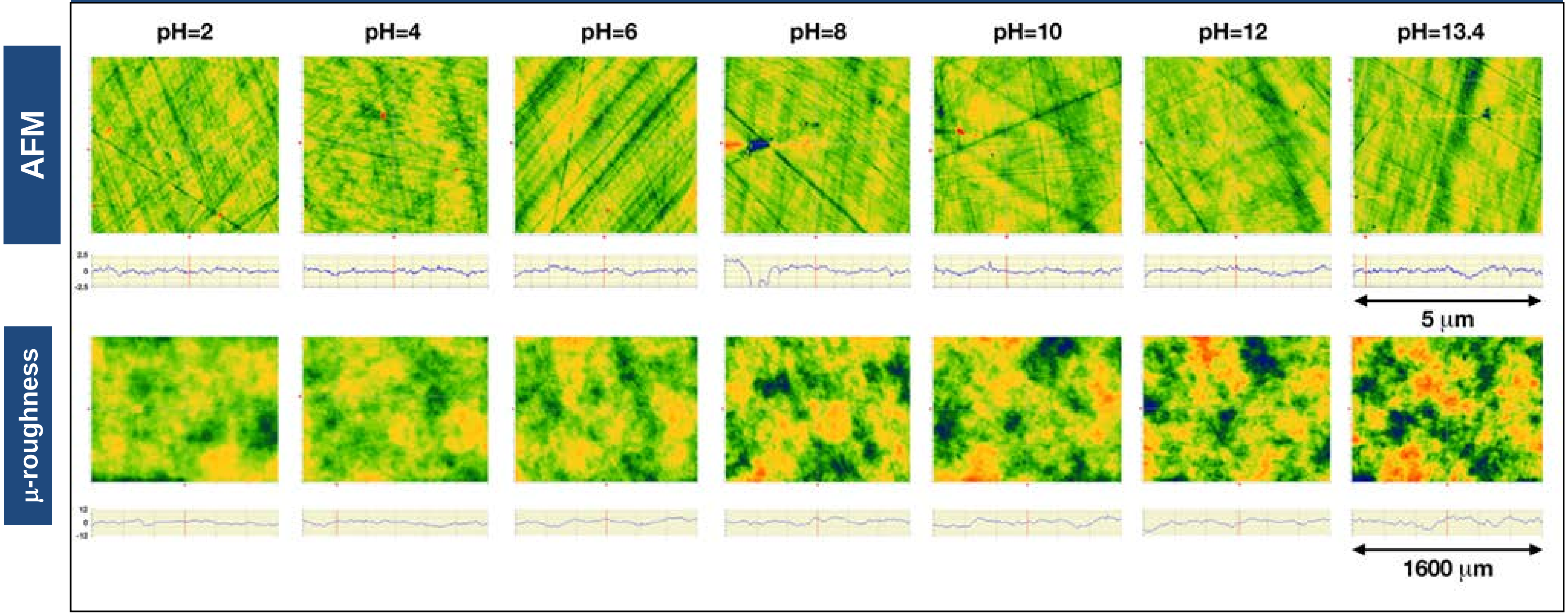

**Note same behavior observed with Stabilized & Unstabilized Hastilite for LHG-8**

# The uniformity of slurry on the pad is greatly improved at lower pH, likely leading to lower m-roughness

## Confocal image of pad surface after polishing

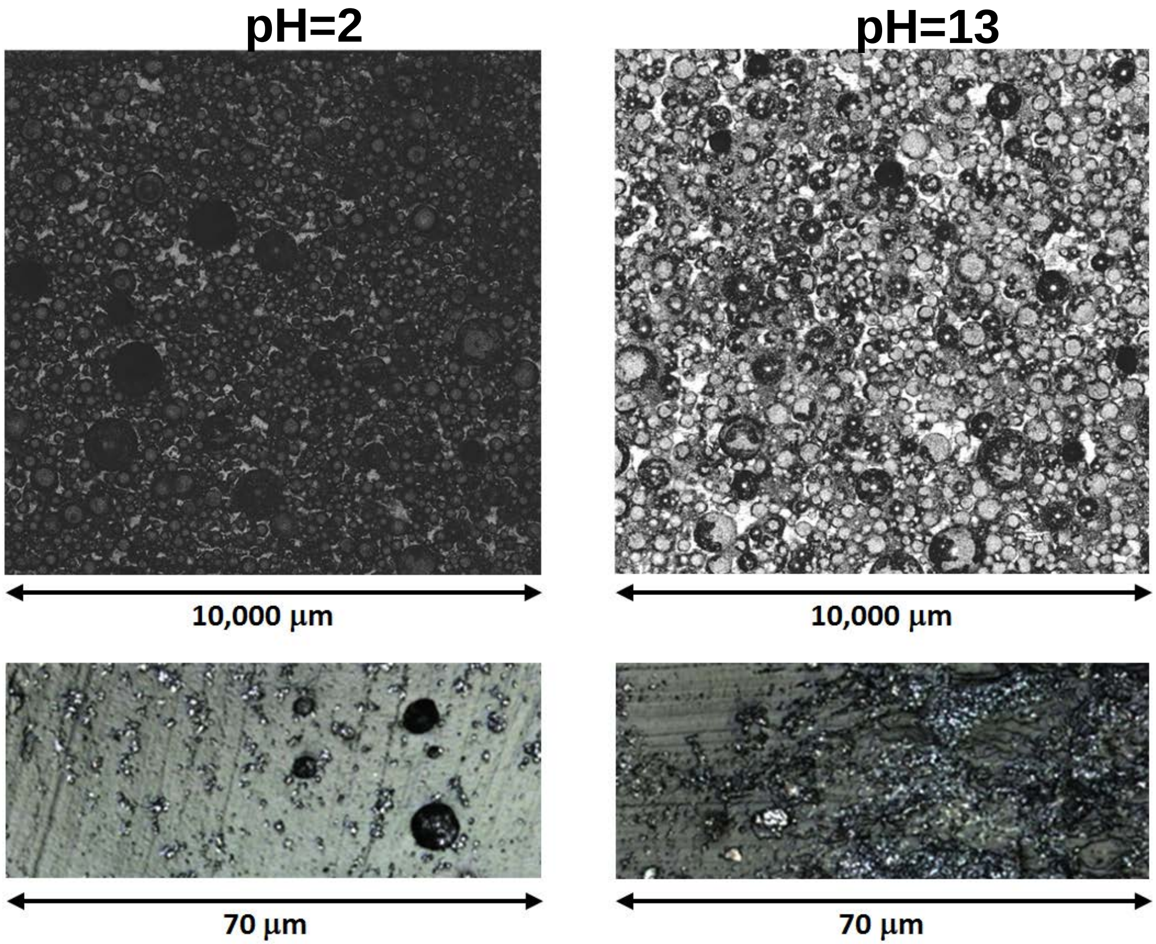

## Slurry Height Distribution

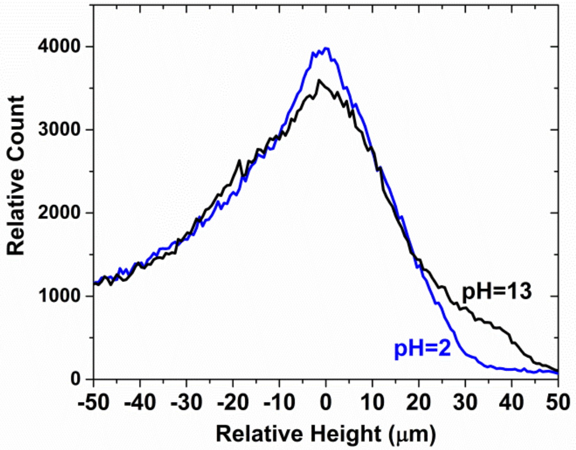

# Impact of glass products on zeta potential is very different depending on the nature of the glass product

## Zeta Potential of Stabilized Hastilite PO as a fn of pH and [$K_3PO_4$]

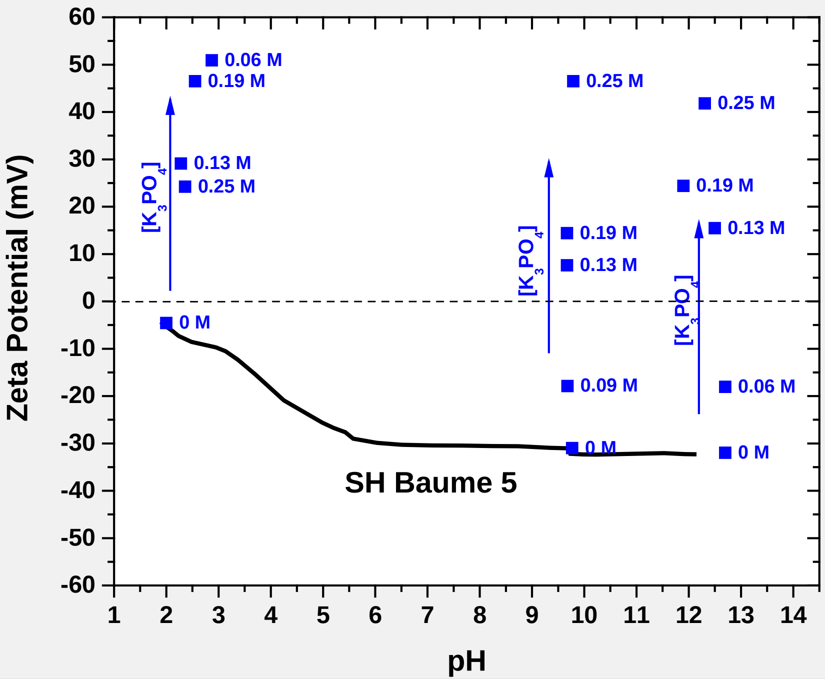

Addition of glass product surrogate for phosphate glass ($K_3PO_4$) make the zeta potential positive with little change in pH

## Zeta Potential of Stabilized Hastilite PO as a fn of pH and [$Si(OH)_4$]

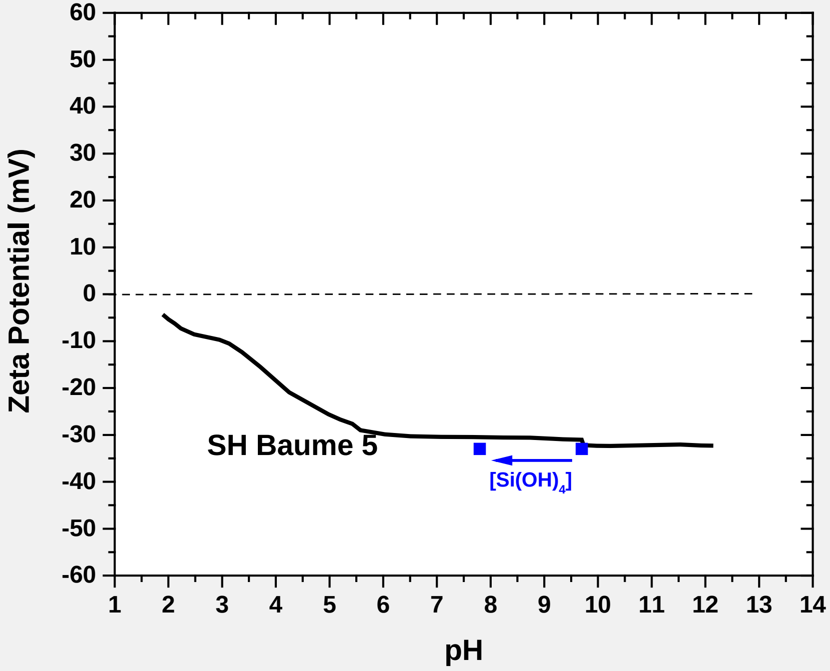

Addition of glass product surrogate for silica glass ($Si(OH_4)$) has little impact to zeta potential

# A model to determine the electrostatic double-layer interaction forces between the 3 components at the interface (as a function of pH and glass products) has been developed

## Electrostatic double-layer interaction forces (two dissimilar surfaces of different radii)*

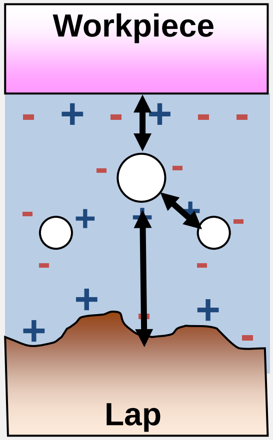

**Particle-Workpiece Force ($F_{P\text{-}WP}$)**

**Particle-Particle Force ($F_{P\text{-}P}$)**

**Particle-Lap Force ($F_{P\text{-}L}$)**

## Force Calculation Results (using measured zeta potential vs pH and glass product conc)

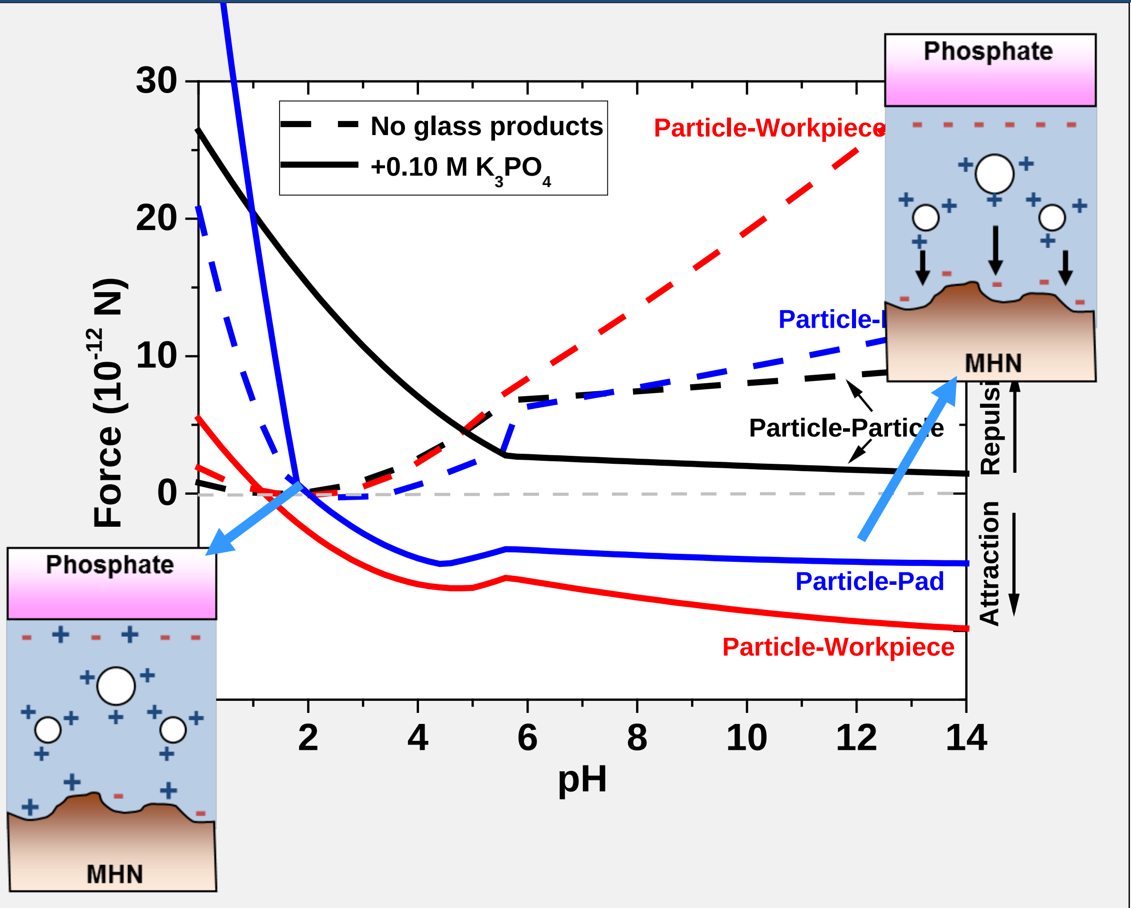

*S. Carnie, D. Chan, J. Gunning *Langmuir* 10 (1994) 2993-3009

# Using the IDG model, simulated μ-roughness compares well with measured data suggesting that slurry spatial distribution is an important contributor to roughness

**Schematic of 'Island' Distribution Gap (IDG) Model**

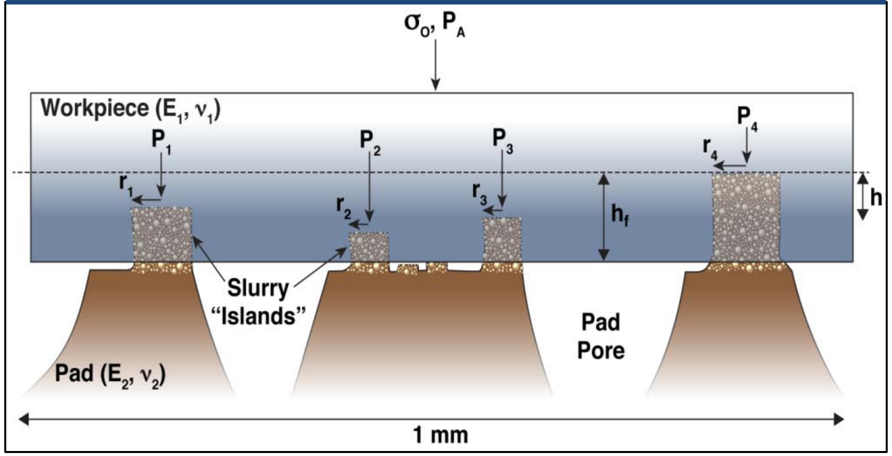

**Comparison between measured and simulated μ-roughness**

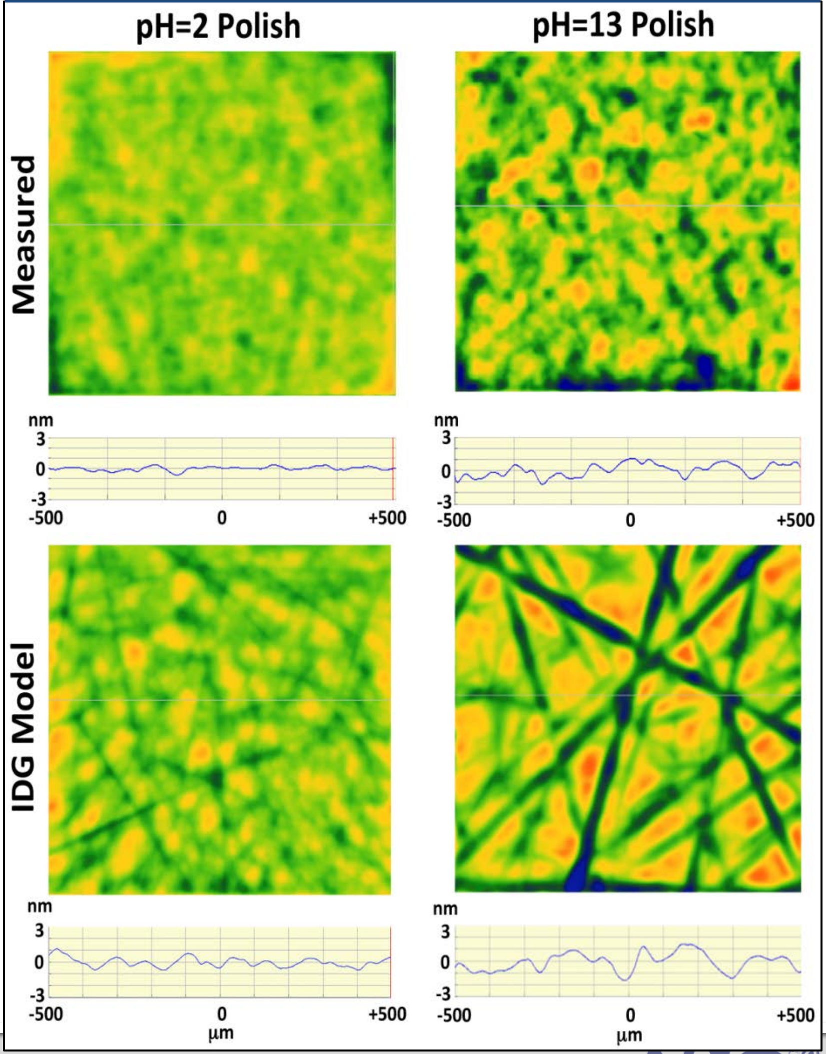

# Increase in pressure resulted in expected removal rate increase and little change in roughness as predicted by the EHMG model

## Plot of measured removal rate & roughness on Fused Silica

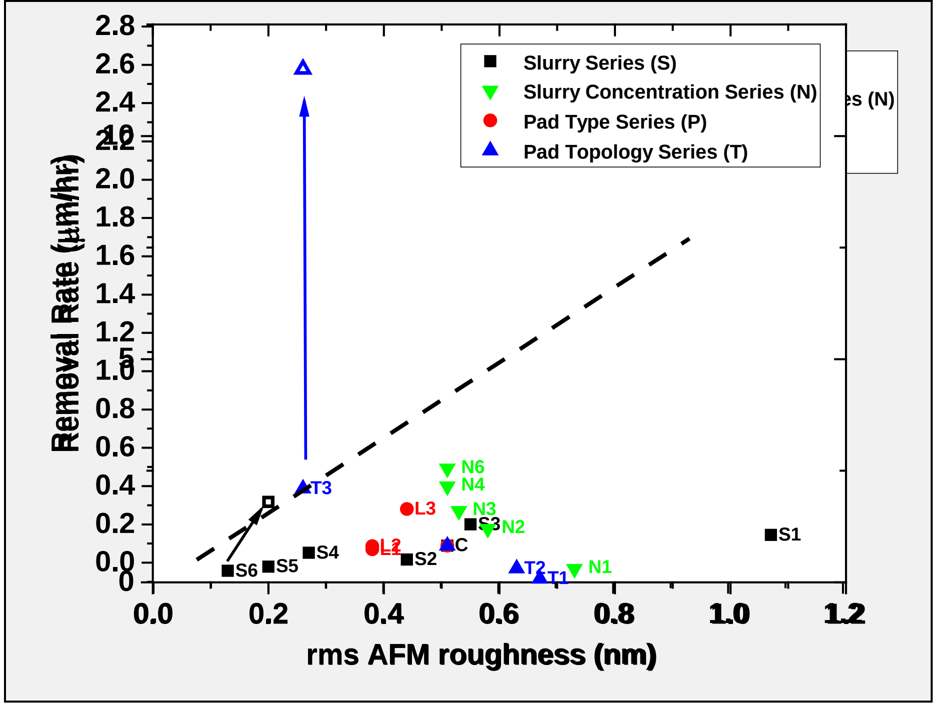

**0.6 psi**
**20 rpm**

**Narrow PSD (S6)**

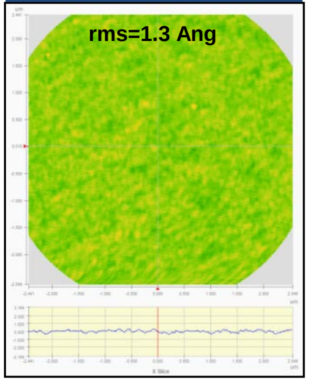

**Flat Pad (T3)**

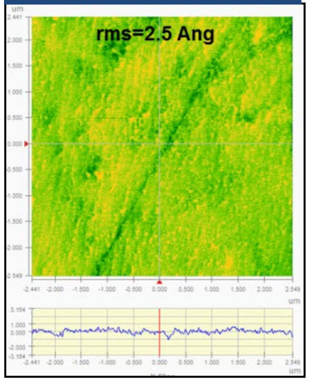

**1.9/2.5 psi**
**50 rpm**

**Flat Pad (ur171)**

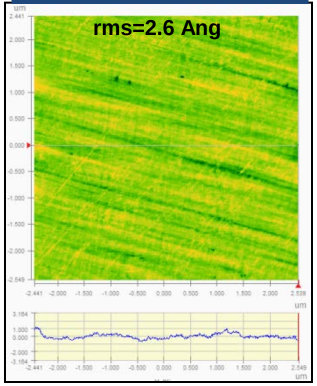

**These results have large practical implications since it is largely believed that low roughness surface are only achieved at low removal rates**

# Schematic model of the parameters that affect roughness during polishing

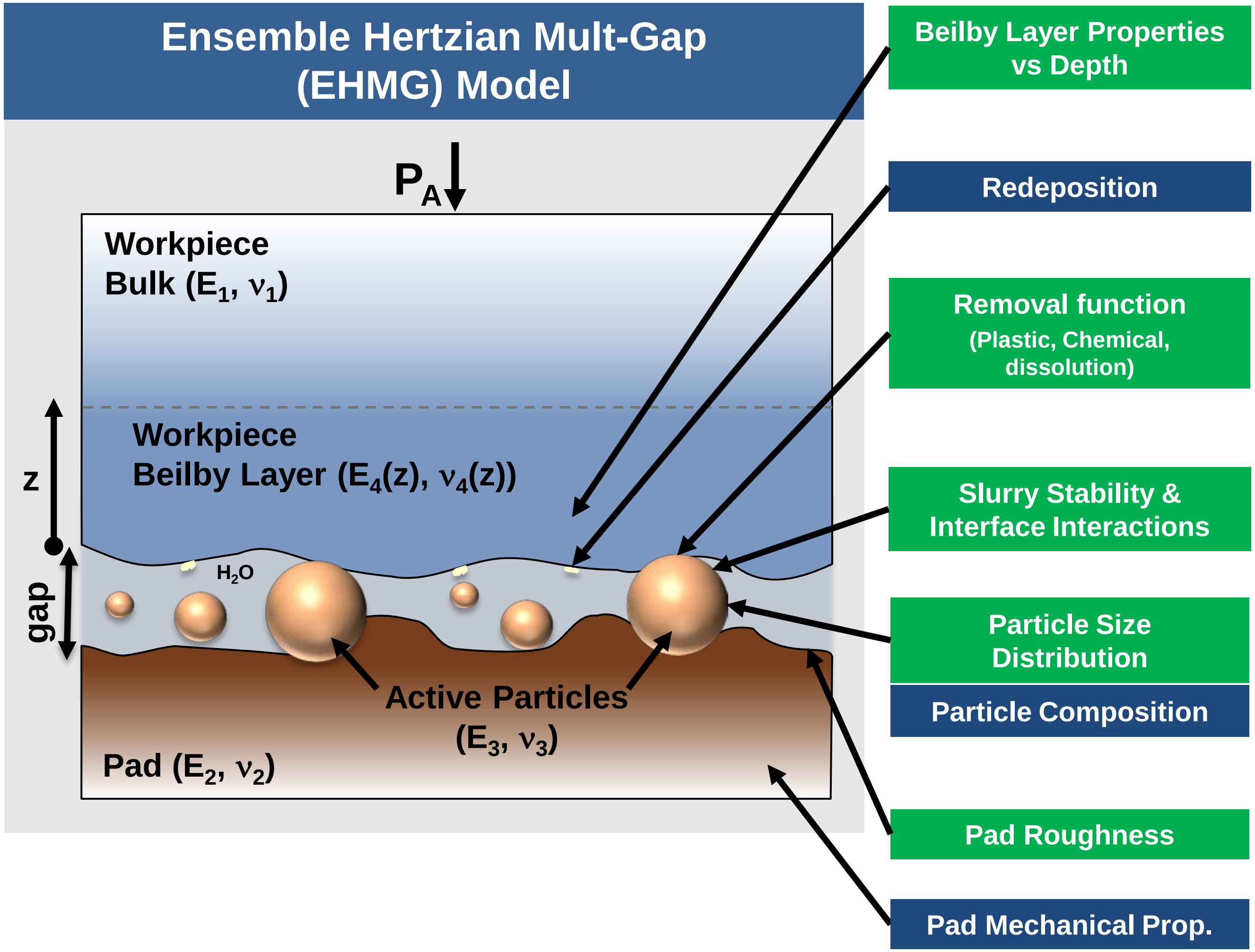

**Ensemble Hertzian Mult-Gap (EHMG) Model**

**Beilby Layer Properties vs Depth**

**Redeposition**

**Removal function**
**(Plastic, Chemical, dissolution)**

**Slurry Stability & Interface Interactions**

**Particle Size Distribution**

**Particle Composition**

**Pad Roughness**

**Pad Mechanical Prop.**

# Strategies to reduce roughness and increase removal rate during polishing

**1) Establish a narrow load/particle distribution**

- **Use slurry with narrow particle size distribution (especially at the tail)**
- **Use a compliant lap**

**2) Remove asperities from lap**

- **Example: Correctly diamond condition polyurethane pad**

**3) Stay within molecular removal regime (avoid plastic regime)**

- **i.e., increase load up until plastic regime is reached**

**4) Control slurry chemistry such that slurry is uniformly distributed at the interface**

- **e.g., pH control and glass products removal**

# The complexities of polishing has made is difficult to scientifically design, optimize a process for a given material

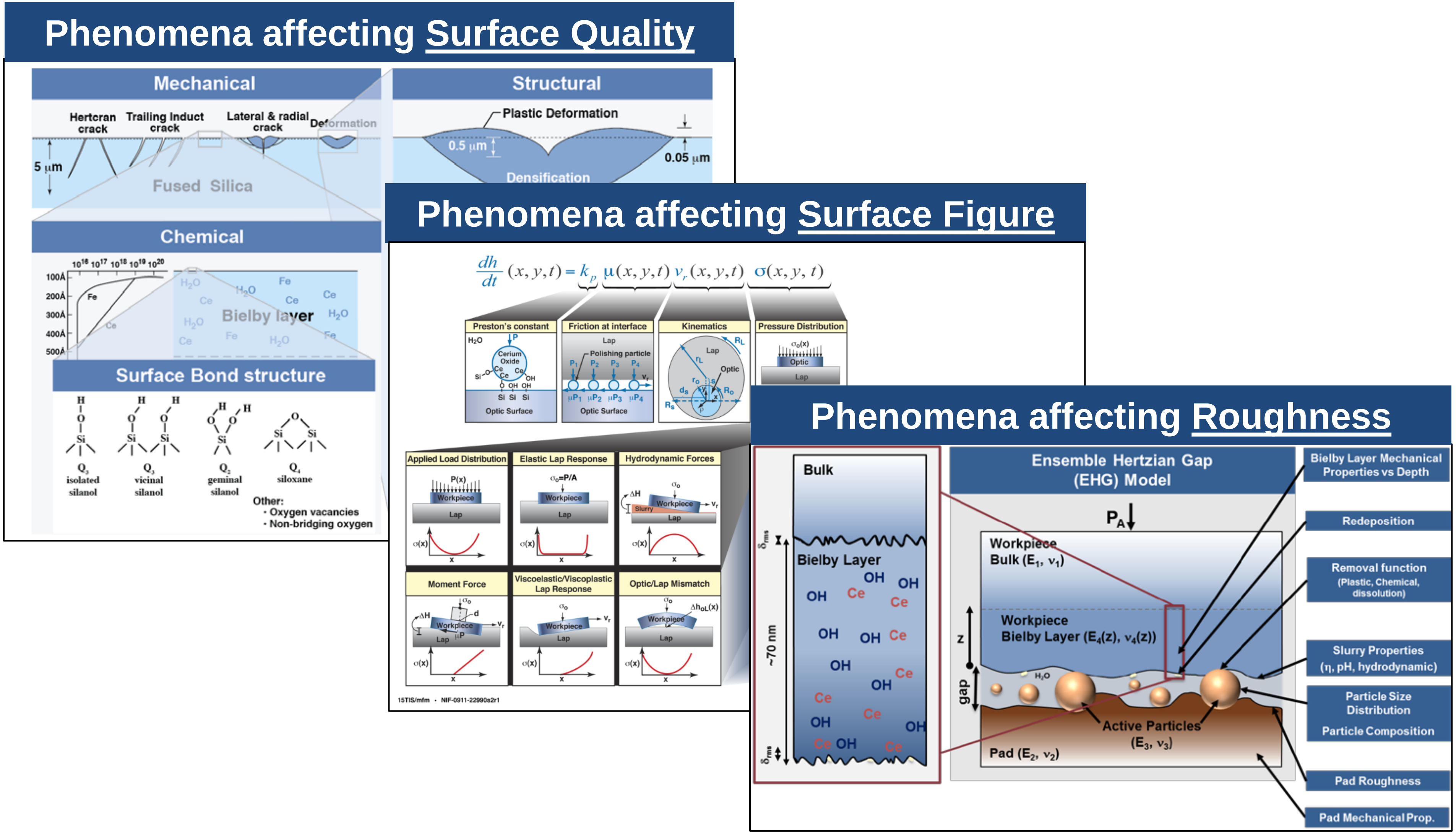

## Phenomena affecting Surface Quality

## Phenomena affecting Surface Figure

$$\frac{dh}{dt}(x,y,t) = \underbrace{k_p}\ \underbrace{\mu(x,y,t)}\ \underbrace{v_r(x,y,t)}\ \underbrace{\sigma(x,y,t)}$$

## Phenomena affecting Roughness